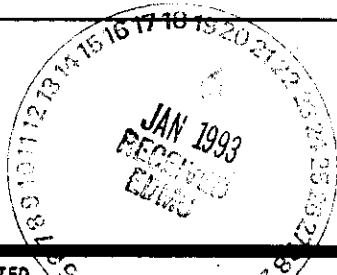


2. To: (Receiving Organization) Distribution	3. From: (Originating Organization) J.R. Kunk - Geosciences	4. Related EDT No.: N/A
5. Proj./Prog./Dept./Div.: Environmental Restoration	6. Cog. Engr.: K.R. Simpson	7. Purchase Order No.: N/A
8. Originator Remarks: Please review the attached report in your area of expertise. Forward Comments to J.R. Kunk as RCRs.		9. Equip./Component No.:
11. Receiver Remarks:		10. System/Bldg./Facility:
		12. Major Assm. Dwg. No.:
		13. Permit/Permit Application No.:
		14. Required Response Date: 1/8/93



15. DATA TRANSMITTED					(F)	(G)	(H)	(I)
(A) Item No.	(B) Document/Drawing No.	(C) Sheet No.	(D) Rev. No.	(E) Title or Description of Data Transmitted	Impact Level	Reason for Transmittal	Originator Disposition	Receiver Disposition
1	WHC-SD-EN-TI-069		0	Phase I Summary of surface Geophysical Studies in the 300-FF-5 Operable Unit.	4	1/4		

16. KEY			
Impact Level (F)	Reason for Transmittal (G)	Disposition (H) & (I)	
2, 3, or 4 (see MRP 5.43)	1. Approval 2. Release 3. Information 4. Review 5. Post-Review 6. Dist. (Receipt Acknow. Required)	1. Approved 2. Approved w/comment 3. Disapproved w/comment	4. Reviewed no/comment 5. Reviewed w/comment 6. Receipt acknowledged

(G)	(H)	17. SIGNATURE/DISTRIBUTION (See Impact Level for required signatures)								(G)	(H)
Reason	Disp.	(J) Name	(K) Signature	(L) Date	(M) MSIN	(J) Name	(K) Signature	(L) Date	(M) MSIN	Reason	Disp.
1/4		Cog. Eng. K.R. Simpson H6-06	<i>K.R. Simpson</i>	1/18/93		K.A. Lindsey H6-06	<i>K.A. Lindsey</i>	18 Jan 1993		1/4	1/4
1/4		Cog. Mgr. A.J. Knepp H6-06	<i>A.J. Knepp</i>								
		QA									
		Safety									
		Env.									

18. J.R. Kunk Signature of EDT Originator <i>J.R. Kunk</i> Date: 1-18-93	19. _____ Authorized Representative for Receiving Organization Date: _____	20. A.J. Knepp Cognizant/Project Engineer's Manager <i>A.J. Knepp</i> Date: 1/18/93	21. DOE APPROVAL (if required) Ltr. No. _____
---	--	--	--

**THIS PAGE INTENTIONALLY
LEFT BLANK**

SUPPORTING DOCUMENT

1. Total Pages 98

2. Title

Phase I Summary of Surface Geophysical Studies in the 300-FF-5 Operable Unit

3. Number

WHC-SD-EN-TI-069

4. Rev No.

0

5. Key Words

Geophysics, Shallow Seismic, GPR, Electromagnetic Hanford/Ringold, Data Acquisition and Processing, Velocity/Depth Profiles.

6. Author

Name: J.R. Kunk

J.W. Fawcett 1-18-93
Signature

Organization/Charge Code 81234/P25AD

APPROVED FOR
PUBLIC RELEASE

1-18-93 N. Solis

7. Abstract

This report documents a geophysical investigation supporting hydrogeology studies of the 300-FF-5 Operable Unit. The report details data acquisition using seismic and ground penetrating radar. Additionally, methodologies, details of equipment used and data processing are described.

8. RELEASE AND USE OF DOCUMENT - This document was prepared and released by the U.S. Department of Energy and its contractors. It is to be used only to perform direct, or integrated work under U.S. Department of Energy contracts. This document is not approved for public release until reviewed.

PATENT RIGHTS - This document copy, since transmitted in advance of patent clearance, is made available in confidence solely for use in performance of work under contract with the U.S. Department of Energy. This document is not to be published nor its contents otherwise disseminated, used for purposes other than specified, or used before patent approval for such release of work has been secured, upon request, from the Patent Counsel, U.S. Department of Energy, Field Office, Richland, WA.

DISCLAIMER - This report was prepared as an account of work sponsored by an agency of the United States Government. Neither the United States Government nor any agency thereof, nor any of their employees, nor any of their contractors, subcontractors or their employees, makes any warranty, express or implied, or assumes any legal liability or responsibility for the accuracy, completeness, or any third party's use or the results of such use of any information, apparatus, product, or process disclosed, or represents that its use would not infringe privately owned rights. Reference herein to any specific commercial product, process, or service by trade name, trademark, manufacturer, or otherwise, does not necessarily constitute or imply its endorsement, recommendation, or favoring by the United States Government or any agency thereof or its contractors or subcontractors. The views and opinions of authors expressed herein do not necessarily state or reflect those of the United States Government or any agency thereof.

10. RELEASE STAMP

OFFICIAL RELEASE
BY WSD
DATE JAN 18 1993
Sta. 21

9. Impact Level 4

9
1
0
9
0
4
1
7
9

**THIS PAGE INTENTIONALLY
LEFT BLANK**

CONTENTS

1.0	INTRODUCTION	1
1.1	PURPOSE OF STUDY	1
1.2	PROJECT OBJECTIVES	1
1.3	SCOPE OF INVESTIGATION	2
1.4	PLAN OF DEVELOPMENT	2
2.0	GENERAL BACKGROUND STUDIES	3
2.1	GEOLOGY	3
2.2	PREVIOUS SEISMIC SURVEYS	5
3.0	SEISMIC REFLECTION STUDIES	5
3.1	INTRODUCTION	5
3.2	DATA ACQUISITION	7
3.2.1	Seismic Source Study	7
3.2.2	Acquisition	8
3.3	DATA PROCESSING	9
3.3.1	Velocity Analysis	9
4.0	DATA ANALYSIS/INTERPRETATION	10
4.1	INTRODUCTION	10
4.2	METHODOLOGY	10
4.3	THE HANFORD/RINGOLD UNCONFORMITY	12
4.4	THE LOWER MUD/BASALT REFLECTOR	12
5.0	CONCLUSIONS	14
6.0	RECOMMENDATIONS	14
7.0	REFERENCES	16
APPENDICES		
A	SUMMARY OF ELECTROMAGNETIC INDUCTION/GROUND-PENETRATING RADAR ANOMALIES	A-i
B	METHODOLOGIES, DETAILS OF EQUIPMENT, AND DATA ACQUISITION AND PROCESSING	B-i
C	VELOCITY/DEPTH PROFILES	C-i
D	INTERPRETED SEISMIC SECTIONS	D-i

9 5 1 1 0 0 4 1 7 9 2

LIST OF FIGURES

1	Site Location Map for the 300-FF-5 Operable Unit, 300 Area	19
2	Seismic Line Locations	20
3	Generalized Stratigraphy From Lindsey (1992)	21
4	Wavelet Processed Seismic Reflection Line From the Basalt Waste Isolation Project Test Survey Over DC-6 Well (Heineck and Beggs 1978)	22
5	Initial Processing of Seismic Reflection Test Line in the "Basalt Waste Isolation Project Reference Repository Location" (Kunk 1986)	23
6	Amplitude Spectra of (a) Betsy Seisgun and (b) Sledge Hammer	24
7	Amplitude Spectra of the Dinoseis Source	25
8	Comparison of Seismic Sources at Seismic Line Intersection	26
9	Symmetrical Split-Spread Configuration of (a) Initial Split-Spread Configuration and (b) Final Split-Spread Configuration	27
10	Seismic Reflection Line 3-5	28
11	Structure Map of the Hanford/Ringold Unconformity	29
12	Structure Contour Map of the Hanford/Ringold Contact, Using Only Borehole Log Depths for Control	30
13	Structure Map on the Ringold Lower Mud Unit	31
14	Structure Contour Map of Ringold Formation Lower Mud Sequence Using Only Borehole Log Depths for Control	32

9 1 1 9 0 4 1 7 9 3

**SUMMARY OF SURFACE GEOPHYSICAL STUDIES
IN THE 300-FF-5 OPERABLE UNIT**

1.0 INTRODUCTION

1.1 PURPOSE OF STUDY

9 3 1 9 0 4 1 7 9 4

This report documents a geophysical investigation supporting hydrogeology studies of the 300-FF-5 operable unit on the Hanford Site (Figure 1). The work was proposed in the *Remedial Investigation /Feasibility Study Work Plan for the 300-FF-5 Operable Unit, Hanford Site, Richland, Washington*, (DOE-RL 1990) Section 5.3.2, Task 2. This remedial investigation/feasibility study (RI/FS) details a study plan to determine the nature and location of hazardous and radioactive substances and pollutants released to the subsurface. To determine the extent of the threat to the environment, an accurate understanding of subsurface fluid migration paths is necessary. This work involves describing the configuration or geometry and location of hydrogeologic boundaries, such as the top and base of the unconfined aquifer, the lateral extent of controlling aquitards, and the location and configuration of lateral and vertical paths of communication. This information will provide the general framework for evaluating the impact of any releases of contaminants and the effectiveness of proposed remediation techniques.

Traditionally, surface geophysical surveys are used to provide subsurface stratigraphic control between boreholes. However, the unusual mix of flood deposits and massive river gravels raises the question of whether these standard surveys can provide useful information. Therefore, the purpose of this study is to use surface geophysical techniques, particularly seismic reflection surveys, in the 300-FF-5 operable unit to determine their feasibility to aid subsurface site characterization.

1.2 PROJECT OBJECTIVES

The geologic goal of the study was to refine the definition of the major lithofacies that may control the hydrofacies between the water table and the top of basalt. The major source of subsurface information at the Hanford Site is provided by borehole control and extrapolations between holes. Consequently, there is no data control from well to well. Geophysical techniques can provide information between boreholes and allow extrapolation of the geology into unknown areas.

Under Section 5.3.2.1, Task 2a, of the RI/FS (DOE-RL 1990), two main objectives using surface geophysical techniques were proposed. The first objective called for a feasibility study ". . . to evaluate the reflective properties of the major sedimentary units, the water table and the top of the basalt." The seismic reflective properties of geologic boundaries are dependent on the acoustic impedance contrast across any given stratigraphic/tectonic unit. This contrast, which involves changes in acoustic velocity and bulk density, must be great enough to allow seismic

energy to be reflected from the boundary and transmitted to receivers on the surface. The impedance contrast in unconsolidated sediments is not always great enough to permit the use of seismic reflection techniques. However, when successful, the detailed resolution can provide the needed geologic control to determine the lateral extent of major stratigraphic units and the structure of the underlying basalt. By evaluating the reflective properties of the controlling stratigraphic horizons, this feasibility study has been able to determine the usefulness of the seismic reflection technique for future site characterization. The RI/FS also specified that extensive ground-penetrating radar (GPR) be run prior to seismic acquisition to delineate the thickness of eolian sediments and the location of paleosol horizons that can adversely effect the quality of seismic data.

The second goal of this study was to determine the existence of a proposed paleochannel (Lindberg and Bond 1979) extending along the eastern boundary of 300-FF-5 operable unit parallel to the present-day Columbia River. Lindberg and Bond (1979) state that excavation in 1958 discovered a channel incised into the Ringold Formation beneath the 300 Area. The eastern side of this channel would consist of Hanford formation flood gravels adjacent to the Ringold Formation forming a flow barrier between the paleochannel and the present-day Columbia River. In the RI/FS (DOE-RL 1990), it was determined that this barrier and any opening in the barrier allowing communication with the river might be mappable utilizing shallow geophysical techniques, such as GPR, electromagnetic induction (EMI) profiling, and seismic refraction studies.

1.3 SCOPE OF INVESTIGATION

In the RI/FS (DOE-RL 1990), survey location lines were laid out to extend between new wells drilled in 1992 to facilitate correlating the geophysical data to well control (Figure 2). About 14.5 km (9 mi) of seismic reflection, GPR and EMI data were collected along these lines. Prior to data acquisition, a series of field tests was performed to optimize the data. Furthermore, three different acoustic sources were tested to investigate problems concerning input frequency versus signal strength. Unfortunately, there were no guidelines in the RI/FS requiring borehole velocity control. Consequently, no data of this nature were acquired. Also, GPR and EMI surveys were carried out along seismic lines to identify thick eolian sections, paleosol locations, and culturally disturbed areas.

Although it is stated in the RI/FS (DOE-RL 1990) that GPR, EMI, and seismic refraction surveys should be used to attempt mapping the proposed paleochannel, several short east-west profiles of reflection and refraction data were collected to ascertain the existence of the proposed north-south-trending barrier (Figure 2). In addition, reflection data were acquired along line 1-3 in several sections locate possible breaks or opening in the proposed barrier.

1.4 PLAN OF DEVELOPMENT

Chapter 2.0 describes pertinent geology and previous seismic studies. Chapters 3.0 and 4.0 briefly describe reflection-seismic source and velocity

9 8 1 2 9 0 4 7 9 5

studies. In particular, an in-depth discussion in Chapter 3.0 describes the importance and results of the initial seismic reflection field testing. The findings of these investigations are relevant, not only to the data quality for this study but also as important documentation to future seismic work at the Hanford Site.

The velocity function, both laterally and vertically, is always an important topic for seismic investigations and, as such, warrants an in-depth discussion to illuminate problems peculiar to the Hanford Site.

In Chapter 4.0, all the data are analyzed with respect to the study objectives as defined in the RI/FS (DOE-RL 1990). Where significant and/or possible, the results of the geophysical surveys have been integrated with the findings of the hydrogeology study to present a more complete subsurface structure of major geologic contacts. Interpreted seismic sections are presented in Appendix D.

The overall results and the significance of this comprehensive geophysical study are discussed in Chapter 5.0. Specific, pertinent recommendations for future geophysical surveys relevant to the 300-FF-5 area and to sitewide investigations are made with respect to the investigative nature of this study.

Examples of each data type are given in the appendices. A comprehensive discussion of EMI/GPR findings is provided in Appendix A, and all the acquisition and processing parameters for each geophysical method used are presented in detail in Appendix B. In addition, documentation of the velocity functions used to process and interpret the seismic reflection survey is presented in Appendix C. This velocity data is provided to aid in planning future sitewide seismic surveys.

2.0 GENERAL BACKGROUND STUDIES

2.1 GEOLOGY

In this section, the basic subsurface lithologic units encountered in the 300 Area are briefly described. These units consist of the Ice Harbor Member of the Miocene age Saddle Mountains Basalt, the late Miocene-to-Pliocene age Ringold Formation, the Pleistocene age Hanford formation, and localized eolian deposits (Figure 3 [Swanson et al. 1992]). The Plio-Pleistocene unit and early "Palouse" soil found further to the west are not present (Swanson et al. 1992).

The Ice Harbor Member is the uppermost unit in the Saddle Mountains Basalt (DOE 1988, Tolan et al. 1989). The source vents are located to the east near Ice Harbor Dam. The Ice Harbor Member extends as far west as Horn Rapids and pinches out just to the north of the 300 Area. In the 300 Area the top of the Ice Harbor Member ranges from 52.4 to 59.7 m (172 to 196 ft) below the surface (Swanson et al. 1992). Where the top of the unit is described, it generally is weathered and oxidized (Ledgerwood 1991).

9 3 1 4 9 0 4 7 9 6

Immediately overlying the basalt is the Ringold Formation. Three of the five Ringold Formation facies associations (Lindsey 1991) are found in the 300 Area. They are the fluvial gravel association, overbank-paleosol association, and lacustrine association. Ringold Formation strata in the 300 Area are divided into an upper gravel-dominated interval and a lower mud-dominated interval (Swanson et al. 1992).

The lower interval is equivalent to the lower mud unit. The lower mud unit probably consists of an upper lacustrine interval and a lower overbank-paleosol interval in the area. The unit thickens to the south, while thinning to the north and west (Swanson et al. 1992). It may be absent north of the 300 Area (DOE-RL 1990). The lower mud unit is separated locally from the underlying basalt by a thin, discontinuous sand-rich interval. The lower mud unit forms the base of the unconfined aquifer in the 300 Area.

The upper part of the Ringold Formation consists dominantly of clast-supported gravels with a fine- to medium-grained sand matrix that is typical of the fluvial gravel facies association (Swanson et al. 1992). These gravels contain two laterally discontinuous mud-dominated intervals that are dominated by the overbank-paleosol association. As a consequence of lateral discontinuity, pinchouts producing a complex interfingering pattern are common. These gravels probably are equivalent to gravel units B, C, and E (Lindsey 1991).

The upper unit of the Ringold Formation, the Plio-Pleistocene unit, and the early "Palouse" soil are missing from the 300 Area as a result of erosion associated with cataclysmic flooding (Swanson et al. 1992). Consequently, the Hanford formation unconformably overlies Ringold Formation gravels. This contact is very irregular and may contain paleochannels. Two of the three main facies in the Hanford formation (Baker et al. 1991, Lindsey et al. 1991, Lindsey et al. 1992), the gravel-dominated and sand-dominated, are found in the 300 Area. The silt-dominated or rhythmite facies found elsewhere on the Hanford Site are absent.

The gravel-dominated facies consists of basalt-dominated granule-to-boulder gravel (Swanson et al. 1992). The facies displays massive bedding, planar and low-angle bedding, and large-scale planar (or foreset) crossbedding. Large-scale scour surfaces also are found. These gravels commonly have little matrix material and, thus, form an open-framework fabric. These open-framework gravels directly overlie Ringold Formation gravels that are significantly more cemented and compacted. Consequently, a sharp contrast in bulk modulus may exist across this contact, allowing reflection of acoustic energy. Hanford formation gravels were deposited by high-energy flood waters in main cataclysmic flood channelways.

The Hanford formation sand-dominated facies in the 300 Area consists of plane-laminated, fine- to coarse-grained basaltic sand with minor gravel (Swanson et al. 1992). Channel-fill sequences may occur locally. Deposition of this facies occurred adjacent to main flood channelways and during waning flood stages.

Where human activities have not modified the ground surface, eolian sands commonly occur. The eolian sands vary greatly in thickness and are Holocene in age.

9 0 1 3 9 0 4 1 7 9 7

2.2 PREVIOUS SEISMIC SURVEYS

Although there have been numerous refraction surveys conducted at the Hanford Site over the years, this discussion is limited to a brief review of past seismic reflection studies. (Donaldson 1963, Heineck and Beggs 1978, Myers et al. 1979, Holmes and Mitchell 1981, Berkman 1984, Berkman 1986, Kunk 1986). These earlier surveys were conducted to study the basalts, to evaluate the method for mapping the basalt/sediment interface, and to determine local basalt structure. None of these studies focused on delineating the sediments. It is important to study the previous work in this area to understand the challenges of this current study.

The seismic reflection method was tested for the Basalt Waste Isolation Project (BWIP) to map the basalt down to the Umtanum flow of the Grande Ronde Basalt (Heineck and Beggs 1978). The data shown in Figure 4 display the basalt starting at 0.15 seconds ramping up onto Gable Mountain. There are, however, no reflections depicting the shallower sediments. In 1979 and 1980, an additional 195 line km (121 line mi) of data were collected sitewide (Myers et al. 1979, Holmes and Mitchell 1981).

Part of this data set was reprocessed for the BWIP to study the upper basalts. The seismic sections were somewhat improved, though did not delineate the suprabasalt stratigraphy (Berkman 1984). Consequently, there was no delineation of shallow sediment stratigraphy.

Additional seismic reflection data was collected in 1985 by BWIP to determine the best acquisition and processing parameters in the area. This was a more involved study that included testing three different energy sources and various other acquisition parameters (Kunk 1986). Early results are shown in Figure 5.

The shallowest coherent reflector near 0.1 second is correlatable to the base of the Plio-Pleistocene layer. Once again, the main goal was to map the basalt top, which is located at about 0.27 seconds near shot point 120. Reflectors can be discerned within the Ringold Formation, but none can be traced across the section. There is no resolution of shallower strata.

These data were reprocessed several times (Berkman 1986, Kunk 1986). Although the character of the coherent reflections within the basalts improved, definition of the shallower strata did not.

3.0 SEISMIC REFLECTION STUDIES

3.1 INTRODUCTION

This section describes data acquisition and processing procedures (detailed description in Appendix B) and results for the seismic reflection testing. The interpretation of the data is presented in Chapter 4.0. There are several problems associated with shallow seismic reflection surveys, especially those conducted in unconsolidated media. The first problem addresses resolution of the subsurface geologic boundaries. Theoretically, to

9 3 1 9 0 4 1 7 9 8

resolve or "sense" a subsurface geologic feature or target, the wavelength of reflecting acoustic waves should be no longer than one-quarter the dimensions of this target. Otherwise, the data cannot resolve and image the feature of interest.

At the Hanford Site, one full wavelength is a more realistic value due to the noisy nature of the data. Therefore, to realistically detect the water table separately from the Hanford/Ringold contact, the seismic wave should have a wavelength no greater than the actual separation. Since the seismic wavelength is dependent on the frequency of the acoustic source and acoustic velocity of the geologic media, for a geologic environment which has a velocity of approximately 610 m/s (2,000 ft/s), a 3-m (10-ft) wavelength equates to a frequency of 200 Hz. To obtain this degree of resolving power, the seismic source must generate energy that has maximum energy near the dominant frequency of 200 Hz. Thus choosing the correct source is critical.

Another problem of shallow seismic surveys concerns attenuation of the energy in unconsolidated media. The magnitude of velocity is dominated by the bulk modulus of the propagating media. The bulk modulus measures the compressibility of the geologic material. A medium with a low velocity is very compressible, and much of the acoustic energy is dissipated as work to allow propagation. Consequently, the depth of penetration is not great. This problem is amplified for dry soils because air is quite compressible while water is almost incompressible. Thus, the seismic source must have enough energy to get through the very shallow, low-velocity sediments.

Three high-frequency sources were tested for this seismic survey. Their amplitude spectra were compared to quantify the amount of energy versus the frequency range that each source could generate at the 300 Area. Data were collected using each source, and a comparison was made between the two most favorable sources.

Proper design of the acquisition configuration is also important to increase the signal-to-noise ratio and also to increase resolution by determining the best acquisition parameters, such as receiver spacing, length of the spread, etc. The nature of shallow reflections in unconsolidated media is extremely site dependent. The same source and acquisition parameters used successfully at one site may produce unsatisfactory results elsewhere. Thus, the seismic source and acquisition parameters had to be field tested for application at the 300 Area. This aspect of the survey is discussed in the next section.

Finally, a variety of complex, quantitative procedures are applied to the data during processing. Decisions of what procedures to apply and how to apply them greatly affect the resulting data. Part of this processing involves a velocity analysis. Detailed sonic borehole logs are often acquired near each seismic line to correlate coherent reflectors to actual geologic horizons. However, these detailed data were unavailable for this survey, and other methods of velocity control were applied.

3.2 DATA ACQUISITION

Field testing of seismic sources and survey geometries is necessary to best match the qualities of the overall data with the project goals and logistics of the survey. Seismic data acquisition tests were conducted at two locations (see Figure 2). A flat area near well S27-E9 in the southwestern part of the study area was used, because of its low topographic relief and nearby borehole data (well 399-5-2). The water table is shallow in this area, which also made the site attractive. The second test site was just north of the 618-7 burial ground near well 8-5 along line 4-5. This area is also relatively flat. This test site is near the center of the study area, which also contributed to its selection.

The goals of the testing were to evaluate source and receiver configuration trade-offs with respect to the objectives of the study. The two main lithologic targets were the Hanford/Ringold contact and the lower mud horizon of the Ringold Formation. Source considerations included the nondestructive and nonintrusive nature of the source, as well as mobility, frequency content of the energy, and amplitude of the energy.

3.2.1 Seismic Source Study

Seismic sources come in a variety of packages. Output energy, frequency, repetition rate, repeatability, availability, cost to operate, mobility, and destructive/nondestructive nature are some of the variables considered in choosing a seismic source.

As the depth of investigation increases, the amount of energy required increases, but the resolution is reduced. Additionally, the lower the frequency, the better the signal propagation, but resolution also decreases with lower frequency. Therefore, the trade-off between depth and resolution must be carefully assessed. Three impulsive seismic sources were tested at this site: the sledge hammer, the Betsy Seisgun Source¹, and the Dinoseis². The sources were tested at two locations to sample different geologic conditions in different configurations to determine the best overall source.

As shown in Figure 6, the Betsy Seisgun and sledge hammer are similar with energy peaks near 45, 70, and 125 Hz; however, the sledge hammer has a slightly wider band width and slightly more amplitude in the high frequencies than the Betsy. The Dinoseis has energy peaks at around 35 and 45 Hz (Figure 7) that will limit its ability to resolve stratigraphic horizons. On the other hand, it has an order of magnitude more energy at frequencies below 75 Hz and a slightly lower amplitude at the higher frequencies than the other two tested sources. Consequently, energy from the Dinoseis can be expected to propagate more deeply into the subsurface.

The Betsy Seisgun was the most repeatable source. This means that the input signal was nearly the same each time the gun was fired. Although the

¹Betsy is a trademark of Betsy Seisgun, Inc.

²Dinoseis is a trademark of Atlantic Richfield Company.

sledge hammer had similar repeatability, it was not tested extensively. Unfortunately, the repeatability of the Dinoseis was not as reliable, primarily due to the variable burn time of the combustible chamber.

Given the Betsy Seisgun and the sledge hammer's similarity, the Betsy was chosen for lines 7-8, 4-5, and 7-4 because of its greater amplitude and better repeatability. The Dinoseis was chosen for the remainder of the survey because it was the only source capable of producing enough energy to consistently penetrate to the lower mud and basalt horizons.

Figure 8 shows two seismic line segments that intersect at borehole S22-E9 (see Figure 2). The Betsy was used as the source for the segment on the left, while the Dinoseis was used for the segment on the right. The trade-off of resolution versus depth of penetration can be seen quite well. The Betsy data reveal two reflectors near 0.05 second. The Dinoseis data only reveal one reflector, which is a combination. This is due to the higher frequency of the Betsy data, which yield higher resolution. The Dinoseis data, however, more clearly reveal a reflector near 0.125 second. This reflector is very weak in the Betsy data and would be difficult to use for interpretation, as seen in the Betsy data.

3.2.2 Acquisition

Initially, a symmetrical split-spread configuration with shots and receivers located every 3.05 m (10 ft) was used (Figure 9[a]). After early data processing, it was determined that this configuration was not "tight" (close-spaced geophones) enough. The acquisition configuration was then altered to having the geophones at 1.5-m (5-ft) intervals and the shot points every 3.05 m (10 ft [Figure 9(b)]).

The acquisition of the seismic data was primarily driven by the drilling of boreholes. Initial testing and data acquisition were done near well S27-E9 in the southwestern corner of the study area (see Figure 2). This was the first well to be drilled. Data were acquired by jumping from line to line to keep away from noise sources. Noise sources included the vibration noise associated with excavation activities at the 618-9 burial ground and 316-5 processing trenches and well drilling. Attempts were also made to acquire data over well sites before well-site preparation activities began. Moving back and forth from line to line does not affect the overall data integrity; however, long-term activities at well 8-5 did prevent the acquisition of data in the immediate area of the well.

Three lines of seismic data were acquired using the Betsy Seisgun (lines 7-4, 7-8, and 4-5). The other lines were acquired using the Dinoseis as the seismic source, except for the far eastern end of line 8-1. The area near well S29-E16 was acquired using the Betsy to acquire the data before the well site was improved for the drilling. The remainder of line 8-1 was acquired using the Dinoseis source.

9 3 1 1 9 0 4 7 9 0 1

3.3 DATA PROCESSING

Once the data are acquired, they are subjected to rigorous data processing schemes. The processing steps and parameters used must be optimized to determine which sets produce the best final stacked seismic section. The reliability of the geologic interpretation depends on the accuracy of the processing sequence and parameters used. The processing sequence used for these data is discussed in Appendix B.

3.3.1 Velocity Analysis

The most critical and difficult processing step involves the determination of seismic velocities. Adequate knowledge of the two-dimensional velocity structure in the vicinity of a seismic reflection line is important for three reasons. First, to apply a proper, normal-moveout correction for each coherent reflector, the processor must assign a realistic velocity to that arrival. Without a prior knowledge of this velocity data, it can be difficult to stack the reflectors coherently. Second, specific reflectors must be related to geologic horizons, such as formation boundaries during the interpretation stage. This requires knowledge of the vertical velocity gradient at some point along the seismic survey line. Third, if it is desirable to map a horizon in depth and not in time, then adequate velocity information is needed.

There were four ways information was obtained to help contain the acoustic velocity gradient. Ideally, the preferred method is to obtain a sonic log in a nearby borehole. In the 300 Area, no borehole data have been acquired. However, several borehole surveys do exist near the reference repository location, and the results of these earlier surveys were used to initially constrain velocities for various horizons (Dresser 1985, Odegard and Mitchell 1987, Kunk 1986). In addition, velocity data derived from vertical seismic profiling surveys conducted by Dresser (1985) and Kunk (1986) in the Western Cold Creek syncline indicate the middle section of the Ringold Formation may have velocities approaching those of basalt (e.g., above 3 km/s (10,000 ft/s)). However, stacking velocities in the 300 Area for the Ringold Formation were seldom found to be that high. This is due to less cementation in the 300 Area.

The second source of velocity control is from the refraction survey. These data were used primarily to guide the velocity selection for processing shallow reflection data. Refraction statics were also tested, but did not prove useful for final processing.

The most reliable velocity estimates were made by fitting hyperbolic normal-moveout curves to the shot point-sorted and common midpoint-sorted data gathers. The selection of these velocities was aided through velocity semblance plots, time-versus-velocity plots, and velocity-contour displays.

Finally, during the interpretation analysis, interval velocities were calculated from stacking velocities to obtain depth estimates. These stacking velocities were adjusted until major reflectors could be correlated to

reasonable geologic horizons. This final correction was done in the immediate vicinity of borehole locations. Velocity/depth profiles are presented in Appendix C.

4.0 DATA ANALYSIS/INTERPRETATION

4.1 INTRODUCTION

There were two primary objectives proposed for this study. The first goal was to determine the usefulness of high-resolution, shallow seismic reflection surveys to delineate and map major geologic horizons in the subsurface. The second goal involved locating a possible major paleochannel incised into the top of the Ringold Formation. In this chapter these goals are specifically addressed. In particular, data and plausible interpretations are presented to evaluate how well significant geologic boundaries can be related to coherent acoustic reflectors that can be mapped.

Although results from GPR and the refraction survey helped to optimize reflection acquisition and to provide velocity control for processing, the seismic reflection data were used to evaluate how well the objectives were met. Consequently this chapter is focussed on an interpretation of the reflection data.

This chapter is divided into three additional sections. The first section describes briefly the manner in which reflectors were matched to specific subsurface boundaries. Limitations of the data are determined, and assumptions associated with the following interpretations are stated. In general, the quality of the reflection data is discussed while in the next two sections, examples of the mapping capability of the data are shown for the Hanford/Ringold unconformity and for the lower Ringold Formation mud. The existence of the paleochannel is addressed under the section on the Hanford/Ringold contact.

Finally, for the purposes of discussions, reflection data are presented in Appendix D for lines 3-5, 2-3, and 4-2. The remaining survey lines are included in a comprehensive data package (WHC-SD-EN-DP-059, Rev. 0 [Kunk 1992]). On each line, wells and tie points are located, and geologic interpretation of reflectors is included. Also, the depth to mapped reflectors at well ties are labelled.

4.2 METHODOLOGY

Normally the relationship between a geologic horizon and a reflector is determined from sonic logs collected in a nearby borehole. In lieu of quantitative control, seismic reflectors were tied to borehole logs by adjusting the stacking velocities until a reasonable match was obtained for the Hanford/Ringold unconformity and the top of the lower Ringold Formation mud. In the 300 Area, the water table is within a few feet of the Hanford/Ringold contact; thus, this was considered one reflector. The

9 8 1 0 9 0 4 1 2 0 3

difference between borehole depths and seismic estimates was less than 3 m (10 ft) for ties to the Hanford/Ringold contact and less than 4.6 m (15 ft) for the lower mud. Lines were tied to each other at intersection points, providing control for those lines with no close wells (see Figures D-1, D-2, and D-3).

Several limitations are placed on the data for various reasons. The frequency of the source signal restricted the resolution of the data. The average velocity for the Hanford/Ringold contact is about 580 m/s (1,900 ft/s), which equates to 7.6 m (25 ft) of resolution for a frequency of 75 Hz. Similarly, resolution for the lower mud appears to be about 12 m (40 ft). Thus, it is not possible to map the water table separately from the Hanford/Ringold contact. This is also true for the lower mud which is within 9 m (30 ft) of the basalt. However, at places double wavelets can be observed that may represent a separate reflection for the water table versus the Hanford/Ringold contact. Figure 10 displays a section of line 3-5 where it intersects well 1-18C at common midpoint 470. Depths from the borehole log are plotted as two-way travel times for the water table and the Hanford/Ringold contact. As can be seen by the distinct double wavelet in Figure 10, in this region it was possible to obtain high-frequency data that could distinguish these two horizons.

Another limiting factor concerns the energy of the source that affects the penetrating depth of the acoustic signal. Since high-frequency seismic sources generate low-energy signals, it becomes increasingly more difficult to obtain coherent reflectors from depth. Given the combination of the Dinoseis source and the unknown filtering function of the subsurface at the 300 Area, an image of the lower Ringold Formation mud was not always seen. As a result, spatial control on the lower mud was not as detailed as that for the Hanford/Ringold contact.

For the data collected along line 1-3 central (see Figure 2), one unique problem did exist. Results from the GPR survey indicate that this area has been extensively disturbed culturally, and the seismic reflection data are also very poor. This degradation of the data is possibly due to inadequate coupling and rapid, shallow attenuation. However, the data from line 1-3 central was not interpreted.

Several assumptions were made during the interpretation process. First is that one reflector represents both the water table and the Hanford/Ringold unconformity. The same assumption is made for the lower mud and the top of the basalt. Although this is not always observed, for the purposes of mapping structure, it is simpler. Furthermore, all coherent, continuous horizons were considered to be reflectors and not refractors. Also, unless a lower reflector appeared to "ghost" an earlier arrival or exact multiple arrival times were observed, no checks were made for multiples. If there was doubt, data were not interpreted for that immediate area.

Frequently seismic data are mapped in time because lateral location of features is more important in geologic interpretations than true depth for hydrocarbon applications. However, the control data from borehole logs for this feasibility project is in depth; thus, travel times were converted into feet. When rapid or extreme velocity changes resulted in loss of data coherency, depth estimates were not mapped in this area. Otherwise, it was

9 3 1 2 9 0 4 7 3 0 4

assumed that relief could be mapped to within 3 m (10 ft) for the Hanford/Ringold contact and to within 6 m (20 ft) for the lower mud reflector. Finally, if a structural trend or feature could be mapped and followed on more than one line, it was given more credence in the discussion.

4.3 THE HANFORD/RINGOLD UNCONFORMITY

The interpretation of the Hanford/Ringold unconformity was combined with borehole log depths and is presented in Figure 11. As a comparison, the structure map based solely on well control is shown in Figure 12. Seismic lines 7-8 and 8-1 were not included in this interpretation.

Several points should be made regarding the Hanford/Ringold reflector (see Figure D-1). This reflector tied in very well with borehole depths usually to less than 2 m (7 ft). The depth from log control to the Hanford/Ringold contact is generally around 12 m (40 ft) in this area, so this is a very shallow horizon. The reflector is also easily recognized from line to line and thus readily mapped. Interval velocities are generally 580 to 610 m/s (1,900 to 2,000 ft/s) with very little lateral variation. This lack of change in the velocity allows greater confidence in the depth estimates and the resulting structural relief.

A comparison between Figures 11 and 12 allows the extension of structural control to be appreciated. The interpretation of this contact as displaying a coalescing, braided stream configuration is confirmed, because the pattern of small, northwest-trending drainages does appear to continue to the north of well 1-18C. Also the east-west-trending drainage in the southern part of the area can be extended to the western edge of the study area.

One important result of mapping the Hanford/Ringold contact is that the data do not show any north-south-trending ancient river channel as proposed in Lindberg and Bond (1979). Between well control and the extension of subsurface coverage with the seismic data, it appears that no ancient river channel existed in the 300 Area. It is possible that one of these small drainages was excavated and appeared like a river channel.

The results of this analysis of the seismic data does show that the Hanford/Ringold contact in the 300 Area can be detected adequately using shallow, high-resolution seismic data. Certainly this horizon can be mapped to produce reasonable results. The data even suggest that with a higher frequency source deviations of the water table from the Hanford/Ringold contact may be detectable and mapped. This data would also be useful to control structure for porous flow modeling to aid in understanding fluid migration routes.

4.4 THE LOWER MUD/BASALT REFLECTOR

Generally, the data quality for the lower mud reflector is not as good as for the shallow horizons. Although the resolving power of the input frequency affected the ability to discern the lower mud separately from the basalt, the energy of the source has also impacted the lower mud interpretation. Not enough energy is returning from these depths of 30 to 52 m (100 to 170 ft) to

consistently see this horizon. Also, the reflector is not seen as a continuous feature along any line. This lack of continuity may have more than one cause. For example, at places the stacking velocities change radically, degrading the data coherency, while other places appear as a distinct decrease in amplitude. These regions may be related to changes in the physical properties of the mud. Consequently, the results are more interpretive. However, the error of the ties between well control and the seismic reflectors is within 4.6 m (15 ft), which indicates that use a higher energy source with better velocity control will obtain a distinctly improved signal.

In Figure 13 the seismic interpretation is combined with the borehole depths to produce a structure map on the top of the lower mud. The contour interval is 6 m (20 ft) except in the northeast of the study area where the data were more coherent. Here the contours are at 3 m (10 ft). This is justified since the tie of line 3-5 to well 1-18C is close. Only the northern survey lines were included in the structure map, because of difficulties in tying wells to the southern lines.

For comparison, the structure map using borehole logs alone is shown in Figure 14. On seismic lines 3-5 and 2-3, interpretation of the data confirms the north-trending structural high seen in Figure 14 (see Figures D-1 and D-2). The feature is mapped from lines 3-5 to 2-3, resulting in a more detailed configuration. Notice that the relief appears to increase to the north and that the difference in elevation goes from close to 3 m (10 ft) near well 1-16C to about 7.6 m (25 ft) further north. Since the lower mud is only 3 m (10 ft) thick in well 1-18C (Swanson et al. 1992), an important question concerns possible pinching out of this unit that would allow vertical communication between the unconfined and lower confined aquifer. There are several scenarios that could explain the existence of this high block in the basalt beneath the mud. First, it is an artifact left after early Ringold Formation erosion, or, alternatively, the block has been faulted up. Regardless, it is unlikely that this 3-m (10-ft) mud extends over this rise as a continuous unit.

Although the data to the west are not as easily mapped, interesting features are also discernable. In particular, a broad rise seen on the northeast end of line 4-2 extends into a very distinctive trough-like feature to the southwest (see Figure D-3). This major feature is about 200 m (650 ft) wide with a maximum drop of 15 m (50 ft). The data quality does not allow the change in elevation to be clearly characterized (e.g., faulted, gradational but continuous, etc.); however, the major change in relief occurs over approximately 13 m (42 ft), indicating a gradual gradient. Generally seismic features should be mapped from line to line to be given credence as a real feature. Unfortunately, there was only sparse control for the lower mud reflector achieved from lines 8-5-2 and 4-5. Consequently, the orientation of this low is unknown. However, the velocity variation was carefully checked during the mapping process to reduce the possibility of this being a spurious structure.

Even though the nature of the Middle Ringold Mud Units was not addressed in this study, corresponding reflectors can clearly be seen in all the data. For example, on line 3-5 shown in Figure D-1, the strong reflectors between the Hanford/Ringold contact and the lower mud reflector represent the middle muds. These reflectors show a complex pattern of rapid pinch outs with an

interfingering, onlapping-offlapping character that would be expected off an overbank flood facies. This observation agrees with the data from the borehole logs (Swanson et al. 1992).

5.0 CONCLUSIONS

In summary, much effort was put into the geophysical investigation for the 300-FF-5 Operable Unit, and a better understanding of the geologic variability within the study area has been derived. Three geologic horizons were mappable with the geophysical methods used. A Holocene soil horizon, typically 0 to 4.6 m (15 ft) below the surface, appears to separate eolian sands and silts from fluvial deposits from the Missoula floods and Columbia River. The Hanford formation/Ringold Formation contact and the lower mud unit of the Ringold Formation are the deeper horizons mapped. The top of basalt was not detected consistently enough to map.

The water table is within a few feet of the Hanford/Ringold contact thus they were considered one reflector and were mapped accordingly. The data supports northwest-trending braided stream configuration north of well 399-1-18C and an east-west-trending drainage in the southern portion of the survey area, consistent with the most current geologic data. However, the data do not support a north-south-trending river channel as proposed by Lindberg and Bond (1979). Several, shallower, small drainage features were detected with the GPR data. It is possible that a similar small drainage was misinterpreted as a river channel.

Even though the lower mud unit was detected with the seismic data, the resolution and mapping of the unit was not as detailed as the Hanford/Ringold contact and showed considerable variation from line to line and, in many cases, within a given line. Interpretations on the source of these variations remain elusive without supporting detailed geologic and geophysical information from other sources.

The seismic refraction data were used primarily for bracketing velocity values for the seismic reflection processing. Deriving geologic structure from the data was not seriously attempted due to the uncertainties in determining first-arrival times. The errors associated with the first-arrival times from the depths of interest were greater than the time variations expected from the signals generated from geologic structure. The deeper refraction information ranged from 23 to 30 m (75 to 100 ft).

6.0 RECOMMENDATIONS

The results from the GPR, EMI, and the refraction survey provided valuable information on the shallower sediments for processing. However, the seismic reflection data were the primary data used to evaluate how well the

7
0
0
4
1
9
0
9
6
9

objectives were met. One of the primary objectives was to determine the feasibility of shallow, high-resolution seismic reflection surveys to delineate and map major geologic horizons.

Shallow, high-resolution seismic reflection work has proved to be extremely labor intensive in this geologic environment, both in data acquisition and processing. Attention to every detail of both acquisition and processing are essential. Standard "production" data acquisition and processing do not apply here.

These data were collected and processed with this philosophy as the guiding factor. The results were a significant improvement over past seismic studies performed on the Hanford Site and the results reflect this level of effort. However, an even greater "attention to detail" would increase the resolving power of the method.

Several factors should be considered in future seismic reflection surveys. First, and extremely important, is the need for detailed velocity information. The highly variable velocities, both laterally and vertically in this glacio-fluvial environment, must be better understood for detailed, shallow seismic processing. Frequent check-shot surveys, vertical seismic profiling, and possibly cross-hole surveys would be extremely useful. Vertical seismic profiling walk-away surveys are recommended to gain insight into the ray paths actually taken by the seismic energy in conventional seismic reflection surveys.

Any method to improve signal-to-noise ratios is always welcome. Cultural noise is a concern for any seismic survey, but particularly is a potential problem in close proximity to industrial sites such as the 300 Area complex. Data collection in the off-shift hours, such as weekend and nighttime, should be considered.

In the Hanford formation environment, the eolian deposits and Hanford formation sands and gravels particularly degrade the signal and often enhance the unwanted "noise." Reduction of shot-related noise, especially ground roll, must be minimized while increasing the percentage of desired signal propagated into the ground. One method for signal-to-noise enhancement includes burying/planting the geophones below the "cone of energy." This allows the earth to "filter" some of the unwanted signals. Applying in-field low-cut filtering is another way to reduce, electronically, some of the unwanted low-frequency energy. Significantly more geophone channels, to allow longer offsets, will allow wanted signal to reach the geophones before the "noise." Reflection geometries and geophone spacing must be studied to avoid spacial aliasing. The use of geophone and shot arrays should be tested thoroughly to determine if certain arrays could improve the signal-to-noise ratio.

Depending upon the objectives of the survey, various energy sources would be appropriate. In general, the shallow, high-resolution objectives anticipated for projects such as hazardous waste characterization would indicate high-frequency sources. Ideally, the sources should have minimal, unwanted lower frequencies and strong, repeatable high-frequency spectra.

Improvements in future data are possible, but will require additional field tests. First, as in the reflection work, much of the desirable seismic energy is attenuated in the eolian deposits. These deposits vary in thickness, but are on the order of a few to 4.6 m (15 ft) thick. Any technique to place the geophones and shots below this layer would yield large dividends in signal quality. Mapping the thickness of the eolian deposits is fast and relatively easy by GPR. This could be a way to define where to place geophones and shots.

Refraction theory requires assumptions such as increasing velocity with depth. This assumption is not routinely valid in the Hanford formation environment. The "hidden" low-velocity layers will reduce resolution of features and layers beneath the low-velocity layers.

Velocity contrasts and layer thickness are other important factors for defining refraction usefulness. Gradational boundaries and thin layers are not normally detectable by refraction methods, especially as depth increases. Both of these factors are significant in this study. The relatively high and variable velocities in the Ringold Formation will make water table detection in the Ringold Formation difficult or impossible by refraction methods, especially if the water table is at or near the Hanford/Ringold contact or in the Ringold Formation.

Reliable depth-to-basalt information is doubtful because of the small velocity contrast between the basalts and the lower Ringold Formation. The Ringold Formation velocities can be as high as 3 to 3.6 km/s (10,000 to 12,000 ft/s), and basalt velocities can start in this same velocity range.

The GPR method was very successful at mapping the thickness of eolian sand dunes and a Holocene soil horizon that is found consistently throughout the Hanford Site. The standard equipment and techniques that were applied achieved an investigative depth of 3 to 4.6 m (10 to 15 ft). A greater depth of investigation may be achieved in portions of the site using new and improved equipment. Data acquisition and signal processing similar to standard seismic reflection surveying are being developed for deeper and higher resolution work. Developments in this industry should be monitored.

The EMI method is good for detecting lateral conductivity variations. However, unique interpretations on the source of these variations remain elusive without supporting detailed geologic and geophysical information from other sources.

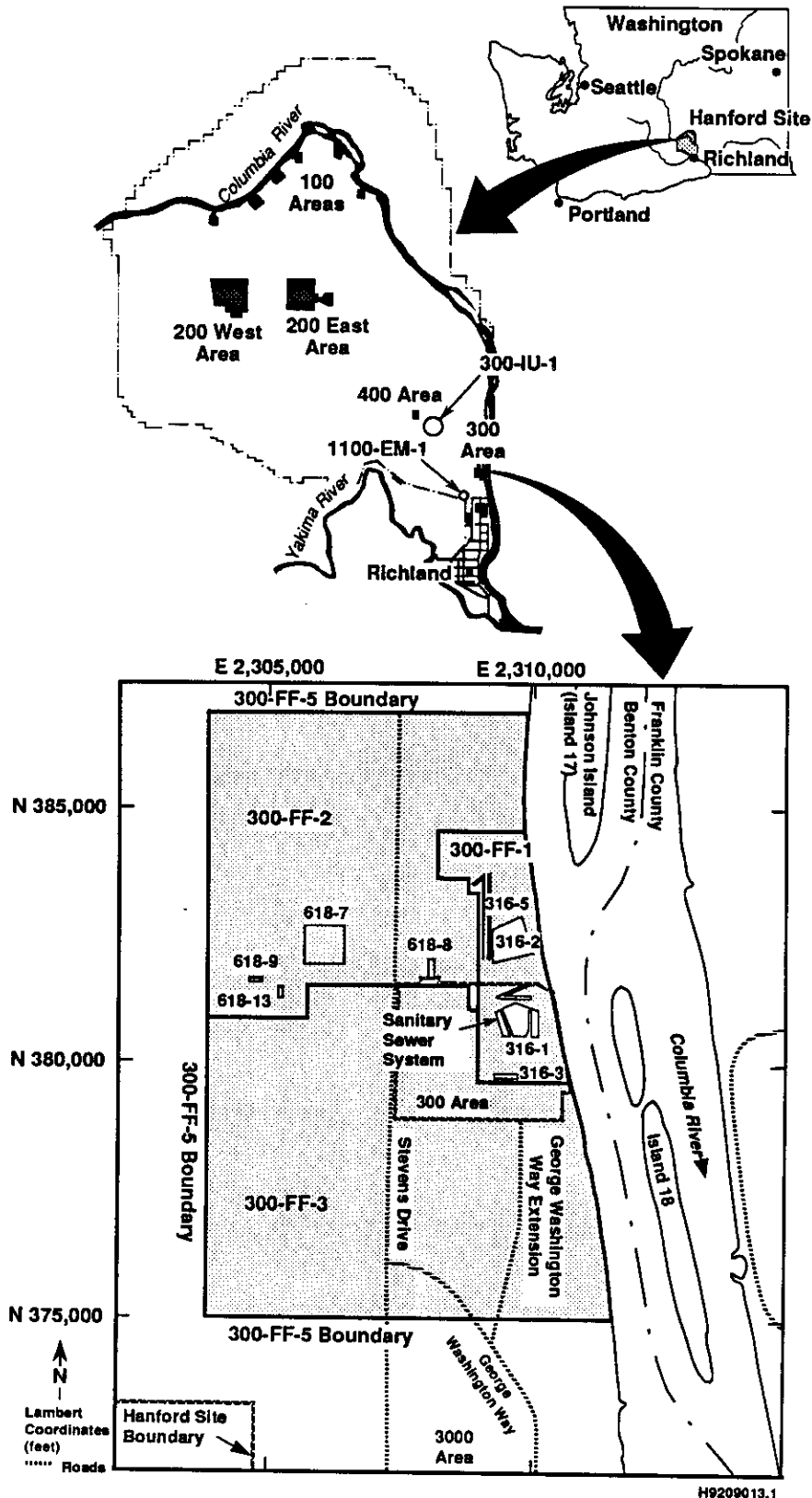
7.0 REFERENCES

- Berkman, E., 1984, *Reprocessing and Interpretation-Seismic Reflection Data, Hanford Site, Pasco Basin, South Central Washington*, SD-BWI-TI-177, Rockwell Hanford Operations, Richland, Washington.
- Berkman, E., 1986, Reprocessing of Two Mile Seismic Test Line, Hanford Site, Emerald Exploration, Austin, Texas.

- 9
1
0
0
4
7
0
1
0
- Dobrin, M. B., 1976, *Introduction to Geophysical Prospecting*, McGraw-Hill, Inc., New York, New York.
- DOE, 1988, *Consultation Draft, Site Characterization Plan, Reference Repository Location, Hanford Site, Richland, Washington*, DOE/RW-0164, Vols. 1-9, Office of Civilian Radioactive Waste Management, U.S. Department of Energy, Washington, D.C.
- DOE-RL, 1990, *Remedial Investigation/Feasibility Study Work Plan for the 300-FF-5 Operable Unit, Hanford Site, Richland, Washington*, DOE/RL 89-14, U.S. Department of Energy-Richland Operations Office, Richland, Washington.
- Donaldson, J. A., 1963, *Seismic Survey, Hanford Atomic Products Operation, Richland, Benton County, Washington*, GEH-26275, Richland, Washington.
- Dresser, 1985, *Report of Borehole Seismic Analysis for Rockwell International RRL-5, -7, -8, -10, and -16, Benton County, Washington*, B066327, B066329, B066331, B066333, and B066335, Dresser Atlas for Rockwell Hanford Operations, Richland, Washington.
- Heineck, R. L., and H. G. Beggs, 1978, *Evaluation of Seismic Reflection Surveying in the Hanford Site, Benton County, Washington*, RHO-BWI-C-20, Rockwell Hanford Operations, Richland, Washington.
- Holmes, G. E., and T. H. Mitchell, 1981, "Seismic Reflection and Multi-level Aeromagnetic Surveys in Cold Creek Syncline Area," *Subsurface Geology of the Cold Creek Syncline*, RHO-BWI-ST-14, Rockwell Hanford Operations, Richland, Washington.
- Kunk, J. R., 1986, *Seismic Reflection Data*, B062650, DAP No. 03-00035, Walker Geophysical Company for Rockwell Hanford Operations, Richland, Washington.
- Kunk, J. R., 1992, *Data Package for Geophysical Studies in the 300-FF-5 Operable Unit*, WHC-SD-EN-DP-059, Rev. 0, Westinghouse Hanford Company, Richland, Washington.
- Ledgerwood, R., 1991, *Summaries of Well Construction Data and Field Observations for Existing 100 Aggregate Area Operable Resource Protection Wells*, WHC-SD-ER-TI-006, Westinghouse Hanford Company, Richland, Washington.
- Lindberg, J. W., and F. W. Bond, 1979, *Geohydrology and Ground-Water Quality Beneath the 300 Area, Hanford Site, Washington*, PNL-2949, Pacific Northwest Laboratory, Richland, Washington.
- Lindsey, K. A., 1991, *Revised Stratigraphy for the Ringold Formation, Hanford Site, South-Central Washington*, WHC-SD-EN-EE-004, Rev. 0, Westinghouse Hanford Company, Richland, Washington.

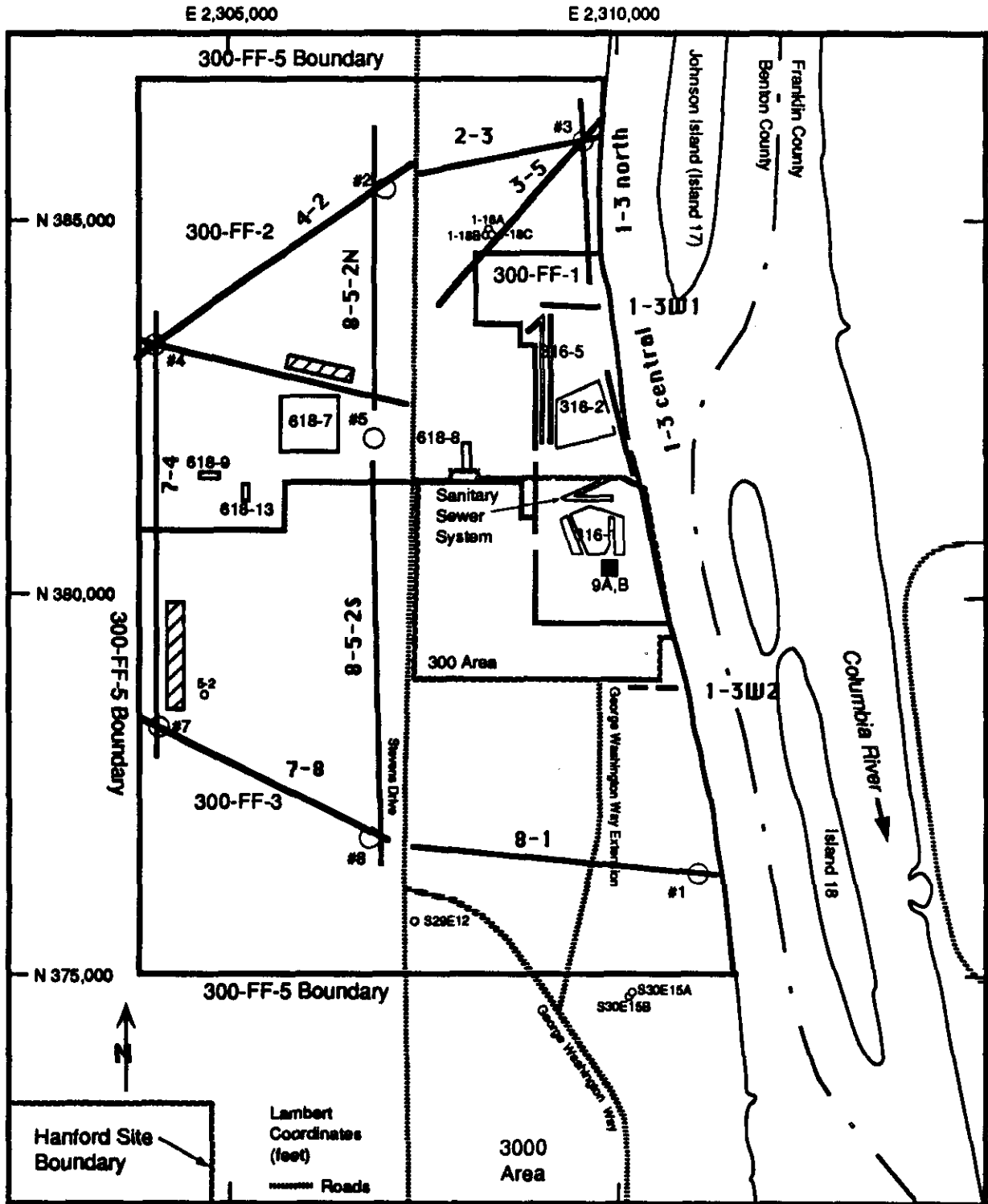
- Lindsey, K. A., 1992, *Geology of the Northern Part of the Hanford Site: An Outline of Data Sources and the Geologic Setting of the 100 Areas*, WHC-SD-EN-TI-011, Rev. 0, Westinghouse Hanford Company, Richland, Washington.
- Lindsey, K. A., B. N. Bjornstad, J. W. Lindberg, and K. M. Hoffman, 1992, *Geologic Setting of the 200 East Area: An Update*, WHC-SD-EN-TI-012, Rev. 0, Westinghouse Hanford Company, Richland, Washington.
- Lindsey, K. A., M. P. Connelly, and B. N. Bjornstad, 1991, *Geologic Setting of the 200 West Area: An Update*, WHC-SD-EN-TI-008, Rev. 0, Westinghouse Hanford Company, Richland, Washington.
- Myers, C. W., S. M. Price, J. A. Caggiano, M. P. Cochran, W. H. Czimer, N. J. Davidson, R. C. Edwards, K. R. Fecht, G. E. Holmes, M. G. Jones, J. R. Kunk, R. D. Landon, R. K. Ledgerwood, J. T. Lillie, P. E. Long, T. H. Mitchell, E. H. Price, S. P. Reidel, and A. M. Tallman, 1979, *Geologic Studies of the Columbia Plateau: A Status Report*, RHO-BWI-ST-4, Rockwell Hanford Operations, Richland, Washington.
- Odegard, M. E., and T. H. Mitchell, 1987, *Seismic Velocity Structure in the BWIP Reference Repository Location from Seismic Refraction and Vertical Seismic Profiling Data*, SD-BWI-TI-359, Westinghouse Hanford Company, Richland, Washington.
- Swanson, L. C., G. G. Kelty, K. R. Simpson, K. A. Lindsey, and S. D. Consort, 1992, *Phase I Hydrogeologic Summary of 300-FF-5 Operable Unit, 300 Area*, WHC-SD-EN-TI-052, Westinghouse Hanford Company, Richland, Washington.
- Tolan, T. L., S. P. Reidel, M. H. Beeson, J. L. Anderson, K. R. Fecht, and D. A. Swanson, 1989, "Revisions to the Extent and Volume of the Columbia River Basalt Group," in *Volcanism and Tectonism in the Columbia River Flood-Basalt Province*, Special Paper 239, Geological Society of America, Boulder, Colorado, pp. 1-20.

Figure 1. Site Location Map for the 300-FF-5 Operable Unit, 300 Area.



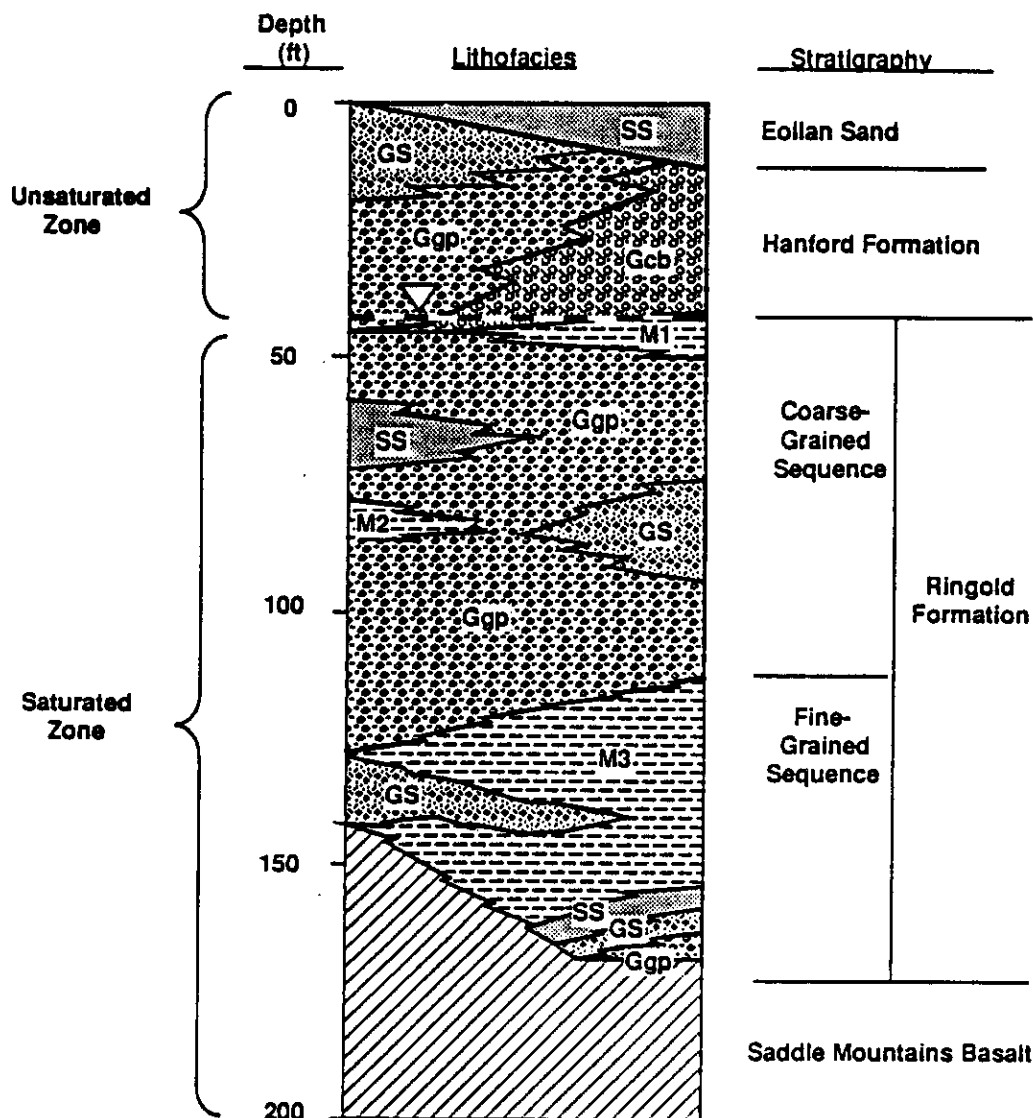
9 3 1 9 9 0 4 1 9 1 2





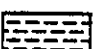

Figure 2. Seismic Line Locations.



2104060116

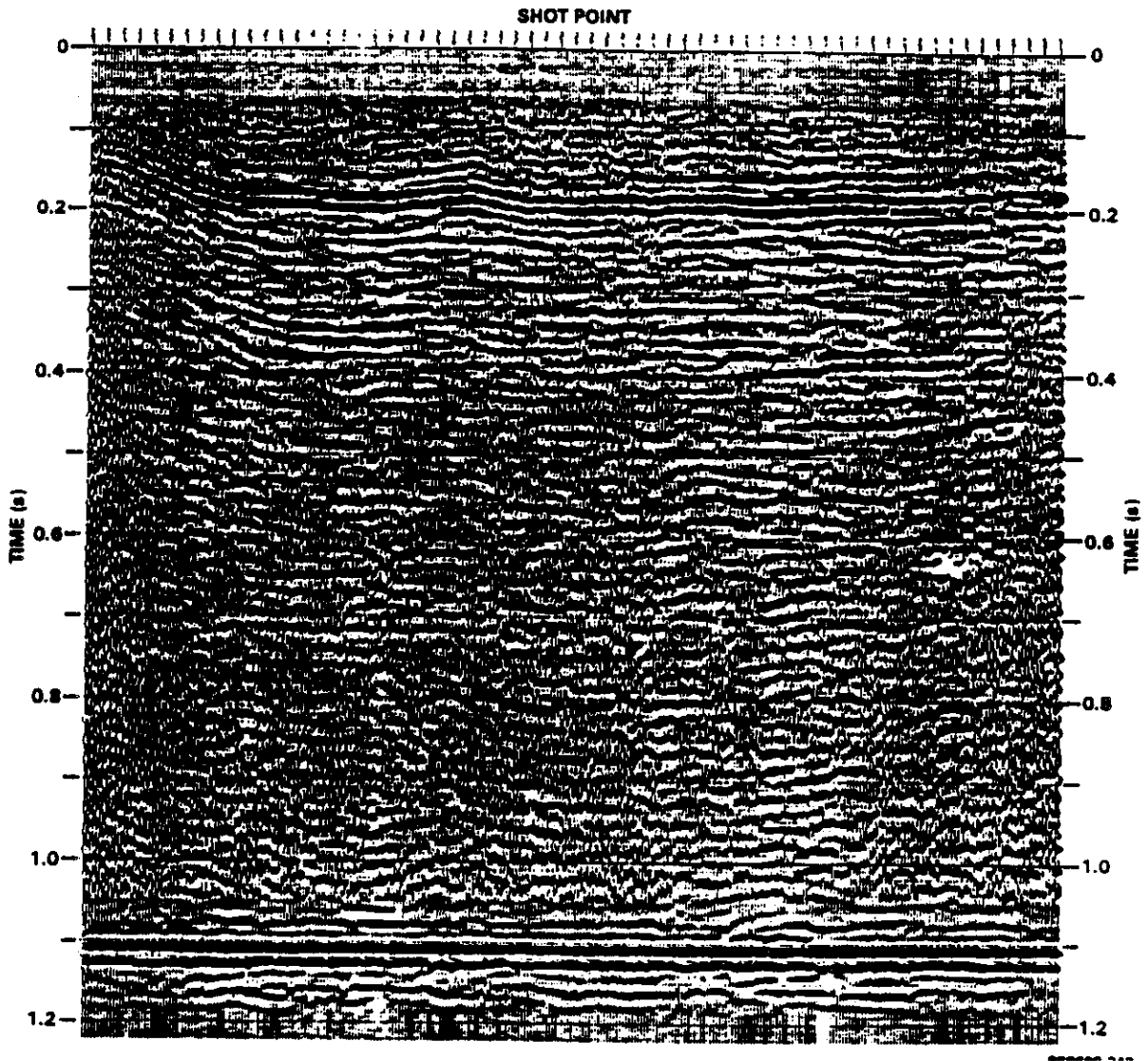
Figure 3. Generalized Stratigraphy From Lindsey (1992).



-  Gcb Sandy cobble-boulder gravel
-  Ggp Sandy granule-pebble gravel
-  GS Gravelly sand
-  SS Sand to silty sand
-  M Mud [silt and clay; M1, M2, and M3 are Ringold Formation mud units (informal names)]
-  Water Table

93129041914

Figure 4. Wavelet Processed Seismic Reflection Line From the Basalt Waste Isolation Project Test Survey Over DC-6 Well (Heineck and Beggs 1978).



9 3 1 9 0 4 7 0 1 5

9 1 1 2 9 0 4 0 8 1 6

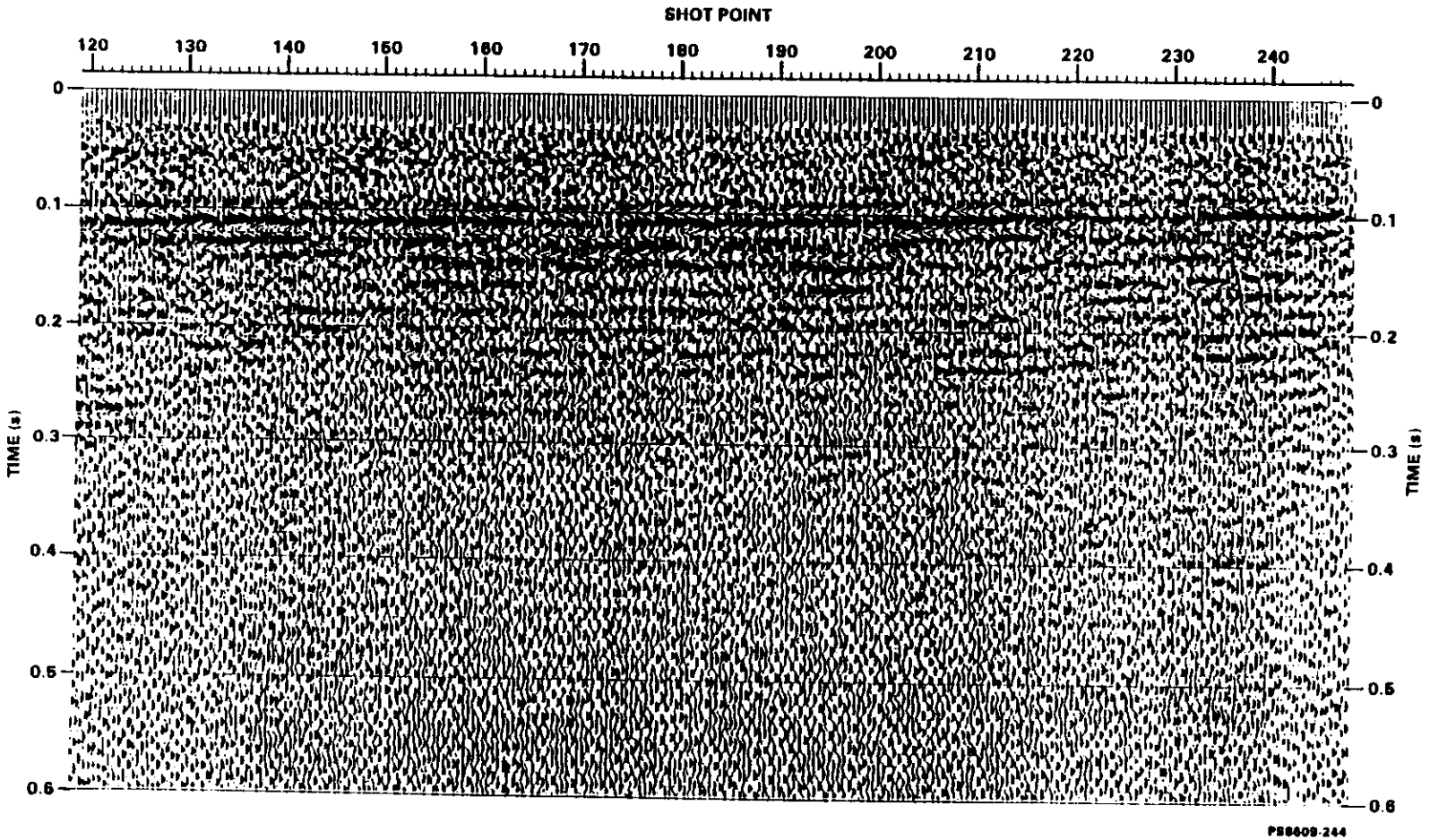
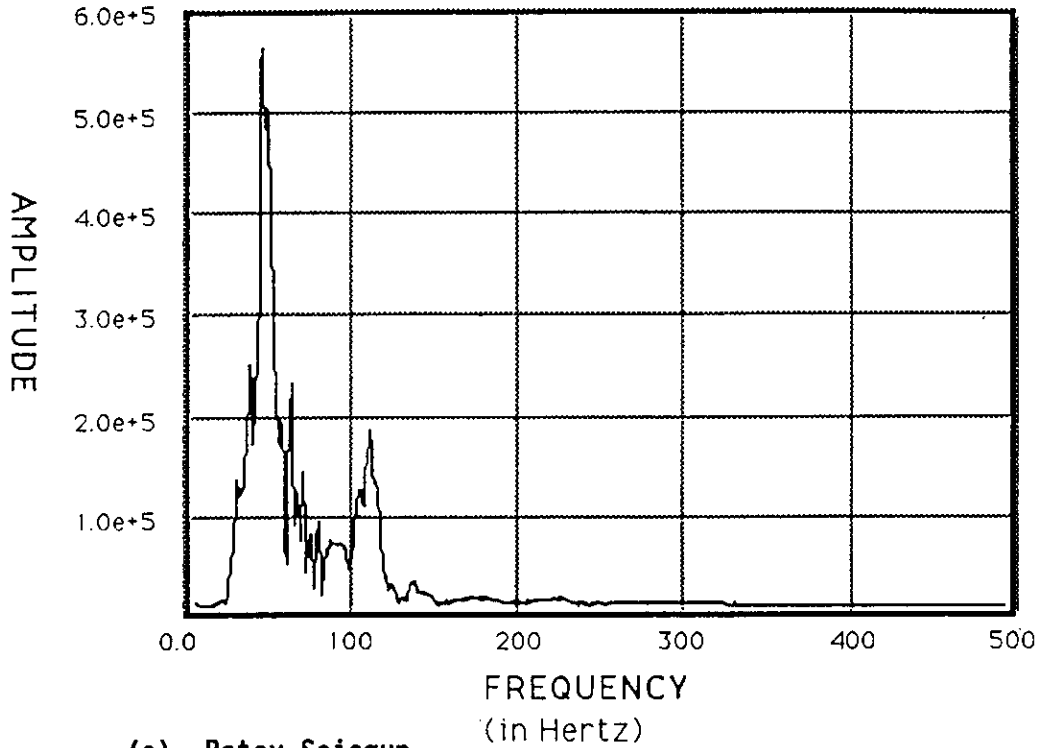
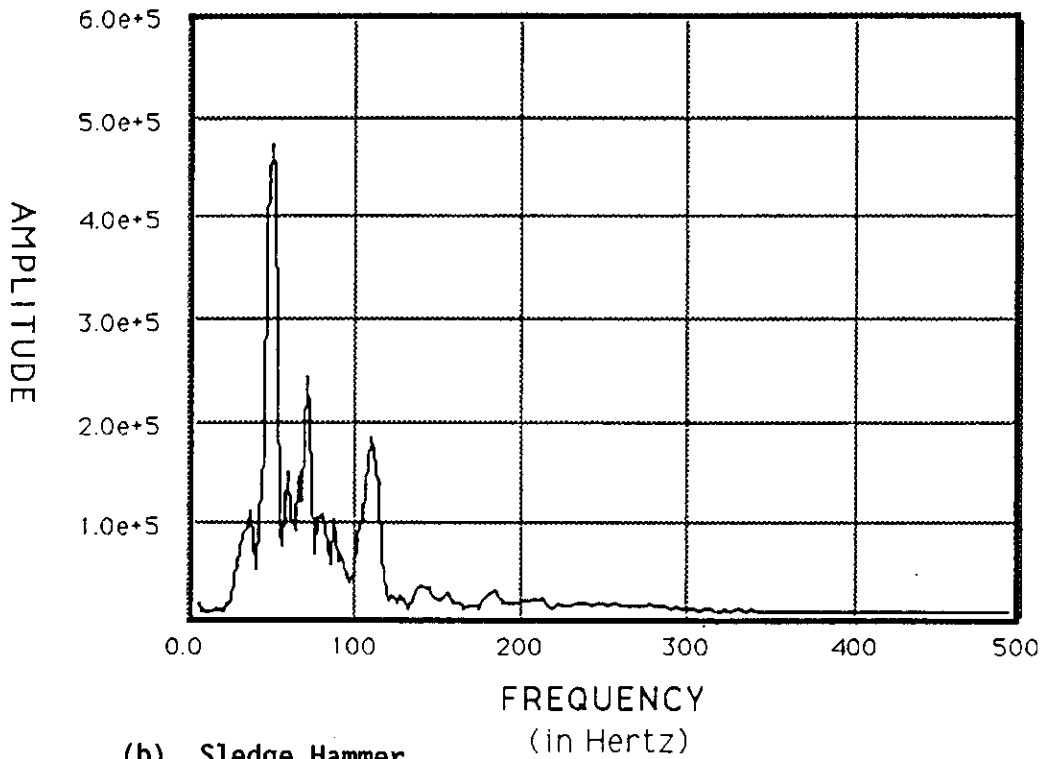


Figure 5. Initial Processing of Seismic Reflection Test Line in the "Basalt Waste Isolation Project Reference Repository Location" (Kunk 1986).

Figure 6. Amplitude Spectra of (a) Betsy Seisgun and (b) Sledge Hammer.



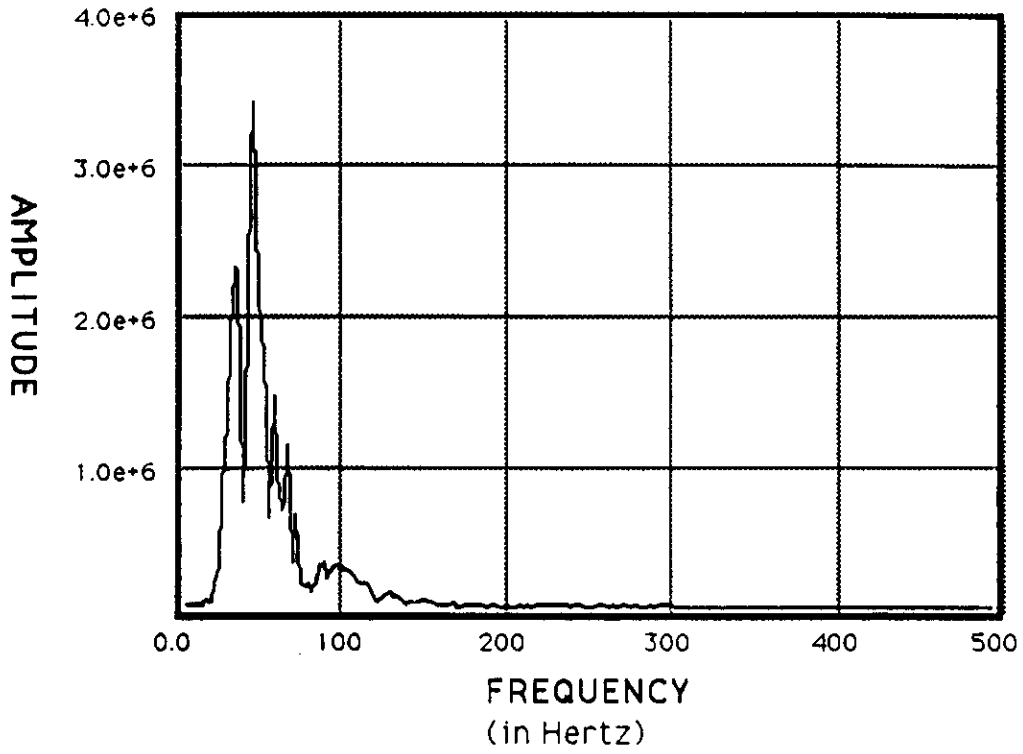
(a) Betsy Seisgun



(b) Sledge Hammer

9 1 1 9 0 4 7 2 1 7

Figure 7. Amplitude Spectra of the Dinoseis Source.



93109041818

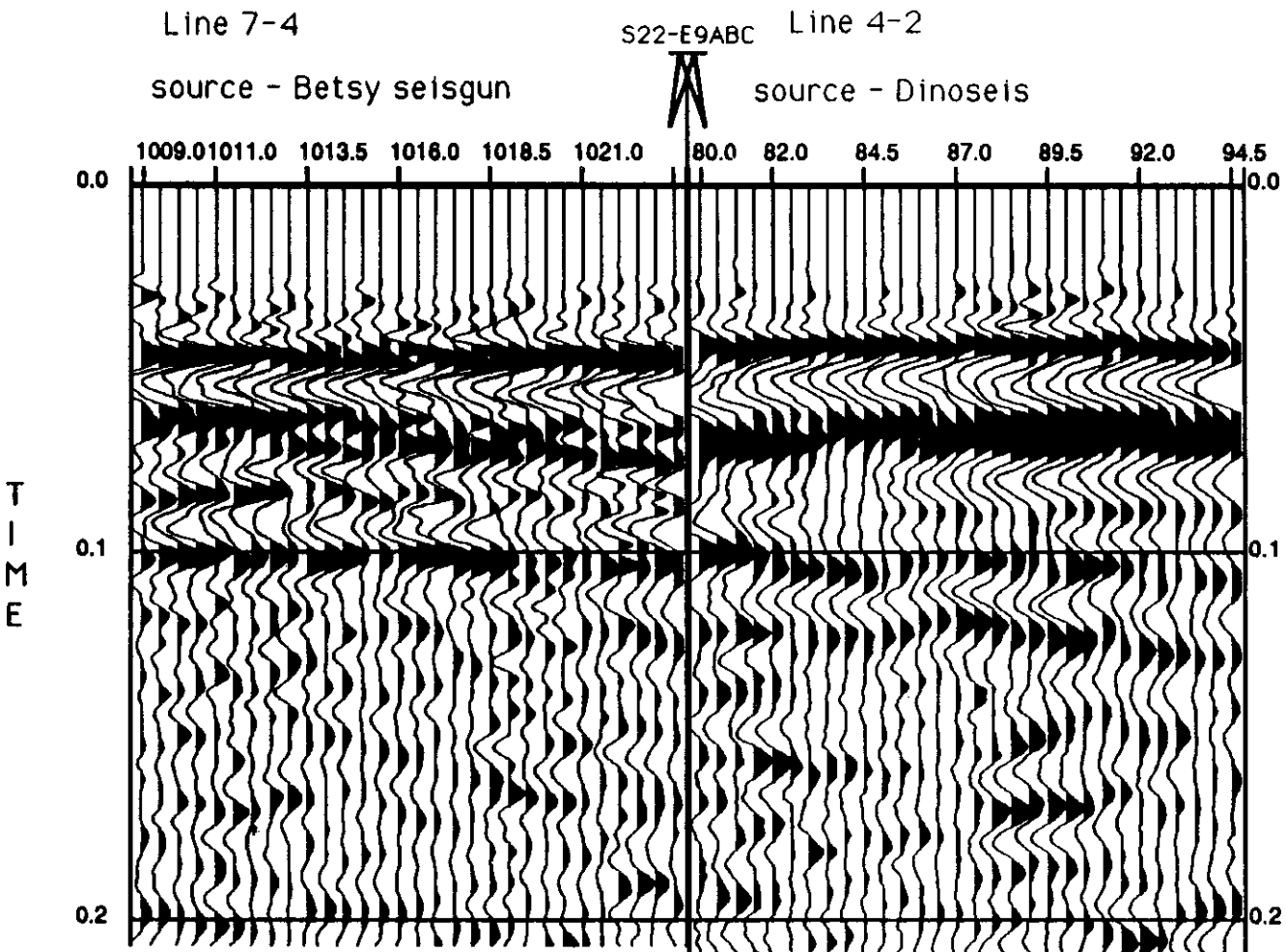
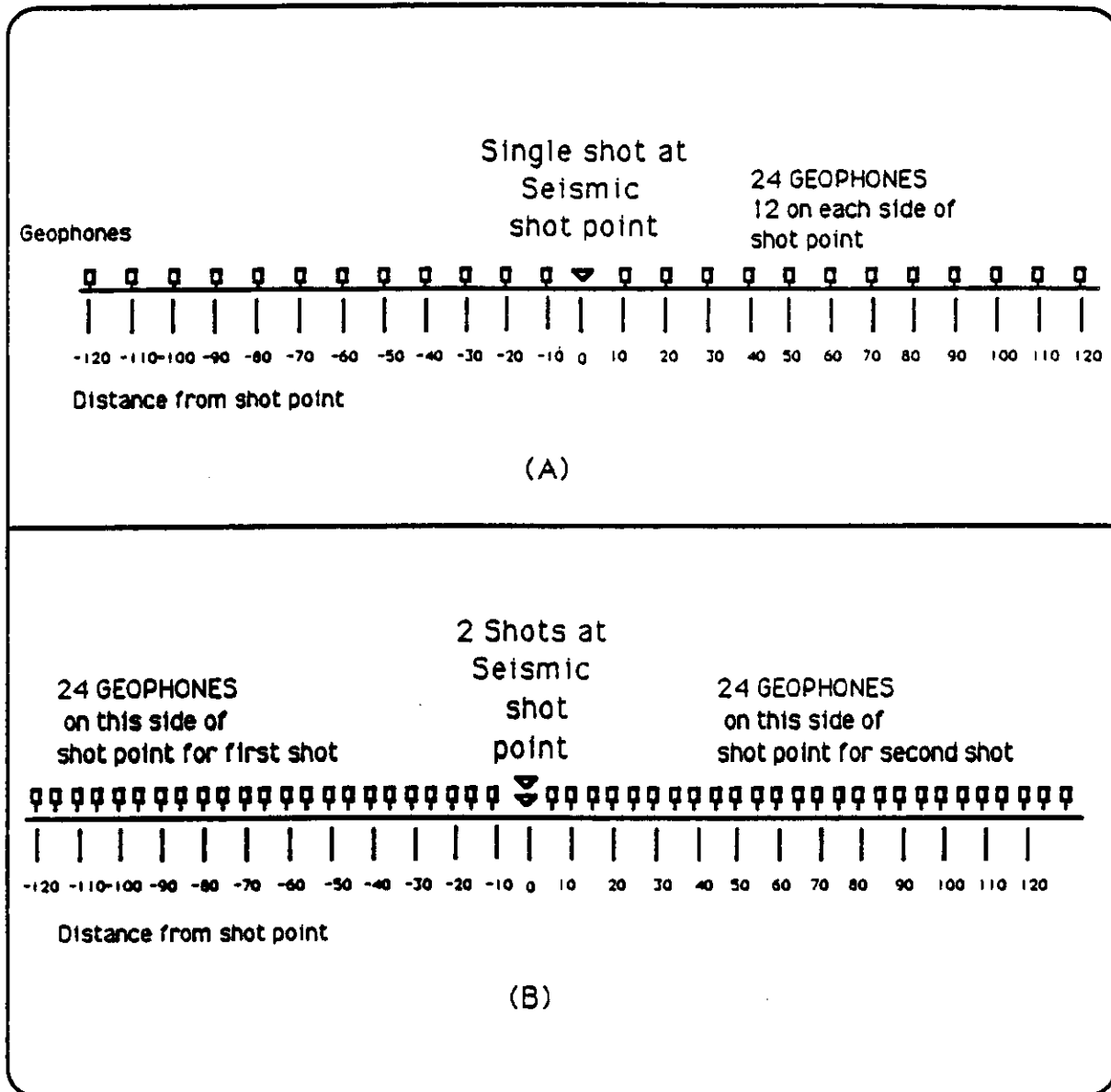


Figure 8. Comparison of Seismic Sources at Seismic Line Intersection.

Figure 9. Symmetrical Split-Spread Configuration of
(a) Initial Split-Spread Configuration and
(b) Final Split-Spread Configuration.



9 3 1 9 9 0 4 7 8 2 0

9 3 1 7 9 0 4 1 3 2 1

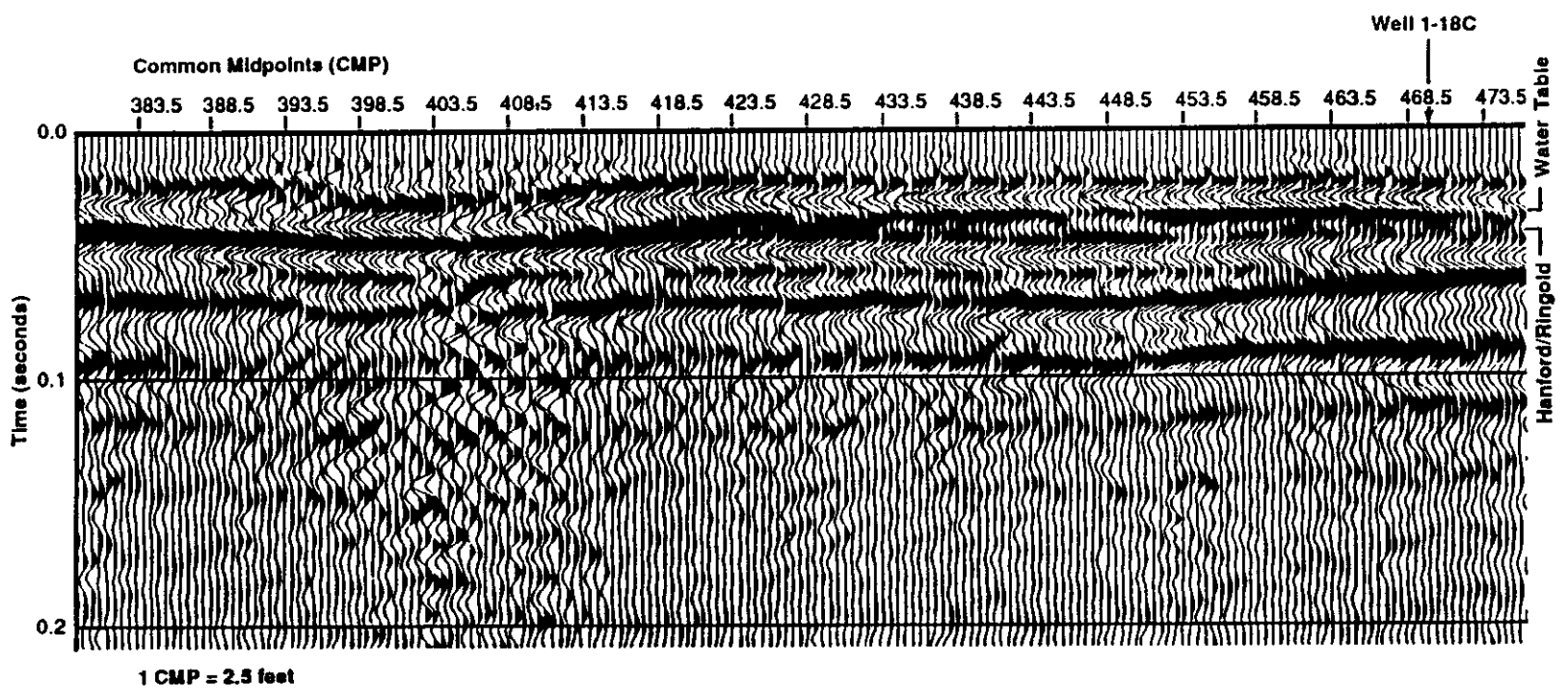
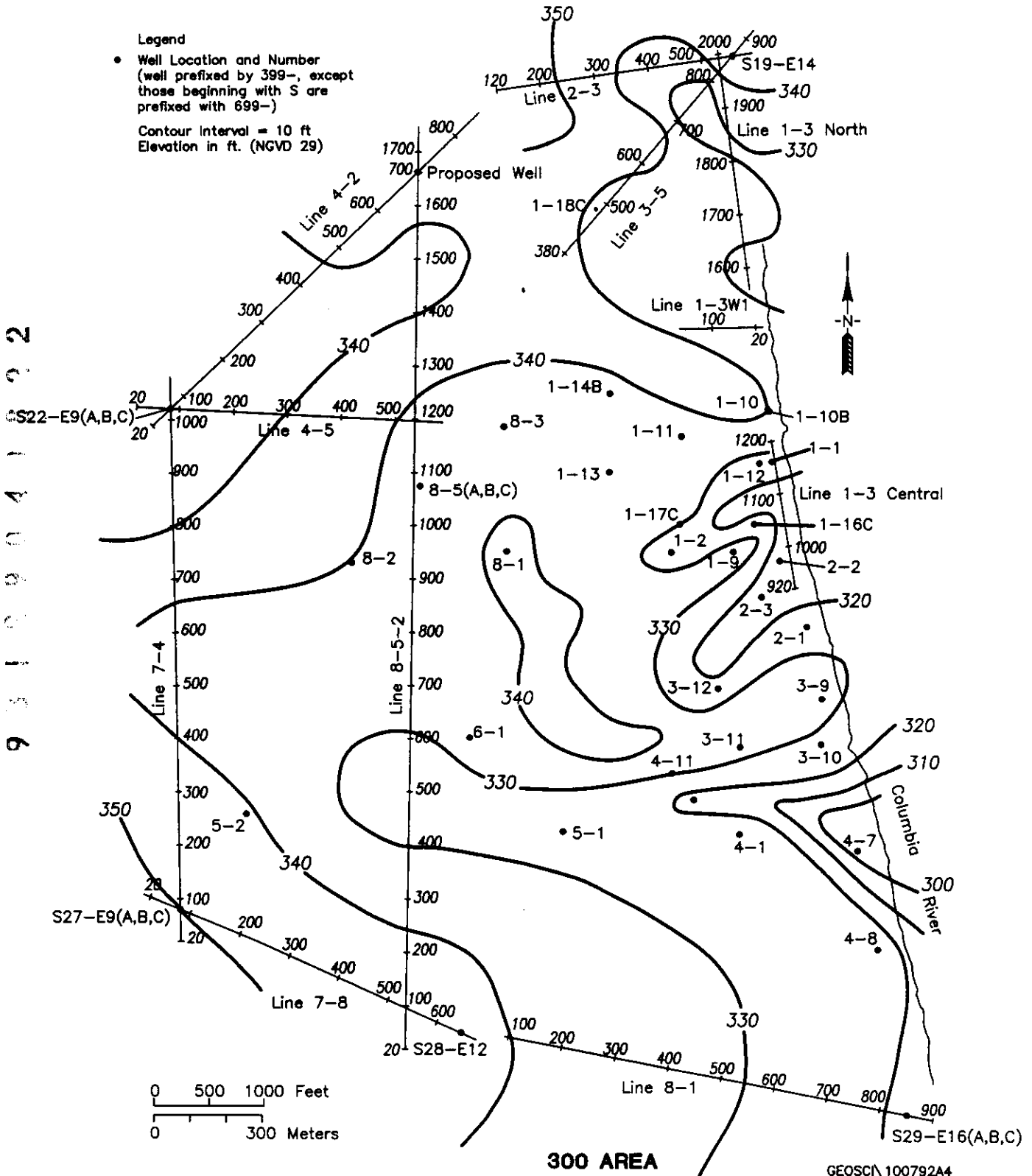


Figure 10. Seismic Reflection Line 3-5.

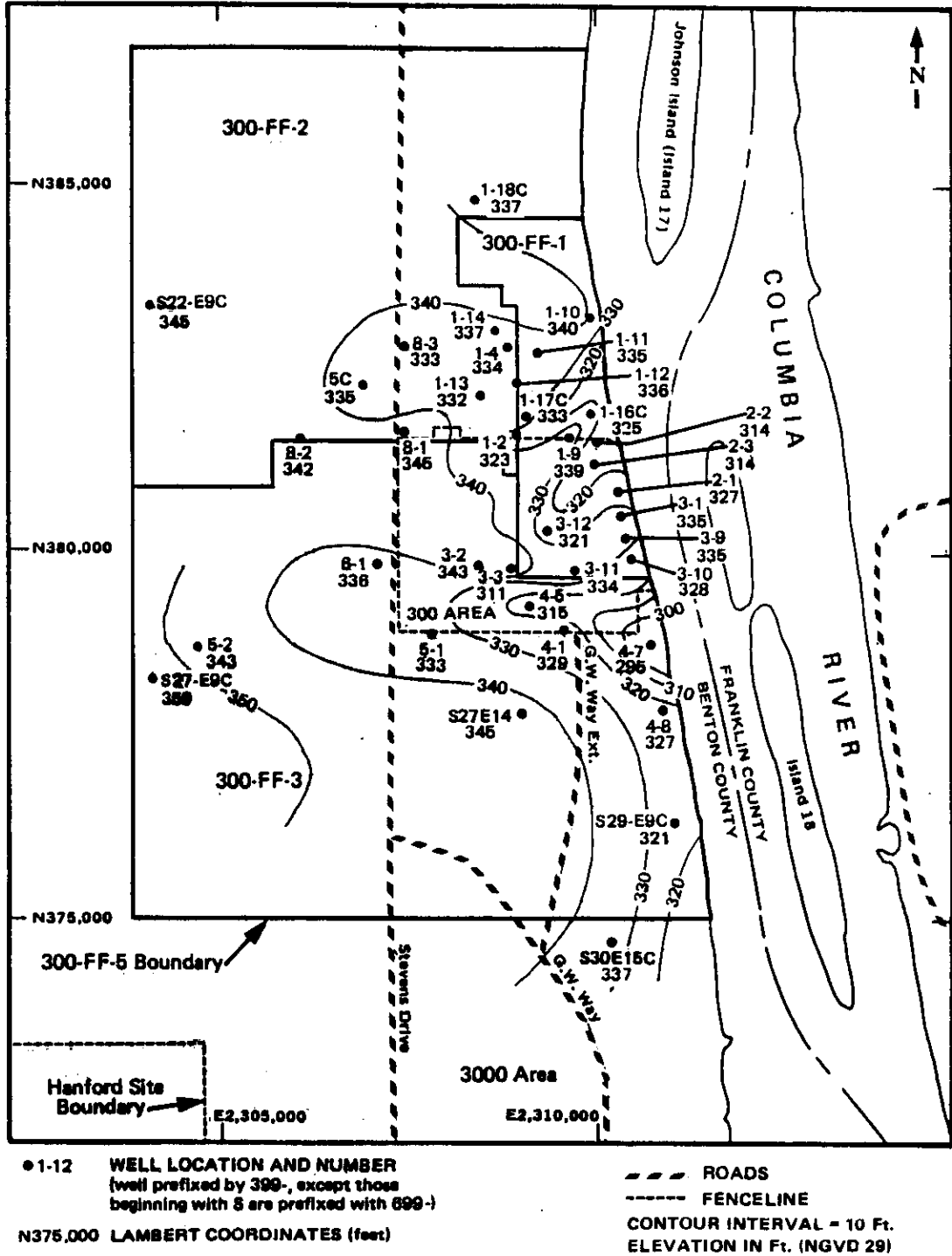
WHC-SD-EN-TI-069, Rev. 0

Figure 11. Structure Map of the Hanford/Ringold Unconformity. The contour interval is 3.05 m (10 ft), and the datum is sea level.



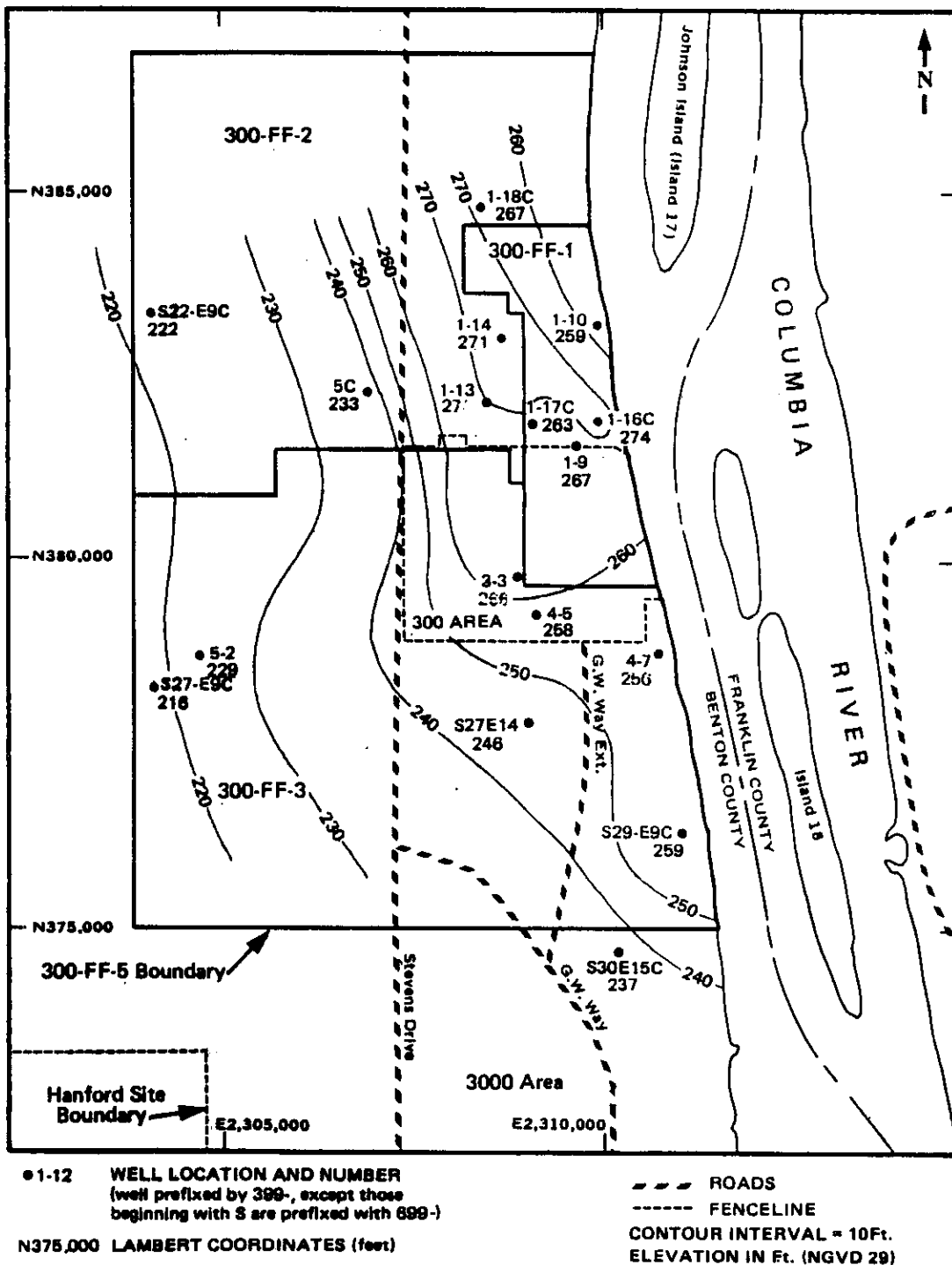
9 3 1 9 9 0 4 1 2 2

Figure 12. Structure Contour Map of the Hanford/Ringold Contact, Using Only Borehole Log Depths for Control (figure courtesy of Swanson et al. 1992). The contour interval is 3.05 m (10 ft), and the datum is sea level.



9 3 1 9 9 0 4 1 9 9 3

Figure 14. Structure Contour Map of Ringold Formation Lower Mud Sequence Using Only Borehole Log Depths for Control (figure courtesy of Swanson et al. 1992). The contour interval is 3.05 m (10 ft), and the datum is sea level.



9 3 1 9 9 0 4 1 0 2 5

APPENDIX A

SUMMARY OF ELECTROMAGNETIC INDUCTION/GROUND-PENETRATING RADAR ANOMALIES

9 7 1 2 0 4 1 9 2 6

This page intentionally left blank.

9 4 1 0 0 0 4 0 0 2 7

APPENDIX A

SUMMARY OF ELECTROMAGNETIC INDUCTION/GROUND-PENETRATING RADAR ANOMALIES

The electromagnetic induction (EMI) and ground-penetrating radar (GPR) data are integrated and presented as a comprehensive interpretation of the shallower strata. The following summarizes the results. Only selected examples of these data are in this report. The complete data set is available in data package WHC-SD-EN-DP-059, Rev. 0 (Kunk 1992).

Data were collected primarily along profiles rather than preferred grids because of the reconnaissance nature of the geophysical surveys and the size of the area being investigated. GPR data were collected along all seismic reflection and refraction profiles (Figure A-1) with additional data concentrated along line 1-3 central (Figure A-2). EMI data were collected along several seismic profiles (Figure A-3). Additional EMI data were collected near well 399-1-18 to trace an anomaly detected along seismic line 3-5 (Figure A-4). The soil conditions limited the maximum depth of investigation of the GPR and EMI to 3 to 4.5 m (10 to 15 ft) in most areas.

The interpretation of the data identified numerous anomalous features. Each anomaly is categorized as one of six types of anomalies (Table A-1). A summary of anomalies identified with the EMI and GPR is presented in Table A-1 along with preferred interpretations. The entire EMI and GPR data set is contained in data package WHC-SD-EN-DP-059, Rev. 0 (Kunk 1992). Approximate locations of the anomalies listed in Table A-1 can be estimated using Figure A-1.

The interpretations of the anomalies were based on available data which is very limited in the study area. Interpretations are based primarily on experience gained from other geophysical investigations conducted on the Hanford Site and knowledge of the Hanford Site geology. There is no supporting borehole geophysical data.

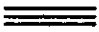


The feature that stands out throughout the operable unit is a pervasive reflector that is found between the depths of 0 to 4 m (14 ft). It is believed to be a Holocene soil horizon that separates eolian silts and sands from the underlying Hanford formation. Based on these data, the thickness of the eolian deposits was calculated and used for the seismic static corrections.

On the GPR records, this interpreted Holocene soil horizon is inversely related to the topography; topographic highs generate apparent lows in this horizon (Figure A-5). However, when topographic corrections are made, this horizon becomes a relatively flat surface. In Figure A-5, soil above the horizon is primarily eolian sands and silts.

The Holocene horizon is absent in several areas. Possible reasons include removed by erosion, human intrusion, never or poorly developed, or coincides with the present topographic surface.

9 3 1 9 9 0 4 7 9 8

Table A-1. Summary of Electromagnetic Induction and Ground-Penetrating Radar Anomalies/Features. Anomalies have been categorized according to the legend below. (sheet 1 of 6)

Anomaly Type	Description
D	Represents an area that appears to have been disturbed by human activity. Examples include; buried debris/garbage, pipes, utilities, excavations etc.
	Area, detected by radar, highlighted by horizontal conductive horizons/layer(s) that appear to be unique relative to the surrounding area.
	A lateral change in the overall "character" of the radar data, but lacking distinct anomalies.
	An radar feature or zone that is an artifact of problems during data collection (i.e. antenna got stuck, going over railroad tracks etc.)
---A---	Anomalous radar zone that is unique relative to the surrounding data or 300-FF-5 and is interpreted as being a geologic feature.
A	Single radar anomaly that could either be human or geologic origin.
E	An electromagnetic induction (EMI) anomaly. If an anomaly was detected with both the EMI and radar, it is listed under radar anomaly.



9 3 0 0 4 0 8 2 9

Table A-1. Summary of Electromagnetic Induction and Ground-Penetrating Radar Anomalies/Features. Anomalies have been categorized according to the legend below. (sheet 2 of 6)

Anomaly Type	Section	Location	Description ; Interpretation
D	1-3W-1 10-400	30-150	Shallow conductive debris; human origin
Line Summary	1-3W-1	All	Most notable feature is a reflector that is believed to be a paleosol that is pervasive throughout 300-FF-5. It varies from 3-6 feet below the surface.
--A--	8-5-2 100-600	400-450	4-5 foot deep reflector becomes convoluted/disturbed; geologic origin.
///	8-5-2 1000-1400	1180-1240	Radar antenna got stuck while going up and down embankments along road
≡	8-5-2 1000-1400 1400-1800	1250-1600	Abnormally high reflective properties of interpreted paleosol at ~6' and 9'. This change occurs North of the Radio Transmission Tower Road.
--A--	8-5-2 3000-3400	3000-3400	Several conductive disturbances that may be related to geologic features such as clastic dikes, clay seams or buried debris.
--A--	8-5-2 3400-3800	3700-3800	5 foot deep anomaly with strong reflective properties; possibly part of paleodrainage that is not apparent from the surface.
D	8-5-2 3800-4200	3800-4170	Area appears to have been altered by human activities. Possibility of scattered buried debris.
A	8-5-2 4200-4600	4300	Anomaly 4' below surface; probably a buried utility line/pipe.
--A--	8-5-2 5800-6200	5930-5980	Distinct anomaly 5 - 6 feet deep; generally correlative with a topographic depression.
A	8-5-2 6200-6600	6410	Anomaly 5' below the surface from questionable source
A	8-5-2 6600-7000	6830	Anomaly 4' below the surface in the center of a small depression. ; geologic origin
A	8-5-2 7000-7400	7000	"U" shaped anomaly 8 feet below the surface; part of paleodrainage system
--A--	8-5-2 7000-7400	ALL	Several small features, 3 - 6 feet, deep all suspected as geologic origin
--A--	8-5-2 7400-7800	7400-7520	Converging dipping layers; Possibly related to paleodrainage.
A	8-5-2 7400-7800	7650&7670	Two "U" shaped anomalies 6 and 8 feet deep in a local depression ; geologic origin
Line Summary	8-5-2	ALL	A shallow, flat reflector, from 0-6 deep, interpreted as a paleosol is pervasive throughout most of the line. There may be an older paleosol below this horizon in some places. Apparent highs and lows of the paleosol are a function of topography.

93199041030

Table A-1. Summary of Electromagnetic Induction and Ground-Penetrating Radar Anomalies/Features. Anomalies have been categorized according to the legend below. (sheet 3 of 6)

Anomaly Type	Section	Location	Description; Interpretation
--A--	7-4 100-600	100-350	Apparent 12 foot deep "U" shaped anomaly, a function of topographic high. Near surface "clutter" probably due to surface roughness/vegetation.
A	7-4 100-600	550	Anomaly 5' below the surface; geologic origin
D, E	7-4 600-700	650	Wire cable laying on surface
D, E	7-4 380-450	430	Wire cable laying at surface
--A--	7-4 600-1200	1000-1200	Dipping reflectors; forsets or crossbedding
D, E	7-4 1350	1350	Wire cable laying on surface
A	7-4 1400-1800 through 3600-4200	ALL	Numerous small shallow (<5') anomaly between 1400 & 4200. Most have a geologic origin but several are most likely buried debris.
D, E	7-4 1450	1450	Negative anomaly, human origin
D	7-4 2400-2800	2450	Conductive debris 3' below the surface; suspected human origin
	7-4 3600-4200	3990	Antenna got stuck going up steep sand dune
--A--	7-4 4800-5400	5130-5300	U shaped anomaly related to topography. Several shallow anomalies within it are most likely human origin. The EMI data suggests it is due to metallic (conductive) debris.
D, E	7-4 5200	5200	Passed by metallic signs
Line Summary	7-4	ALL	The persistent paleosol that is observed throughout 300-FF-5 is prevalent in the southern portion of the line. It appears that a significant portion of the line has been disturbed by human activities.
--A--	4-5 1200-1800 1800-2400	1750-1850	Topographic induced high with a deep (10') anomaly beneath; geologic origin
A	4-5 2400-2950	2770	Shallow anomaly most likely a function of localized drainage pattern
Line Summary	4-5	ALL	Western portion of the line appears to have higher concentrations of near surface boulders and cobbles scattering of the radar signal. The interpreted paleosol is intermittent in this area. In the eastern portion, the paleosol is prevalent with notable highs and lows; a function of the topography.
	1-3 North Powerline rd to 8400	ALL	Uncharacteristically "quiet zone" with a lack of anomalies, debris, and reflective material.

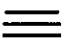


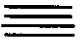
9 3 1 0 0 4 1 0 3 1

Table A-1. Summary of Electromagnetic Induction and Ground-Penetrating Radar Anomalies/Features. Anomalies have been categorized according to the legend below. (sheet 4 of 6)

Anomaly Type	Section	Location	Description; Interpretation
--A--	1-3Cent/ North 1-3W-1N	ALL	Dipping reflector that is a function of topography. Layers most likely are relatively flat.
EMI	1-3 North 8000-8400	8200-8300	EMI conductivity high is probably associated with debris/coal clinkers, ashes etc observed in the vicinity of the anomaly.
≡//	1-3North 8800-9200	8900-9050	High degree of reflective horizons relative to the south and north; possible human origin
--A--	1-3North 9200-9600	---	Good figure showing topography affects on apparent dipping horizons which in reality are relatively flat.
A	1-3North 9600-10000	9500-9800	"U" shaped anomaly; function of topography.
≡//	1-3Cent ALL	4600-6000	Area with poor resolution; fill material covers most of original surface, affecting data. Extensive near surface "clutter".
--A--	1-10B 5800-well	Near well 1-10-B	Possible combination of more than one anomaly. Near surface features are likely human induced. Deeper portion (<6') is probably of geologic origin.
Line Summary	1-3Cent through 1-3North	ALL	1-3 Central has very poor data resolution. Data collection on road between 1-3 Central and 1-3 North was able to detect the paleosol; 1-3 North has a quiet zone that is an enigma. Paleosol was detected in the Northern portion.
≡	4-2 1000-1400	1220-1270	Dipping reflectors; crossbedding/forset bedding.
A	4-2 1400-1800	1720	Buried anomaly 12' below the surface; suspected geologic origin.
≡//	4-2 1800-2200	ALL	Variety of dipping reflectors and anomalies; buried depositional features (crossbedding, forsets etc.)
A	4-2 3000-3400	3000	Anomaly 6' below surface; origin not clear. Possible paleodrainage feature.
A	4-2 3000-3400	3090	Anomaly 5' below surface; origin not clear. Possible paleodrainage feature.
A	4-2 3400-3800	3420	Anomaly 10' below surface; possibly related to paleodrainage that predates paleosol development.
A	4-2 3800-4300	3980	Anomaly 7' below the surface; possibly related to paleodrainages.
≠	4-2 3800-4300	4280	Radar antenna got stuck during data collection.
Line Summary	4-2	ALL	Paleosol prevalent through most of line. Several features detected may be related to paleodrainage system that may still influence localized moisture patterns.

93199041932





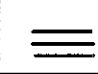
Table A-1. Summary of Electromagnetic Induction and Ground-Penetrating Radar Anomalies/Features. Anomalies have been categorized according to the legend below. (sheet 5 of 6)

Anomaly Type	Section	Location	Description; Interpretation
A	2-3 1400-1800	1460	Anomaly 5' below the surface; origin??
--A--	2-3 2200-2600 2600-2930	2450- well #3	Two reflectors, 3' and 10' below the surface merge with the lower, pinching out in the vicinity of well #3.
Line Summary	2-3	ALL	The interpreted paleosol is prevalent throughout the majority of the line. A second, deeper reflector with similar properties is observed in places. It too is most likely a paleosol.
A	7-8 100-600	300	"U" shaped anomaly 6' below surface; part of a paleodrainage system.
D, E	7-8 450	450	Crossed cable at surface
A	7-8 600-1200	770	Anomaly 3' below surface; geologic origin.
	7-8 600-1200	880	Apparent gap in reflector with offset. More a function of the differences between horizontal and vertical scales than true offset.
D, E	7-8 1800	1800	Crossed fence
--A--	7-8 1800-2400	2300	Significant increase in reflective properties; most likely lithologic variation (i.e. increase in clay/silt content)
	7-8 2400-3000 3000-3400	2600-3400	Increase in "conductive debris." Combination in gravel/cobbles content (geologic origin) and human induced debris.
D, E	7-8 2900	2900	Power line
D, E	7-8 3000-3400	3000-3400	Metallic Debris scattered around at surface.
Line Summary	7-8	ALL	Paleosol is intermittent along the line, there is more "conductive debris" along the eastern portion of the line.
	8-1 600-1000	590	Radar antenna got stuck going up a sand dune.
	8-1 600-1000	900	Reflector beneath upper paleosol at a depth of 7', probably geologic origin.
A	8-1 1000-1400	1080	"U" shaped anomaly 5'-7' below surface; paleodrainage?
A	8-1 1000-1400	1180	"U" shaped anomaly 5'-9' below surface; paleodrainage?

9 3 1 1 9 0 4 0 3 3

Table A-1. Summary of Electromagnetic Induction and Ground-Penetrating Radar Anomalies/Features. Anomalies have been categorized according to the legend below. (sheet 6 of 6)

9 1 1 2 9 0 4 0 3 3 4

Anomaly Type	Section	Location	Description; Interpretation
	8-1 1000-1400 1400-1800	1250-1550	Character change in radar signature; more "conductive/disturbed" subsurface; possibly due to higher percentage of boulders/cobbles.
	8-1 1800-2200	1820-1890	Relatively high conductive layer 6' below surface with single anomaly. Anomaly 2' below surface; combination of human induced and geologic origin. EMI anomaly suggests buried utility/pipe.
A, E	8-1 1800-2200	1970	Anomaly 2' below surface; human origin. correlates with EMI anomaly (pipe or utilities).
A	8-1 2600-3000	2640	Anomaly 2' below surface; human origin. Correlates with EMI anomaly (pipe/utility?)
	8-1 2600-3000	2820	Antenna got stuck during data collection.
	8-1 2600-3000	2820-2900	Disturbed area; caused by crossing road.
E	8-1 3000-3400	3180&3210	Two relatively minor EMI anomalies; human origin.
	8-1 3400-3800	3520	Horizontal reflector, 40-50 feet wide, Origin??.
E	8-1 4200-4400	4300	EMI anomaly associated with cultural features on well pad.
Line Summary	8-1	All	Interpreted paleosol is present throughout most of the line. A second intermittent reflector is present 4-5 feet below the first.
E	3-5	2500-2800	EMI anomaly; no GPR associated anomaly; possibly paleodrainage.
D, E	3-5 3400-4000	3900	Disturbed appears to be human induced. EMI associated anomaly suggests buried "debris."
E	3-5	4200	EMI anomaly; human origin no obvious GPR anomaly associated with it.
E	3-5	4500	EMI high; result of getting close to river and topography.
Line Summary	3-5	ALL	Interpreted paleosol is very persistent from 1000-3800. Portions of eastern end cluttered with GPR anomalies associated with human activities.

There are several locations where trough-shaped GPR anomalies coincide with a missing section of the interpreted Holocene soil horizon. Several of these anomalies have been interpreted as paleochannels (Figure A-6). In Figure C-6, the Holocene soil horizon is not apparent, suggesting the interpreted channel is a relatively recent development. Most paleodrainage/channels interpreted from this data are shallow, 0 to 4.5 m (15 ft), and less than 30 m (100 ft) wide. There are no paleodrainage/channels that were detected that are the size, depth, or magnitude as predicted by Lindberg and Bond (1979).

Two possible explanations for the shallow "channels" detected are considered. They could have developed during the waning stages of the Missoula floods or during erosional episodes of "regular" Columbia River flooding. Erosion by creeks is unlikely because there is no surficial expression for such creeks. Such paleochannels appear to influence movement/infiltration of surface water.

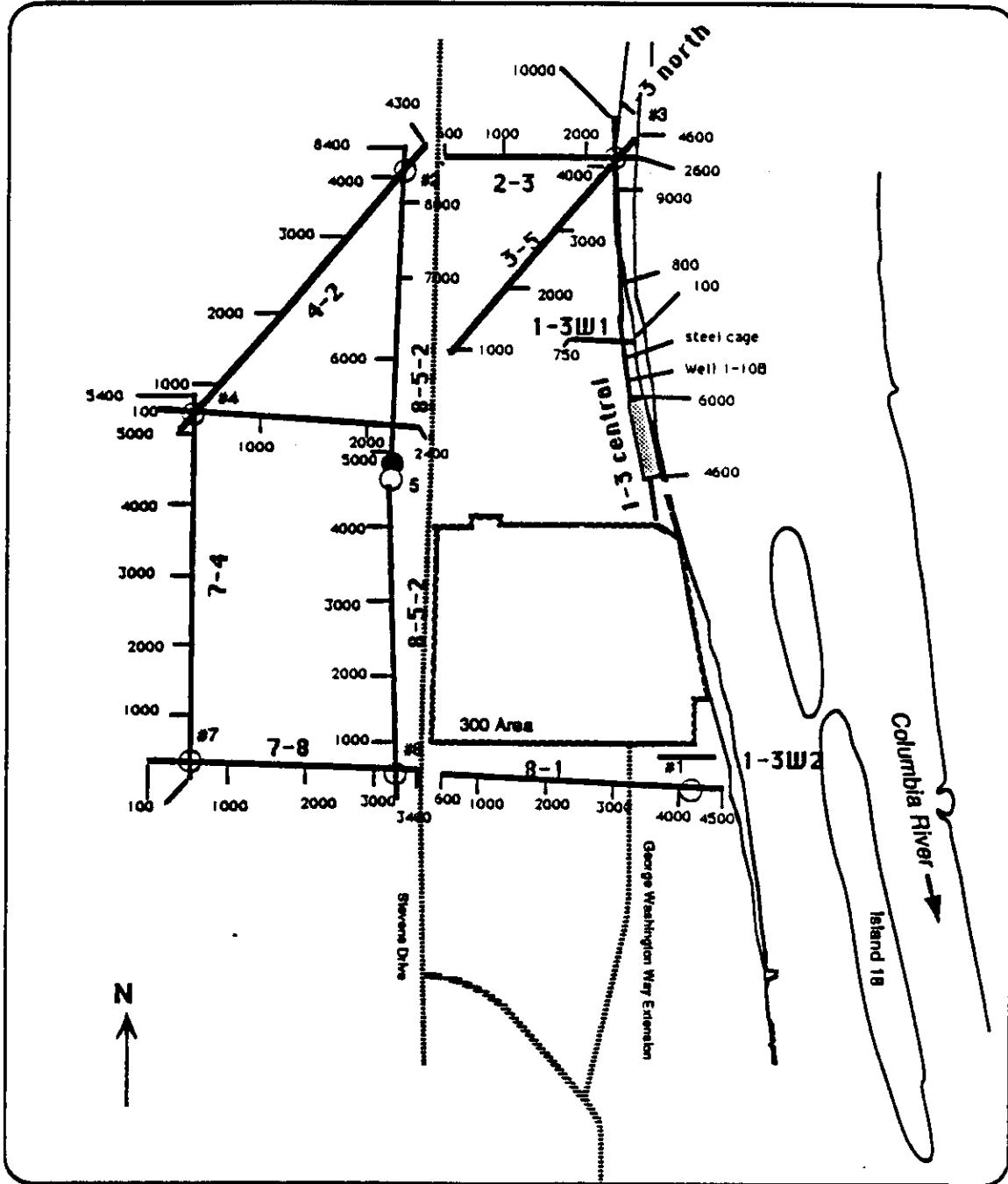
The Holocene soil remains intact across one interpreted paleochannel (Figure A-7), suggesting it developed during the waning stages of the flood and the soil horizon developed after the channel. But most of the interpreted paleochannels appear to postdate the Holocene soil horizon.

A second reflecting horizon was detected on several profiles, usually 1.22 to 1.52 m (4 to 5 ft) below the upper horizon. It is most likely a paleosol of unknown extent. An example of the upper Holocene soil with the underlying paleosol is shown in Figure C-8. A complex relationship between the paleochannel, dune development, soil horizon development, and topography is notable between 2800-2930.

Most variations in the EMI data can be directly attributed to the topography (i.e., high EMI values read from the meter correspond with topographic lows, usually hardpack surface soils; and EMI lows correspond with topographic highs, generally sand dunes elevated above the hardpack). The EMI data correlates with the GPR data throughout most of the areas where both were collected.

An EMI anomaly was identified near well 1-18, line 3-5 (Figure A-9). Data coverage was expanded to the northwest and southeast of the anomaly to aid in its interpretation (Figure A-10). Radar data collected along line 3-5 shows an intact Holocene soil over the anomaly, suggesting that the anomaly is located within the Missoula flood deposits. It may extend to depths greater than 4.5 m (15 ft). The increased conductivity suggests a much higher concentration of moisture than in the surrounding soils, which could be related to current, near-surface water movement. The anomaly does not correspond with local topography.

Figure A-1. Ground-Penetrating Radar Survey Location Map.



9 1 1 2 0 0 4 2 0 3 6

— Ground Probing Radar (GPR) Profiles

■ Concentrated GPR Data

○ 1991 Boreholes

Figure A-2. Location Map of Ground-Penetrating Radar Profiles in the I-3 Central Area.

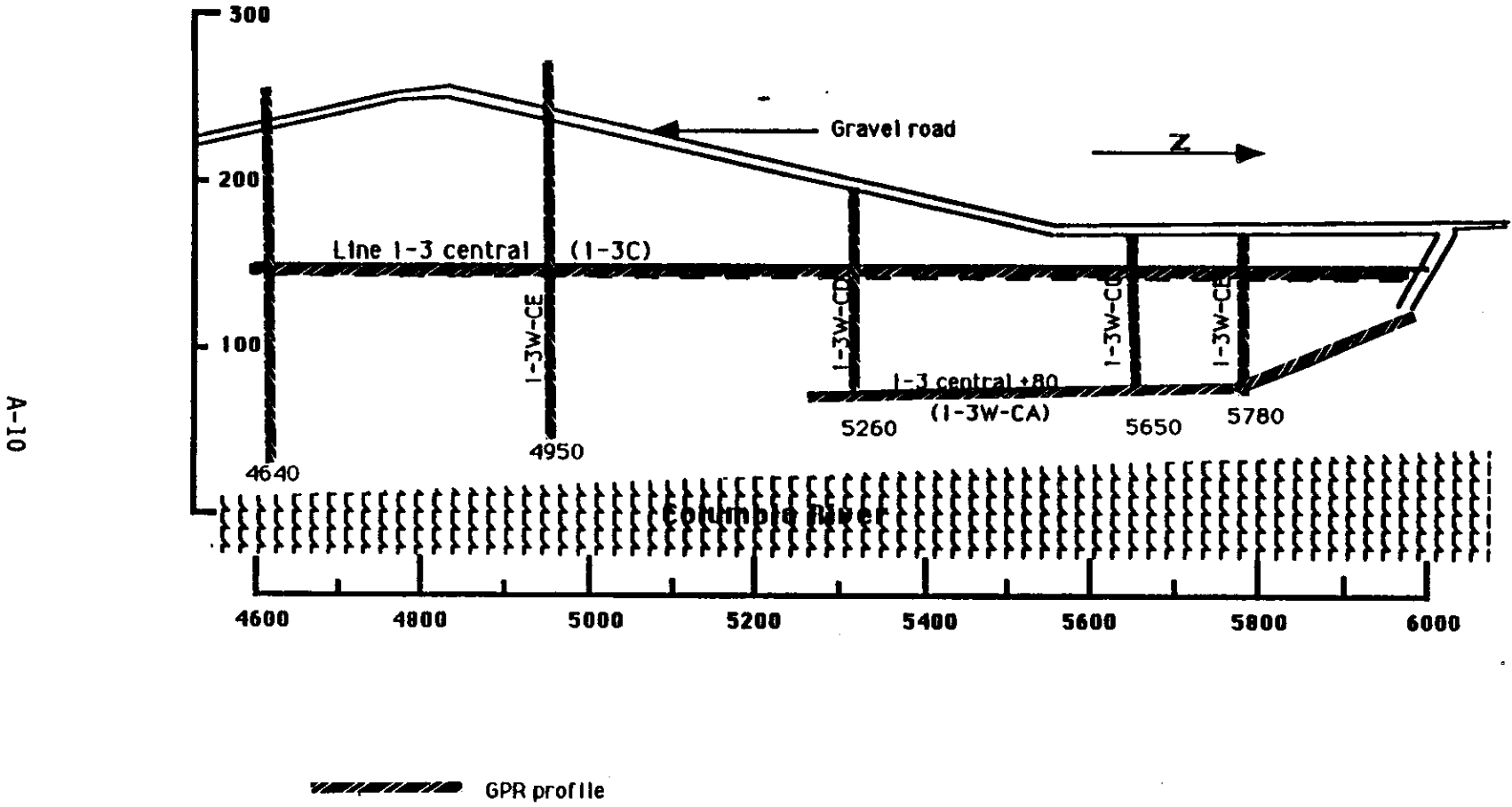


Figure A-3. Electromagnetic Induction Profile Location Map.

8
2
0
1
9
0
6
6
1
5
6

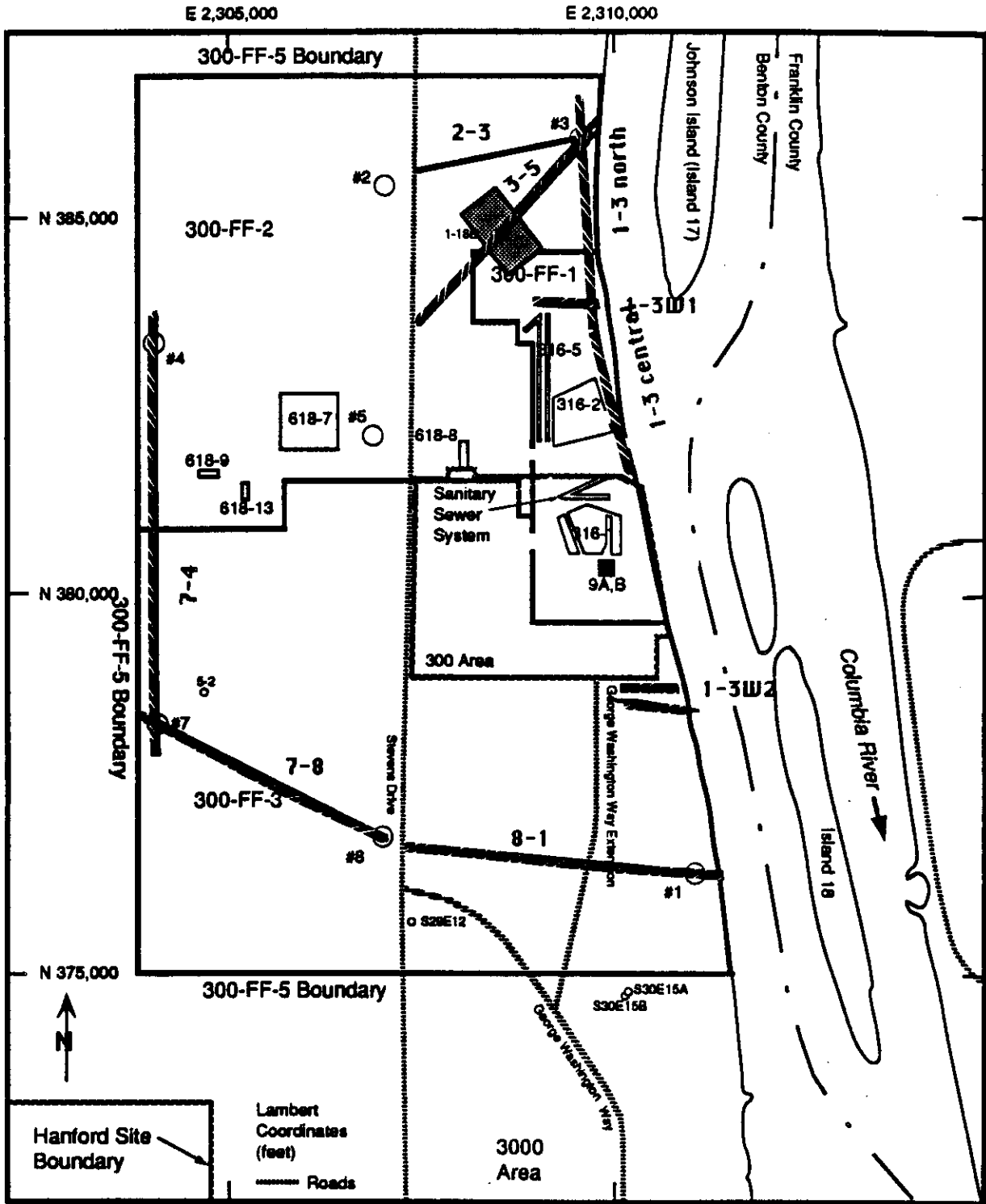
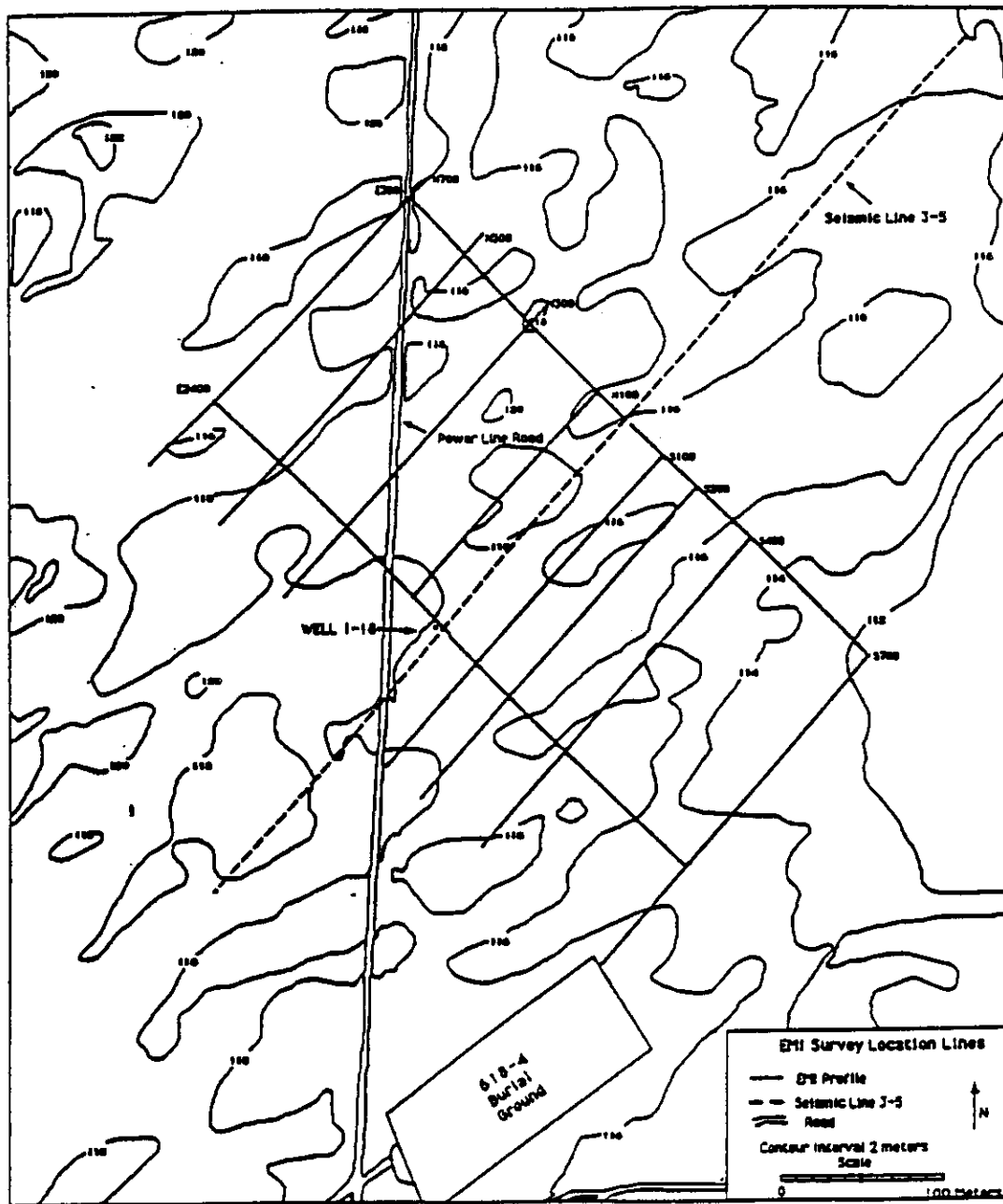


Figure A-4. Electromagnetic Induction Line Locations Near Well 399-1-18.



93139941379

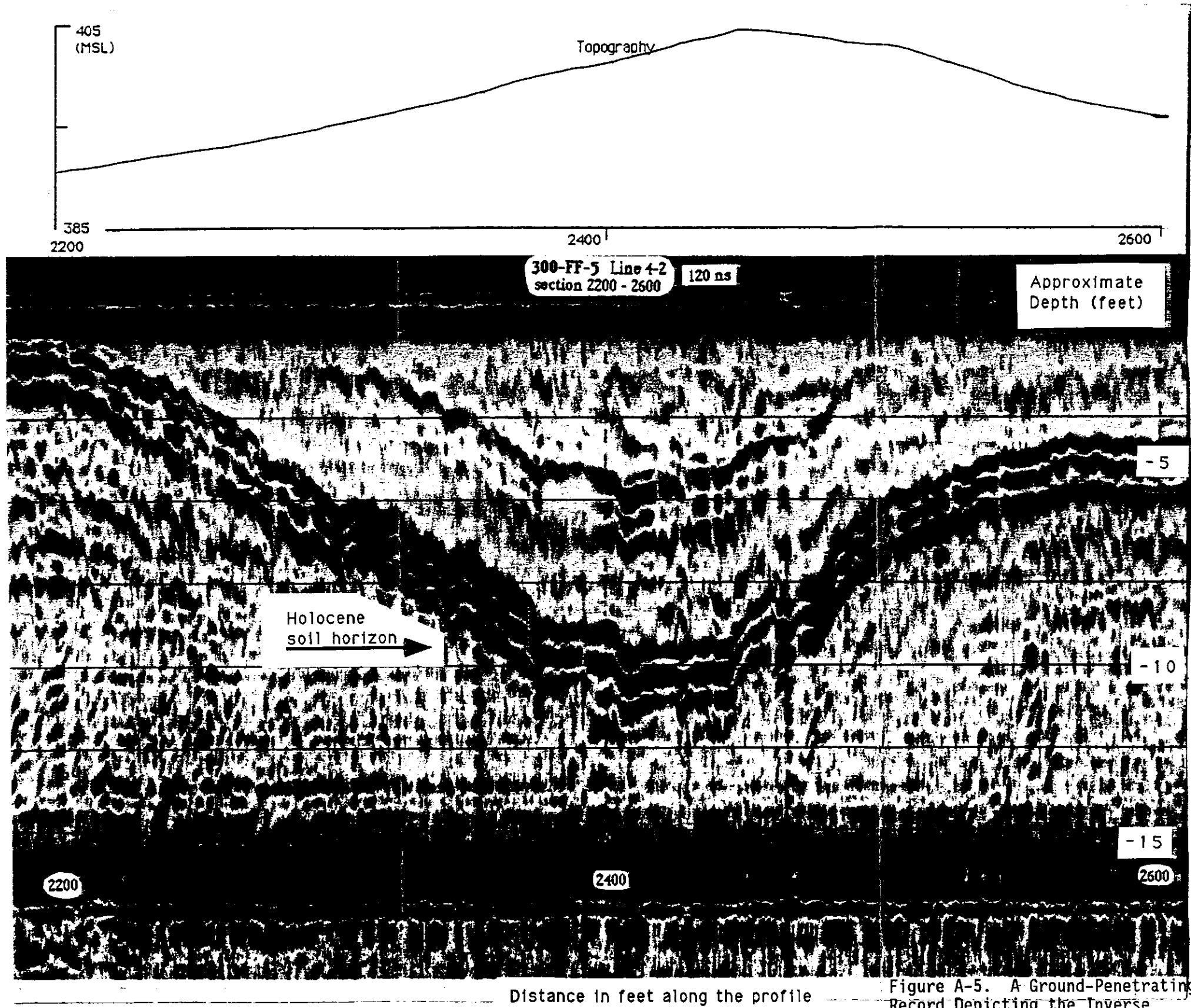


Figure A-5. A Ground-Penetrating Radar Record Depicting the Inverse Relationship of the Holocene Soil Horizon to Topography.

931120041040

**THIS PAGE INTENTIONALLY
LEFT BLANK**

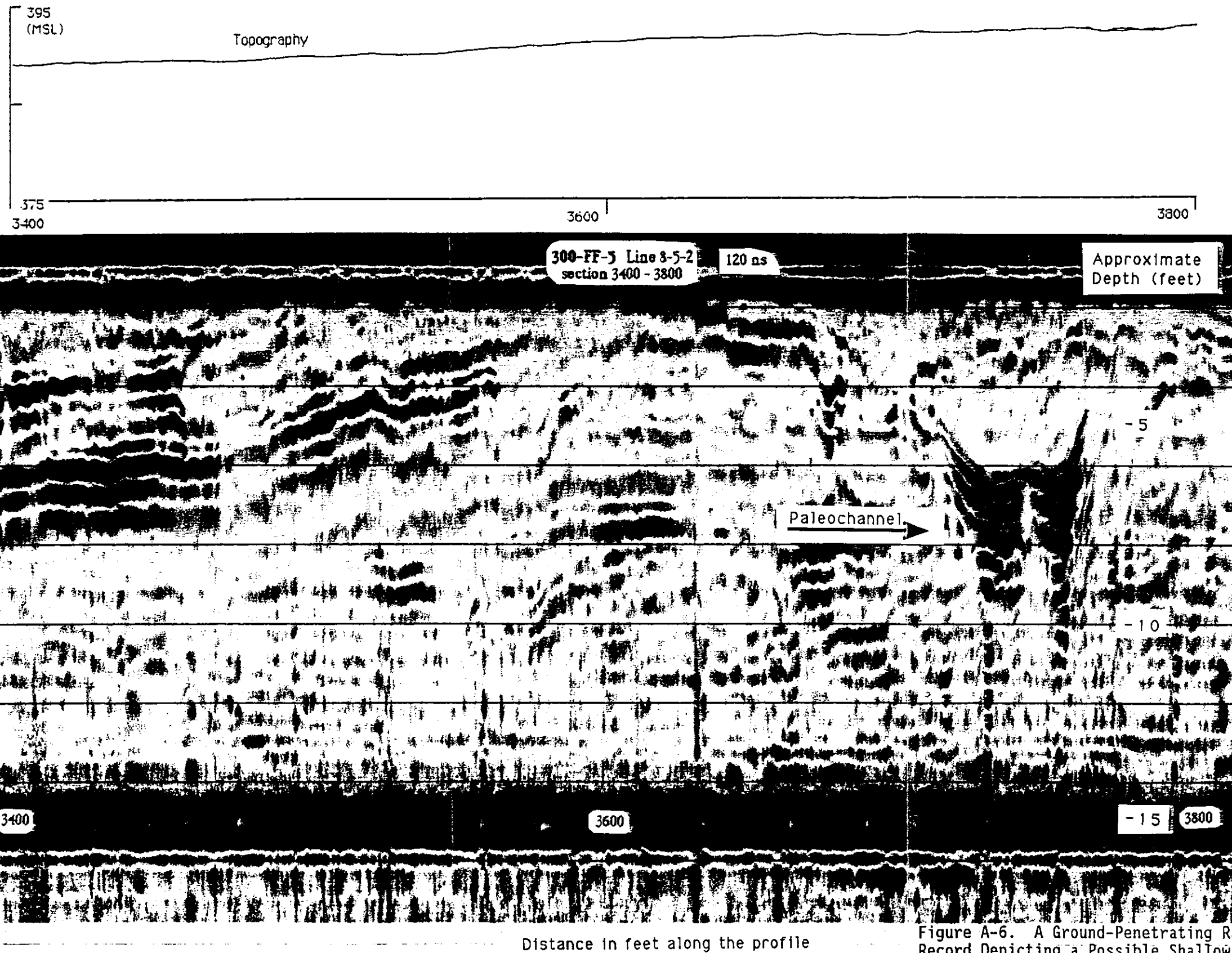


Figure A-6. A Ground-Penetrating Radar Record Depicting a Possible Shallow, Buried Paleochannel Within the Holocene Sediments.

9 3 1 3 3 4 1 2 2 1

THIS PAGE INTENTIONALLY
LEFT BLANK

93199040342

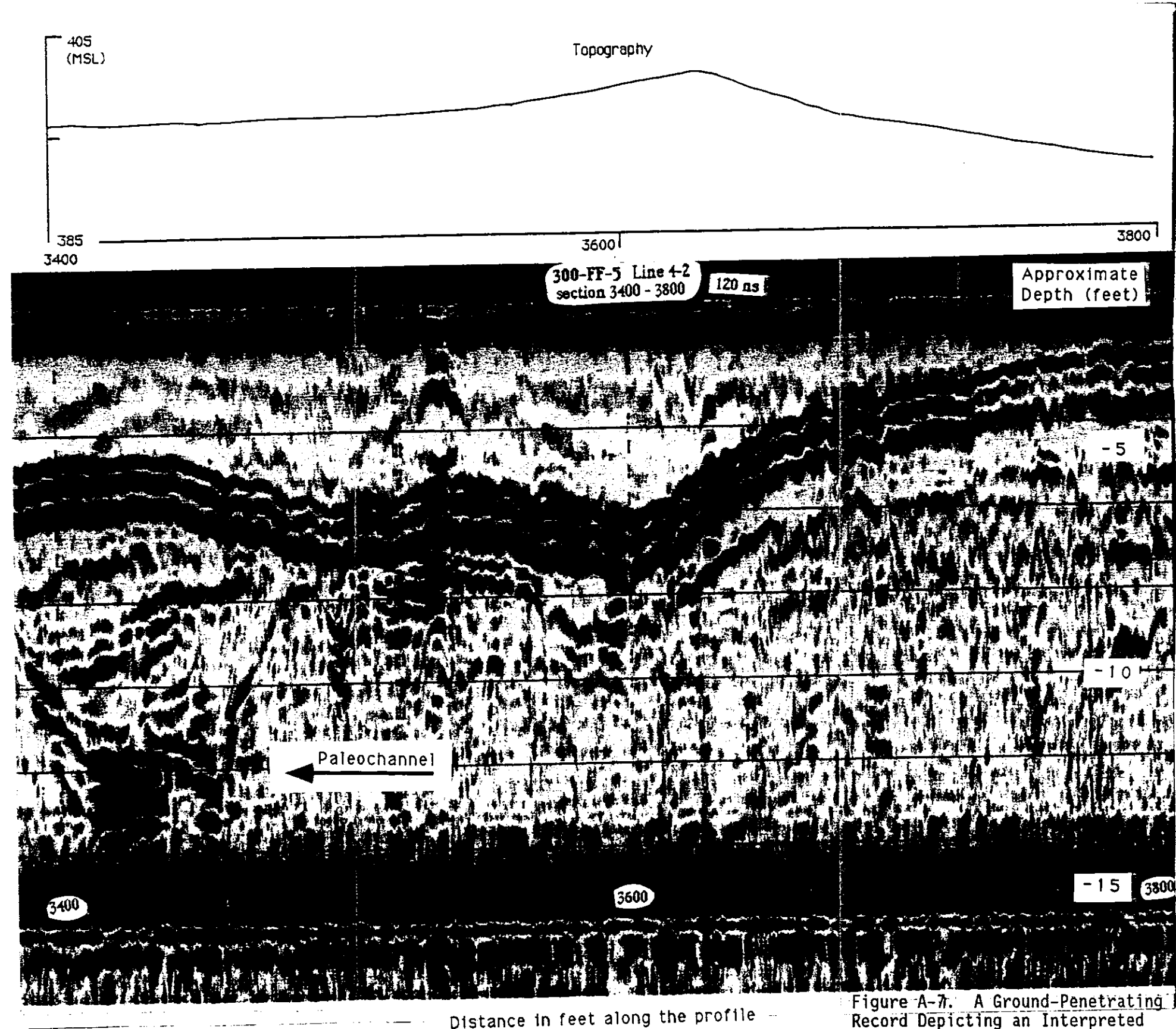
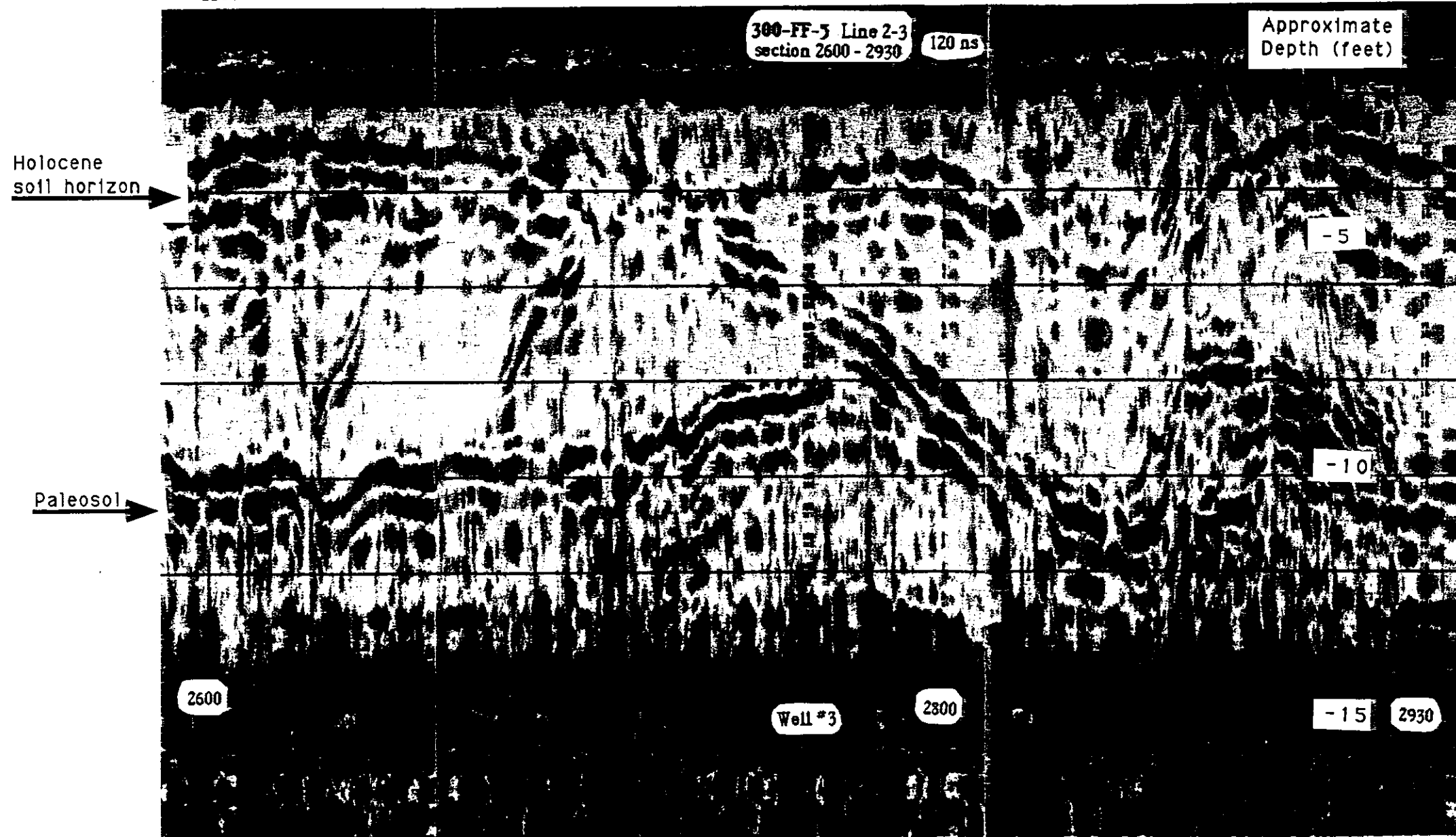
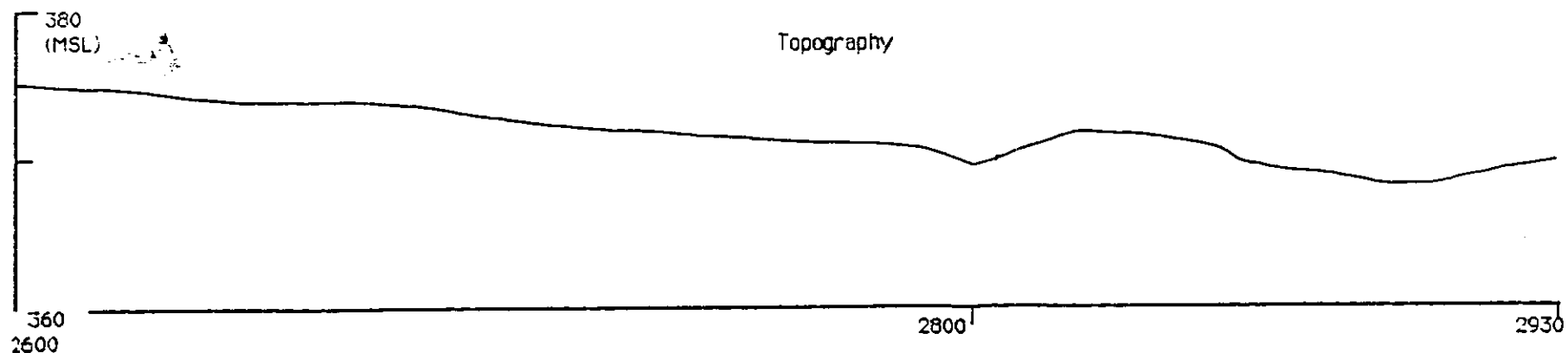


Figure A-7. A Ground-Penetrating Radar Record Depicting an Interpreted Paleochannel With Holocene Soil Horizon Overlying.

**THIS PAGE INTENTIONALLY
LEFT BLANK**



Distance in feet along the profile Figure A-8. A Ground-Penetrating Radar Record Depicting a Holocene Soil Horizon Overlying a Paleosol.

3 4 1 3 3 4 3

**THIS PAGE INTENTIONALLY
LEFT BLANK**

Figure A-9. Electromagnetic Induction Anomaly
Near Well 399-1-18.

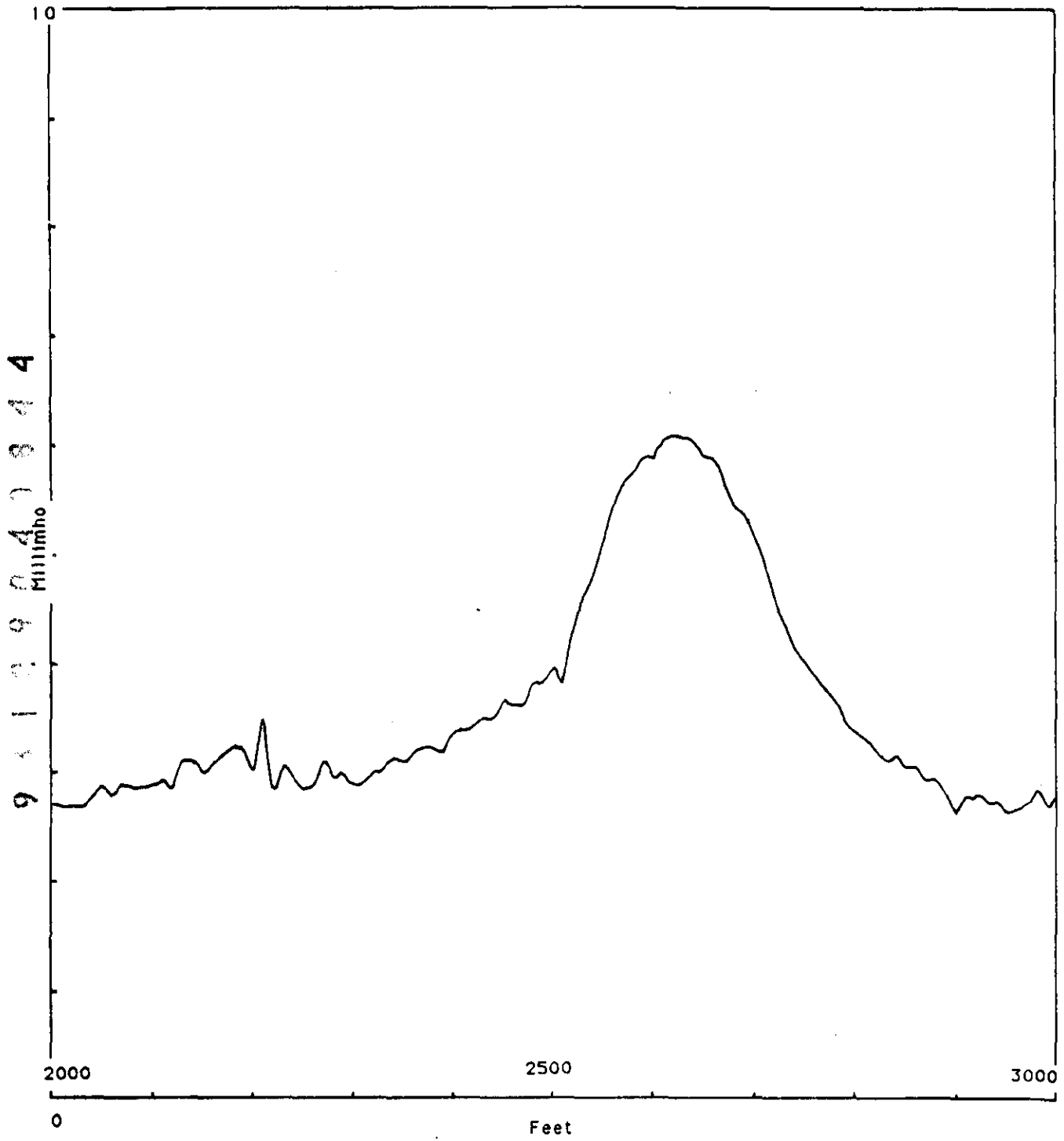
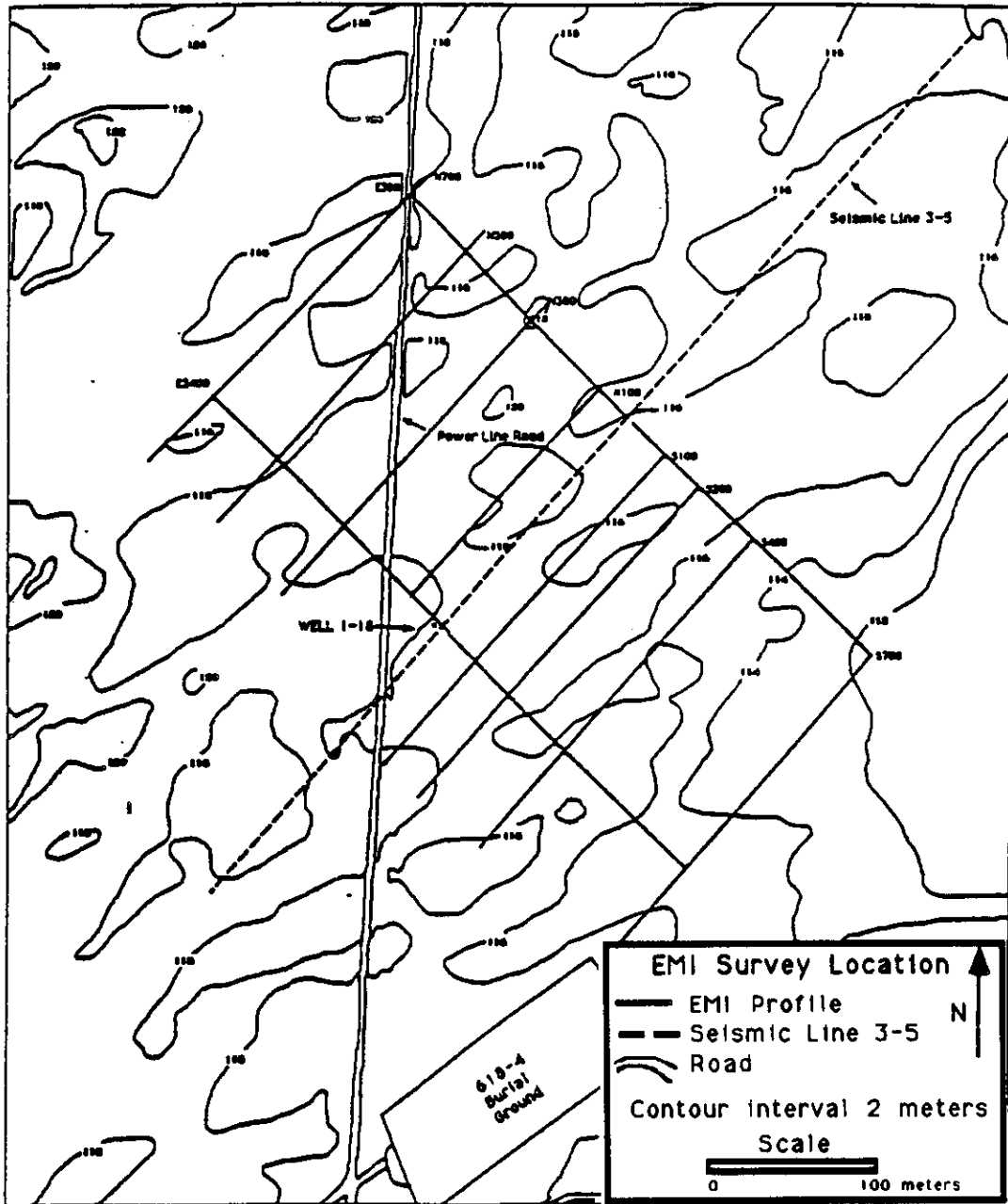


Figure A-10. Expanded Electromagnetic Induction Data Coverage Near Well 399-1-18.



9 3 1 0 0 4 1 3 4 5

This page intentionally left blank.

9 3 1 0 9 0 4 0 8 4 7

APPENDIX B

METHODOLOGIES, DETAILS OF EQUIPMENT, AND DATA ACQUISITION AND PROCESSING

B.1.0 REFLECTION DATA ACQUISITION AND PROCESSING PARAMETERS

B.1.1 DATA ACQUISITION

As briefly discussed in Section 3.2, initially a symmetrical split-spread configuration with shots and receivers located every 3 m (10 ft) was tried (Figure 8[a]). After early data processing, it was determined that this configuration was not tight enough. The acquisition configuration was then altered to 1.5-m (5-ft) geophone spacings as shown in Figure 8(b). Two shots were made at each 3.05-m (10-ft) interval. For one shot, the geophones selected were on one side of the shot, and for the second shot, the geophones selected were on the other side of the shot. This acquisition setup resulted in sampling the subsurface every 0.75 m (2.5 ft). There was a 3-m (10-ft) gap between the shot and the first active geophone in both configurations. Geophones were buried as much as 0.5 m (1.5 ft) in sandy areas to improve coupling.

Table B-1 lists key acquisition and equipment parameters for seismic data acquisition.

Table B-1. Seismic Acquisition and Equipment Parameters.

Instrumentation and settings for data acquisition include:

RECORDING UNIT	- Geometrics ES-2401
GEOPHONES	- 40 Hz Mark Product with 10-cm (4-in.) spikes
DATA FORMAT	- SEG -2
SAMPLE RATE	- 0.2 millisec
NUMBER OF CHANNELS	- 24
LOW-CUT FILTER	- 30 Hz
HIGH-CUT FILTER	- 250 Hz
NOTCH FILTER	- In most lines
RECORD LENGTH	- 0.409 seconds
SHOT SPACING	- 3.05 m (10 ft)
RECEIVER SPACING	- 1.52 m (5 ft)
NEAR RECEIVER	- 3.05 m (10 ft)
FAR RECEIVER	- 38.1 m (125 ft)

B.1.2 DATA PROCESSING

The data acquired using the Dinoseis as a source required application of a "Record Static" shift to each seismic record to correct for an apparent inconsistent start pulse from the accelerometer. Additionally, trigger

The velocities for the material encountered do not appear to be as high as anticipated. Refraction information indicates horizons exist near the surface that have velocities near 0.9 to 1.1 km/s (3,000 to 3,700 ft/s) with higher velocity material a short distance below that. Velocities estimated using velocity semblance, constant velocity stacks, and normal-moveout correction estimates indicate much lower velocities are needed to stack the data.

This may be explained in a number of ways: (1) The refracted waves may be following thin, high-velocity layers. The velocities of the other material (nonrefracting layers) are then much lower. (2) Another possibility may be that most of the energy is shear waves rather than compressional waves. (3) Finally, multiple reflections may be more predominant than primary reflections.

The velocities used for processing the data are those of the lower end. Measured velocities down boreholes in the form of a check-shot survey or vertical-seismic-profile survey would be needed to unequivocally resolve this discrepancy. Because of these lower-than-expected velocities, reflections from the top of the basalt surface were not reliably obtained.

The processing sequence for all the seismic reflection lines was similar. The largest changes were between lines of different sources. The lines shot with the Betsy Seisgun were filtered with a lower cut-off frequency. This was to allow for reflection information from as deep as possible from the geologic section.

B.2.0 SEISMIC REFRACTION INVESTIGATIONS

B.2.1 INTRODUCTION

Seismic refraction investigations differ from seismic reflection primarily in how the seismic waves interact at subsurface boundaries. The seismic waves of interest in refraction surveys are the refracted waves. These waves travel along the top of a layer that is overlain by lower velocity material.

Numerous factors affect a refraction survey and are partially controllable. These factors include source frequencies, source amplitude, recording sensitivity, noise reduction, and survey configurations. Also, three important geologic constraints are (1) the velocity must increase with depth, (2) a layer(s) of interest must have a significant velocity contrast with the layer above, and (3) the layer(s) of interest must be sufficiently thick to be detected.

If the velocity decreases with depth or a horizon of interest has no velocity contrast with the overlying horizon, then the layer is not directly detectable and is termed a "hidden layer." Layers are also hard or impossible to directly detect if the layer thickness is thin compared to overlying layers or the layer is thinner than the seismic wavelength. The stratigraphy of the sediments in this study area may include combinations of all of these factors.

Refraction information can be obtained from layers below a "hidden layer," but additional interpretive assumptions must be made that decrease the reliability of interpretations.

Two objectives were established for the refraction surveys: first, to attempt to detect the Hanford formation/Ringold Formation contact and, second, to determine if refraction could detect contrasts in the sediments that might be associated with potential hydrologic channeling. Both of these objectives push the method to the limit in that they involve potentially thin interfaces with small velocity contrasts.

B.2.2 DATA ACQUISITION

The same equipment was used for both the seismic reflection and seismic refraction surveys. Section B.1.1, Table B-1, lists the equipment.

The geophone and shot positions are annotated as in the reflection work. The refraction spreads were shot in most cases in conjunction with and during the roll-along process of the seismic reflection work. Typically, the refraction spreads consisted of geophones at 1.5-m (5-ft) intervals, with the first geophone at the shot point and the last geophone about 70 m (230 ft) offset from the shot point (Figure B-1). This layout, using the reflection cables and geophones at 1.5-m (5-ft) intervals, required more than 24 channels to achieve. Therefore, two series of shots were required for each refraction direction.

Using the roll-along box, the first 24 channels/geophones were selected, starting with the geophone at the shot point. The information from the near geophone was used primarily to confirm/adjust time zero for the shot. This configuration provided data for the first 35 m (115 ft) of offset. Then, 24 channels/geophones, starting at 35 m (115 ft) and extending to 70 m (230 ft), were selected. For this longer offset, typically two to three shots were stacked in order to achieve first breaks that could be used. The long-offset configuration overlapped with the near-offset configuration to "tie" the data. This was desirable since all the data were not from the same shot.

B.2.3 DATA PROCESSING

The field data were stored on 3-1/2-in. diskette, accompanied with observer logs. The combination of these provided the raw data for processing.

The seismic refraction processing was extended to different levels, depending upon the intended use. Some of the refraction data were utilized for velocity information for input to reflection processing. For this usage, full refraction analysis was not necessary. Travel-time curves and simple depth calculations were all that were considered.

In-depth analysis of the refraction data utilized the generalized reciprocal method (GRM). In GRM, seismic waves from opposing shots traveling along the same refractor in conjunction with reciprocal times between the

shots are used to determine the depth from a geophone to a refractor. The sequence of steps for the refraction data processing essentially proceeded as follows:

- Combine shot records and gaining as appropriate
- Edit and pick first breaks
- Tabulate elevations for shot point and geophone locations
- Develop time-distance curves
- Assign layers
- Determine apparent velocities and intercept times
- Determine reciprocal times
- Apply the GRM analysis
- Develop time-depth-velocity sections
- Develop final velocity and depth sections.

B.2.4 RESULTS

Several generalities can be drawn from the refraction data. The data depicts three to four velocity layers in the upper 30 m (100 ft). These layers are variable, which is, in part, a function of geology. Unfortunately, uncertainties in the data also contributed to the apparent layer variability. Nonetheless, the general velocity structure and depths were useful for guidelines into the seismic reflection processing. Some generalities drawn from the refraction data are discussed here. General recommendations for improving refraction data are presented in Chapter 5.0.

The first layer is interpreted as unconsolidated eolian silts and sands, varying in thickness from 0 to about 6 m (20 ft). This layer has seismic velocities ranging from 305 m/s (1,000 ft/s) to possibly as high as 760 m/s (2,500 ft/s). The eolian layer is evident in Figure B-2 from line 1-3W-1. Figure B-2 shows a typical seismic refraction section with travel-time curves, depth sections, and velocity sections. The eolian layer, as interpreted from the refraction data, is pervasive throughout the study area and correlates well with information from the ground-penetrating radar (GPR) data.

Refraction layer 2 corresponds generally with the Hanford formation. This layer is sufficiently thick with a good velocity contrast with the overlying eolian silts and sands. The velocity of this layer appears to range from 0.9 to 1.5 km/s (3,000 to 5,000 ft/s). On line 1-3W-1, this layer appears to vary in thickness from 3 to 15 m (10 to 50 ft). Unfortunately, layer 2 may not have a sufficiently large or sharp enough velocity contrast with layer 3 to define this boundary clearly. Factors like these must be carefully considered before drawing conclusions from refraction data.

Layer 3 is interpreted as Ringold Formation. Velocities of this layer may vary widely, ranging from 1.5 to 3.0 km/s (5,000 to 10,000 ft/s). Stratigraphic horizons, such as the lower mud and basalt, were not detected in this survey.

B.3.0 GPR

B.3.1 INTRODUCTION

GPR uses a high-frequency signal that is transmitted into the ground, operating typically in the 10's-to-100's-MHz range. The transmitted energy is reflected back to a receiving antenna where variations in the return signal are recorded. The results are a continuous profile of the subsurface conditions. The recorded reflections are from materials having a variety of electrical properties. Common reflectors include natural geologic conditions, such as bedding, cementation, moisture, and clay, or artificial objects, such as pipes and buried wires. Depth of penetration at the Hanford Site is generally between 1 to 5 m, depending on the subsurface conditions, which can vary from site to site.

The GPR surveys were expected to provide shallow stratigraphic information, especially at shallow depths where seismic methods tend to be ineffective. In addition, identifying variations in the shallow horizons could help define potential hydrologic channeling.

B.3.2 DATA ACQUISITION

Data were collected with a Geophysical Survey Systems Inc. Subsurface Interface Radar System 8, model 4800, and digitally stored on tape. Both 100-MHz and 300-MHz antennas were used.

The 100-MHz antenna did not penetrate appreciably deeper than the 300-MHz antenna, but did have lower resolution than the 300-MHz antenna. Therefore, the majority of the GPR surveys utilized the 300-MHz antenna.

Recording "windows" ranging from 90 to 150 nanoseconds (two-way travel time) were tested. Minimal data were detected below 120 nanoseconds; therefore, profiles were primarily collected with a 120-nanosecond window to maximize resolution.

The GPR data were collected along profiles coincident with the seismic reflection profiles (Figure A-1). Additional data are concentrated along line 1-3 central (Figure A-2). Surveyed locations are marked on the GPR profiles every 61 m (200 ft). Locations between these known points are interpolated.

B.3.3 DATA PROCESSING

The display and interpretation of the data are similar to seismic reflection data. Sections are presented with the horizontal distance across the section. The vertical scale on the sections is two-way travel time. As in seismic reflection, this time can be generally related to depth if velocity is known. Throughout most of the Hanford Site, electromagnetic velocities for the radar signal in the sediments is on the order of 3 ns/0.305 m (1 ft).

9 1 1 9 0 4 1 3

This results in a two-way travel time of 6 ns/.3 m (1 ft), and is what is plotted on the GPR sections. Therefore, with a 100-nanosecond window, full scale on the sections is about 5 m (16 ft).

Postacquisition processing was minimal for the data collected for this survey. Filtering of the data was attempted, but the data were not significantly enhanced.

B.3.4 RESULTS

The GPR data was used extensively as a "stand-alone" method to depict the near-surface geologic setting, to be a tool in the overall integrated geologic interpretation, and to evaluate velocities and topography for the seismic processing/interpretation. The data quality is good throughout most of the survey area, yielding usable data down to depths of 3 to 4.6 m (10 to 15 ft). Discussion and interpretations of the data are integrated into Chapter 4.0, "Data Analysis/Interpretation." The entire set of GPR profiles are contained in data package WHC-SD-EN-DP-059, Rev. 0 (Kunk 1992).

B.4.0 ELECTROMAGNETIC INDUCTION (EMI)

B.4.1 INTRODUCTION

EMI surveys are used to determine the electrical conductivity/resistivity structure of the subsurface soil, rock, and groundwater. The tools used for this work are generally used for shallow investigations, ranging from a few meters to tens of meters. The method is based on a transmitting coil radiating an electromagnetic field that induces eddy currents in the earth. A resulting secondary electromagnetic field is measured at a receiving coil and can be linearly related to the subsurface conductivity.

Ground conductivity is a function of the natural soil matrix and pore fluid electrical conductivity. The depth of investigation is primarily dependent upon the electrical conductivity of the subsurface, the distance between the transmitting and receiving coils, and the operating frequency. The conductivity value resulting from a measurement is a "composite," representing the combined effects of the thickness of the stratigraphic layers; their depths; their specific conductivities; and any artificial conductive objects that may be present, such as metal objects. Metallic objects generally overwhelm the natural conductivity.

The EMI surveys were utilized to explore for shallow zones of anomalous conductivities. Anomalous ground conductivities can be a function of several parameters, including texture and composition of the sediments, that might be correlative to hydrologic barriers/channels.

B.4.2 DATA ACQUISITION

The Westinghouse Hanford Company operates for the U.S. Department of Energy a Geonics' EM-31¹ ground conductivity meter. This instrument was used for the initial reconnaissance EMI surveys. The EM-31 has an intercoil spacing of 3.66 m (12 ft), operating frequency of 9.8 kHz, yielding a depth of exploration of about 6 m (20 ft).

The data are digitally stored in the field for "dumping" to computer later. This allows for display in profile form and in contour map form when appropriate.

Data were collected primarily along seismic profiles rather than preferred grids because of the reconnaissance nature of the geophysical surveys and the size of the area being investigated (Figure A-3). Station spacing was 3 m (10 ft) at surveyed locations on the profiles. EMI stations are the same as the GPR locations, which, in turn, are related to the seismic reflection locations by a factor of five. Additional data were collected near well 1-18 to trace an anomaly detected along seismic line 3-5 (Figure A-4).

B.4.3 DATA PROCESSING

The data are plotted in profile form. A contour map of the gridded data that was collected near well 1-18 was produced using a computer contouring package.

B.4.4 RESULTS

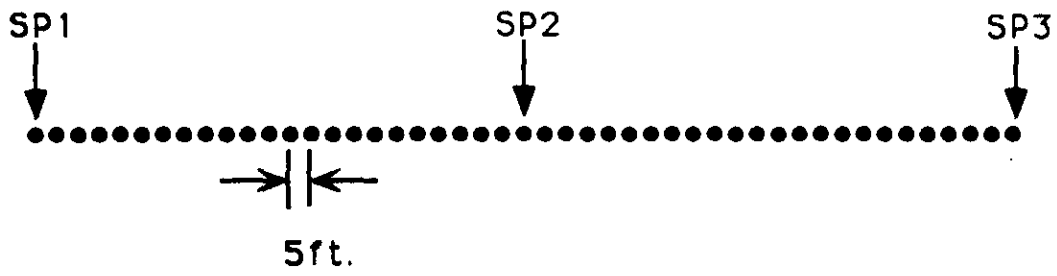
Most variations in the EMI data can be inversely attributed to the topography (i.e., the EMI lows correspond with topographic highs, and EMI highs correspond with topographic lows). The EMI data correlates with the GPR data throughout most of the areas where both were collected.

The EMI and GPR data are integrated and presented as a comprehensive interpretation of the shallower strata as discussed in Chapter B.4.0 and Appendix A. The complete data set is available in data package WHC-SD-EN-OP-059, Rev. 0 (Kunk 1992).

¹Geonics EM-31 is a trademark of Geophysical Instrument and Supply Company, Incorporated.

9 1 1 3 0 4 0 9 5

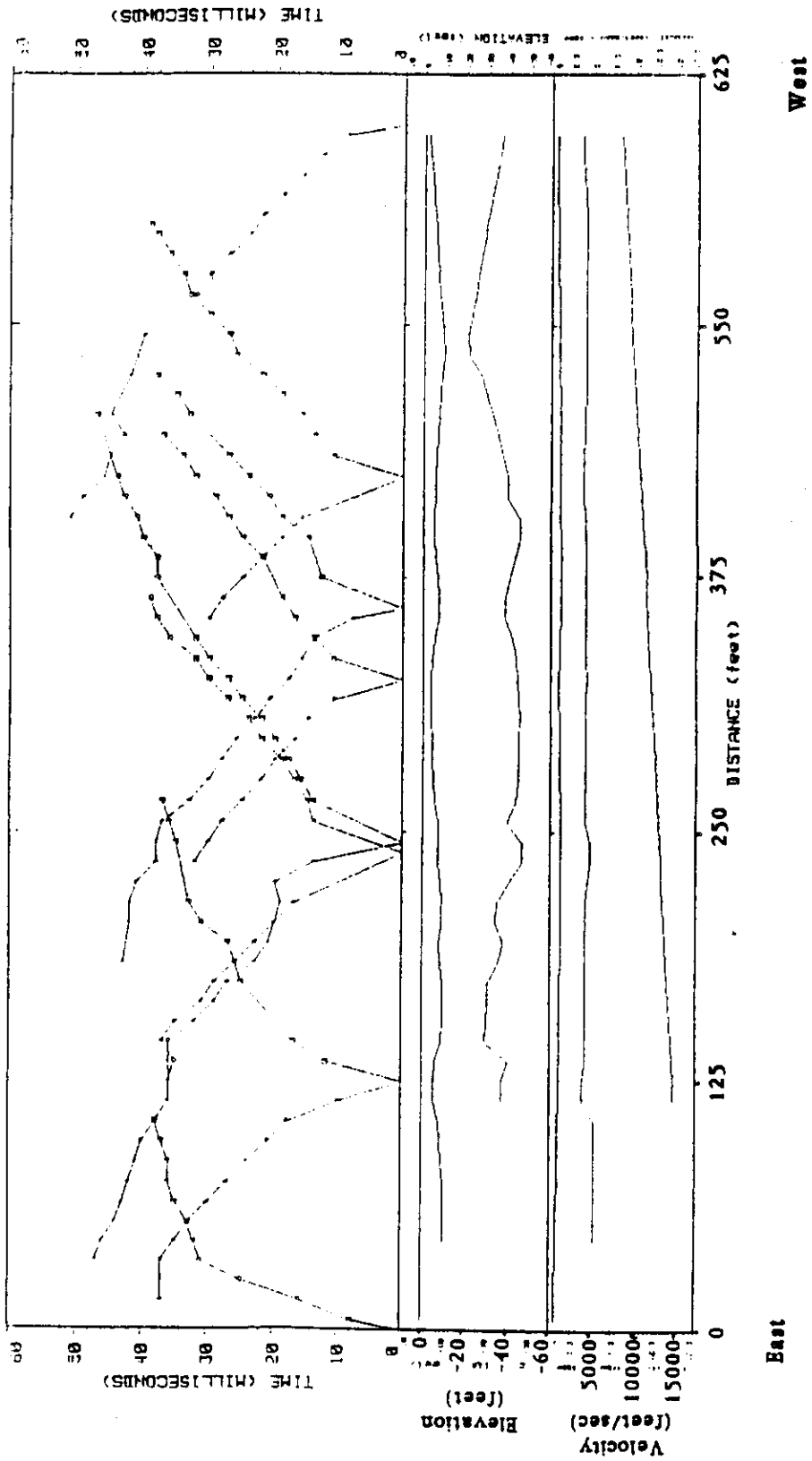
Figure B-1. Seismic Refraction Layout.



- SP1 - Shot Point Location
- - Geophone Location

9 1 3 0 4 0 8 5 6

Figure B-2. Interpreted Seismic Refraction Profile Along Line 1-3W-1, Utilizing the Generalized Reciprocal Method.



9 1 1 9 0 4 1 9 9 7

APPENDIX C

VELOCITY/DEPTH PROFILES

9 0 1 4 9 0 4 7 3 8 8

This page intentionally left blank.

9 1 2 3 4 5 6 7 8 9

APPENDIX C

VELOCITY/DEPTH PROFILES

In general, a sonic log represents direct measurements of the velocity of the strata. Seismic reflection data collected from the surface, on the other hand, provide an indirect measurement of velocity. Based on these two types of information, numerous velocity values used in seismic processing are derived, such as apparent, interval, average, root-mean-square, instantaneous, phase, group, normal moveout (NMO), stacking, and migration velocities. All of the velocities are related. Due to the lack of direct borehole information (i.e., sonic logs, velocity profiling, etc.), selecting the appropriate velocities became a very laborious task using primarily "trial and error." The velocities tabulated below are those that yielded the best stack. It is believed that with additional velocity analysis and direct measurements of the velocity from boreholes, the final seismic sections could be improved upon.

The following data are the interval and NMO velocity data used to process the seismic reflection data for the 300-FF-5 operable unit. The data are listed according to common midpoints (CMP) along each line. The NMO velocities are those used to correct the seismic data for NMO due to the geometry of the data acquisition. The interval velocities were calculated from the average velocities using Dix's equation (Dobrin 1976). As can be observed, there are considerable horizontal variations between interval velocities that are consistent with sediments deposited in a fluvial environment.

LINE 1-3N							
CMP	TIME	NMO VELOCITY	INTERVAL VELOCITY	CMP	TIME	NMO VELOCITY	INTERVAL VELOCITY
1594.0	54	2229.0	2229.0	1604.0	51	2200.0	2200.0
	74	2450.0	2965.5		72	2446.0	2959.5
	94	2648.0	3278.2		90	3200.0	5221.9
	190	6000.0	8024.0		193	6000.0	7649.1
1618.0	47	2300.0	2300.0	1624.0	53	2272.0	2272.0
	62	2750.0	3831.8		86	2592.0	3036.2
	90	3250.0	4147.9		114	3000.0	4000.9
	115	3600.0	4646.6		188	6000.0	8808.8
	135	4000.0	5786.2				
	190	6000.0	9224.5				

9 1 1 9 0 4 0 9 6 0

CMP	TIME	NMO VELOCITY	INTERVAL VELOCITY	CMP	TIME	NMO VELOCITY	INTERVAL VELOCITY
1652.0	40	2273.0	2273.0	1672.0	47	2281.0	2281.0
	67	2517.0	2840.2		67	2354.0	2517.2
	97	2911.0	3640.1		106	2653.0	3100.1
	187	5673.0	7598.4		128	3111.0	4732.6
200					6000.0	9099.1	
1700.0	41	2126.0	2126.0	1726.0	40	2300.0	2300.0
	76	2369.0	2625.2		54	2450.0	2835.2
	93	2857.0	4423.1		79	2600.0	2897.6
	174	5855.0	8016.8		111	3100.0	4079.9
190					6000.0	8548.7	
1756.0	53	2011.0	2011.0	1822.0	47	2361.0	2361.0
	65	2300.0	3285.2		65	2400.0	2499.0
	92	2679.0	3423.4		95	3062.0	4148.5
	190	5000.0	6460.0		113	3400.0	4804.9
183					6000.0	8686.4	
1878.0	53	2077.0	2077.0	1908.0	54	2078.0	2078.0
	71	2250.0	2695.7		76	2369.0	2964.5
	84	2786.0	4743.8		97	3000.0	4610.9
	97	3000.0	4123.2		178	5800.0	7946.5
	190	6000.0	8010.1				
1950.0	46	1744.0	1744.0	1970.0	46	1744.0	1744.0
	65	2182.0	2987.4		56	1969.0	2778.5
	83	2500.0	3409.8		81	2500.0	3400.8
	137	4100.0	5748.1		137	4100.0	5664.3
	178	5800.0	9480.3		172	5800.0	9975.8
1984.0	46	1744.0	1744.0				
	56	1969.0	2778.5				
	81	2500.0	3400.8				
	137	4100.0	5664.3				
	172	5800.0	9975.8				

9 1 0 0 4 0 0 6 1

LINE 2-3

CMP	TIME	NMO VELOCITY	INTERVAL VELOCITY	CMP	TIME	NMO VELOCITY	INTERVAL VELOCITY
144.0	56	2100.0	2100.0	238.0	50	1744.0	1744.0
	78	2236.0	2549.7		80	2208.0	2816.3
	94	2780.0	4585.9		103	2800.0	4260.5
	175	5500.0	7509.1		181	5500.0	7735.8
346.0	60	2250.0	2250.0	368.0	67	2193.0	2193.0
	81	2399.0	2781.1		95	2445.0	2962.2
	95	2445.0	2695.8		120	3000.0	4525.9
	190	5500.0	7383.9		190	5500.0	8165.7
410.0	53	2033.0	2033.0	426.0	50	2022.0	2022.0
	67	2193.0	2714.6		78	2307.0	2743.2
	90	2445.0	3063.1		137	4100.0	5656.6
	120	3000.0	4250.4		172	5500.0	9102.6
	190	5500.0	8165.7				
444.0	54	2200.0	2200.0	510.0	62	2058.0	2058.0
	69	2330.0	2747.5		78	2195.0	2660.0
	128	3500.0	4497.5		118	3000.0	4141.8
	172	5500.0	9089.2		178	5500.0	8487.7
556.0	46	1744.0	1744.0				
	56	1969.0	2778.5				
	81	2500.0	3400.8				
	137	4100.0	5664.3				
	172	5500.0	9102.6				

LINE 3-5

368.0	61	2200.0	2200.0	392.0	58	2200.0	2200.0
	78	2400.0	3010.2		78	2400.0	2903.1
	127	3600.0	4941.8		91	2500.0	3031.5
	180	5500.0	8466.4		110	3200.0	5417.6
					140	4000.0	6092.6
					167	5500.0	10204.8

93113040952

CMP	TIME	NMO VELOCITY	INTERVAL VELOCITY	CMP	TIME	NMO VELOCITY	INTERVAL VELOCITY
400.0	61	2100.0	2100.0	414.0	49	2300.0	2300.0
	75	2250.0	2811.7		65	2400.0	2683.2
	108	3000.0	4236.6		106	2800.0	3337.3
	142	4000.0	6183.5		138	4300.0	7332.7
	170	5500.0	10125.1		165	6600.0	13103.3
442.0	49	2150.0	2150.0	450.0	49	2200.0	2200.0
	69	2300.0	2631.6		72	2350.0	2641.3
	106	2750.0	3435.2		106	2550.0	2928.8
	138	4300.0	7395.1		138	3200.0	4756.1
	165	6000.0	11202.5		165	6600.0	14624.0
476.0	49	2200.0	2200.0	486.0	49	2200.0	2200.0
	69	2300.0	2528.3		70	2300.0	2517.9
	90	2400.0	2702.6		97	2900.0	4061.9
	101	2500.0	3203.0		144	4300.0	6268.4
	138	3200.0	4596.9		175	5000.0	7432.4
	165	6000.0	12948.4				
492.0	53	2200.0	2200.0	502.0	52	2250.0	2250.0
	72	2450.0	3040.6		68	2300.0	2455.5
	98	2900.0	3882.9		90	2400.0	2685.7
	175	6500.0	9236.8		103	2600.0	3699.1
				153	4000.0	5919.0	
				175	6000.0	13232.2	
510.0	52	2250.0	2250.0	564.0	60	2050.0	2050.0
	68	2300.0	2455.5		80	2200.0	2598.6
	90	2400.0	2685.7		105	2638.0	3706.7
	103	2600.0	3699.1		137	4500.0	7991.3
	153	4000.0	5919.0		179	6000.0	9347.5
	175	6000.0	13232.2				

9 1 1 0 0 4 0 6 3

CMP	TIME	NMO VELOCITY	INTERVAL VELOCITY	CMP	TIME	NMO VELOCITY	INTERVAL VELOCITY
580.0	60	2000.0	2000.0	600.0	60	2000.0	2000.0
	80	2200.0	2712.9		80	2200.0	2712.9
	105	2249.0	2399.1		105	2470.0	3183.7
	137	3000.0	4683.4		137	2739.0	3478.5
	179	5000.0	8785.8		167	3180.0	4693.9
620.0	47	2000.0	2000.0	632.0	47	1800.0	1800.0
	58	2116.0	2552.9		62	2500.0	3960.0
	99	2740.0	3434.3		97	3000.0	3724.4
	155	5500.0	8393.8		155	5500.0	8111.0
656.0	47	1800.0	1800.0	680.0	46	2140.0	2140.0
	62	2500.0	3960.0		65	2300.0	2647.6
	97	3150.0	4053.2		92	2600.0	3209.2
	155	5500.0	8015.4		122	3750.0	6037.9
					156	5700.0	9930.4
698.0	53	2000.0	2000.0	712.0	60	2100.0	2100.0
	67	2100.0	2441.7		83	2370.0	2960.6
	101	2600.0	3375.0		106	2600.0	3299.3
	122	3750.0	7013.1		142	4000.0	6573.2
	160	5000.0	7753.4				
726.0	60	2100.0	2100.0	742.0	64	2200.0	2200.0
	88	2370.0	2864.1		83	2350.0	2796.7
	110	2600.0	3366.4		110	2600.0	3250.3
	142	4000.0	6911.0		145	4000.0	6711.2
					175	6000.0	11518.1
750.0	60	2200.0	2200.0	846.0	48	1744.0	1744.0
	83	2350.0	2702.4		56	1969.0	2981.5
	110	2600.0	3250.3		81	2500.0	3400.8
	145	4000.0	6711.2		137	4100.0	5664.3
	175	6000.0	11518.1		172	5500.0	9102.6

9 1 1 2 0 4 2 3 6 4

CMP	TIME	NMO VELOCITY	INTERVAL VELOCITY	CMP	TIME	NMO VELOCITY	INTERVAL VELOCITY
894.0	50	1739.0	1739.0				
	70	3200.0	5317.9				
	81	3500.0	5004.1				
	96	4000.0	6020.8				
	134	4450.0	5423.0				
	165	5200.0	7637.1				
LINE 4-2							
46.0	42	1729.0	1729.0	48.0	43	1650.0	1650.0
	65	1809.0	1946.6		78	1950.0	2264.8
	81	2198.0	3341.2		97	2500.0	4037.0
	109	2368.0	2802.3		112	2600.0	3171.4
	144	3500.0	5739.1		158	3700.0	5528.4
	190	6000.0	10504.7		175	6000.0	15599.7
54.0	42	1800.0	1800.0	80.0	42	2244.0	2244.0
	80	2169.0	2514.6		51	2362.0	2848.8
	102	2477.0	3367.4		65	2500.0	2948.6
	124	3601.0	6681.4		81	2811.0	3822.5
	181	5600.0	8448.2		132	4437.0	6197.2
					167	5800.0	9287.8
124.0	43	1800.0	1800.0	158.0	47	1840.0	1840.0
	74	1900.0	2030.6		62	1907.0	2103.2
	85	2005.0	2603.5		85	2005.0	2248.0
	106	2400.0	3578.1		110	2400.0	3417.0
	144	3000.0	4247.1		141	3000.0	4527.3
	180	5557.0	10881.2		180	6000.0	11559.2
200.0	48	1860.0	1860.0	224.0	51	1777.0	1777.0
	71	2012.0	2297.0		71	1951.0	2336.8
	124	2500.0	3033.1		87	2052.0	2450.5
	149	3000.0	4758.2		100	2467.0	4317.0
	180	6000.0	12875.3		148	3800.0	5643.0

9 1 1 9 0 4 0 6 5

CMP	TIME	NMO VELOCITY	INTERVAL VELOCITY	CMP	TIME	NMO VELOCITY	INTERVAL VELOCITY
230.0	48	1900.0	1900.0	250.0	48	1900.0	1900.0
	83	2040.0	2217.7		71	2000.0	2194.1
	94	2100.0	2506.8		90	2127.0	2546.1
	113	2500.0	3918.3		123	2600.0	3585.8
	147	3050.0	4409.9		147	3050.0	4725.8
	191	3808.0	5645.2		191	6000.0	11189.0
264.0	50	1825.0	1825.0	270.0	50	1940.0	1940.0
	81	2050.0	2368.3		79	2100.0	2350.4
	119	2718.0	3765.2		95	2300.0	3104.0
	156	3700.0	5827.5		142	3058.0	4190.5
	175	6000.0	14804.6		201	7000.0	12017.7
290.0	50	1940.0	1940.0	346.0	56	1900.0	1900.0
	79	2200.0	2587.6		79	2030.0	2316.2
	115	2675.0	3498.2		105	2200.0	2650.5
	147	4000.0	6912.6		140	3500.0	5872.0
	183	6000.0	10847.4		162	4200.0	7206.9
				180	5500.0	11989.2	
374.0	58	1950.0	1950.0	376.0	55	1900.0	1900.0
	82	2030.0	2211.4		82	2030.0	2271.9
	100	2672.0	4570.7		100	2700.0	4661.2
	134	3040.0	3927.3		137	3050.0	3839.5
	158	5000.0	10629.4		163	6000.0	13291.9
422.0	60	1879.0	1879.0	488.0	65	2050.0	2050.0
	82	2100.0	2609.3		78	2127.0	2476.3
	99	2800.0	4938.1		94	2600.0	4202.4
	130	3500.0	5131.6		142	3600.0	5010.2
	163	5800.0	10858.3		163	5700.0	12827.7

9 3 1 1 9 0 4 1 0 5 6

CMP	TIME	NMO VELOCITY	INTERVAL VELOCITY	CMP	TIME	NMO VELOCITY	INTERVAL VELOCITY
490.0	65	2100.0	2100.0	500.0	59	1950.0	1950.0
	76	2127.0	2280.0		80	2275.0	3005.6
	93	2800.0	4760.7		101	2575.0	3489.1
	137	4200.0	6193.0		131	2900.0	3794.8
	160	6000.0	12056.6		179	6000.0	10549.8
538.0	58	1950.0	1950.0	586.0	59	2100.0	2100.0
	77	2200.0	2829.7		74	2200.0	2555.6
	103	2325.0	2661.0		109	2375.0	2708.0
	135	3150.0	4945.8		143	3000.0	4446.3
	177	6000.0	10946.3		174	6000.0	12670.8
604.0	57	2200.0	2200.0	624.0	58	2200.0	2200.0
	95	2300.0	2442.3		77	2300.0	2581.4
	115	2400.0	2827.1		102	2400.0	2684.7
	136	3200.0	5896.9		119	2600.0	3572.1
	174	6200.0	11805.4		141	3300.0	5764.5
				182	6500.0	12251.4	
630.0	58	2200.0	2200.0	646.0	58	2200.0	2200.0
	74	2300.0	2630.8		72	2300.0	2674.7
	102	2500.0	2964.3		104	2600.0	3172.9
	138	3200.0	4641.7		128	3000.0	4325.1
	182	6600.0	12168.1		172	6200.0	11139.3
672.0	57	2200.0	2200.0	690.0	44	2000.0	2000.0
	107	2600.0	2991.5		60	2200.0	2673.9
	174	6000.0	9093.8		84	2578.0	3340.9
					106	3210.0	4926.6
				176	6000.0	8655.1	
706.0	58	2056.0	2056.0	738.0	40	2025.0	2025.0
	87	2672.0	3600.6		67	2150.0	2322.9
	109	4092.0	7397.8		99	3100.0	4478.0
	135	5351.0	8858.6		128	3875.0	5785.3
	156	6200.0	10073.9		172	6000.0	9851.2

9 1 9 0 4 1 9 5 7

LINE 8-5-2 NORTH

CMP	TIME	NMO VELOCITY	INTERVAL VELOCITY	CMP	TIME	NMO VELOCITY	INTERVAL VELOCITY
1104.0	57	2350.0	2350.0	1120.0	54	1920.0	1920.0
	82	2500.0	2812.2		72	2071.0	2469.2
	102	2700.0	3399.1		95	2500.0	3519.8
	119	3695.0	7199.4		142	3519.0	4978.0
	178	6000.0	9004.0		178	6000.0	11364.6
1122.0	48	1960.0	1960.0	1128.0	59	2150.0	2150.0
	72	2158.0	2507.5		73	2227.0	2525.8
	110	2500.0	3044.4		87	2600.0	4018.5
	138	3500.0	5985.1		126	4009.0	6070.0
	174	6000.0	11271.3		149	4600.0	7002.4
				181	6000.0	10251.8	
1136.0	57	2000.0	2000.0	1150.0	63	2259.0	2259.0
	74	2115.0	2461.7		79	2390.0	2847.8
	87	2262.0	2963.0		138	3370.0	4349.2
	126	4009.0	6364.8		181	6000.0	10727.9
	149	4600.0	7002.4				
181	6000.0	10251.8					
1160.0	49	2068.0	2068.0	1170.0	45	2075.0	2075.0
	76	2232.0	2502.3		60	2228.0	2634.2
	94	2529.0	3516.6		74	2400.0	3028.4
	126	3800.0	6170.1		104	3000.0	4122.1
	149	5000.0	9102.2		136	5000.0	8775.0
	181	6000.0	9339.1		181	6000.0	8321.3
1180.0	45	2000.0	2000.0	1194.0	49	2215.0	2215.0
	60	2141.0	2517.0		65	2400.0	2893.9
	85	2664.0	3623.3		85	2664.0	3382.6
	118	3500.0	5052.0		115	3500.0	5181.7
	149	4600.0	7421.3		151	4600.0	7044.3
	181	6000.0	10251.8		181	6000.0	10521.2

91100040968

CMP	TIME	NMO VELOCITY	INTERVAL VELOCITY	CMP	TIME	NMO VELOCITY	INTERVAL VELOCITY
1236.0	46	2215.0	2215.0	1248.0	62	2278.0	2278.0
	62	2400.0	2866.1		78	2722.0	4001.5
	78	2664.0	3503.9		94	2977.0	3993.4
	119	3500.0	4696.1		121	3300.0	4236.6
	151	4600.0	7368.4		144	4548.0	8497.7
	181	6000.0	10521.2		175	5900.0	10021.3
1268.0	64	2300.0	2300.0	1302.0	63	2100.0	2100.0
	78	2468.0	3123.0		81	2250.0	2710.4
	126	3400.0	4521.8		103	2723.0	4009.4
	144	4548.0	9195.3		121	3062.0	4538.5
	175	5900.0	10021.3		146	4500.0	8537.0
					189	6000.0	9459.2
1320.0	54	2030.0	2030.0	1342.0	39	2111.0	2111.0
	78	2300.0	2814.3		61	2300.0	2601.5
	92	2370.0	2727.3		78	2468.0	2994.2
	115	3000.0	4746.8		92	2648.0	3484.6
	144	4548.0	8186.5		144	4548.0	6698.8
	175	5900.0	10021.3		175	5900.0	10021.3
1356.0	39	2110.0	2110.0	1404.0	61	2200.0	2200.0
	62	2241.0	2447.2		80	2362.0	2819.9
	99	2900.0	3753.3		95	2600.0	3613.6
	119	3066.0	3781.9		123	3015.0	4122.7
	150	3800.0	5812.5		178	5500.0	8807.4
	181	6000.0	11845.8				
1442.0	51	2200.0	2200.0	1456.0	57	2238.0	2238.0
	65	2350.0	2830.0		76	2496.0	3145.5
	85	2545.0	3095.0		90	2600.0	3104.4
	180	5700.0	7467.6		124	3200.0	4410.4
					179	5900.0	9497.6

9 1 1 0 0 4 1 9 3 9

CMP	TIME	NMO VELOCITY	INTERVAL VELOCITY	CMP	TIME	NMO VELOCITY	INTERVAL VELOCITY
1482.0	54	2238.0	2238.0	1502.0	55	2193.0	2193.0
	70	2400.0	2880.2		87	2500.0	2954.0
	87	2600.0	3298.1		138	3266.0	4266.3
	179	5900.0	7831.7		187	6050.0	10471.2
1516.0	58	2162.0	2162.0	1562.0	45	2300.0	2300.0
	80	2434.0	3036.5		61	2400.0	2661.2
	105	3000.0	4340.7		107	3000.0	3646.4
	149	4000.0	5718.8		167	6000.0	9173.3
	181	6000.0	11363.3				
1576.0	47	2300.0	2300.0	1584.0	47	2250.0	2250.0
	60	2407.0	2759.4		60	2357.0	2708.8
	75	2550.0	3055.8		75	2500.0	3004.7
	100	3152.0	4498.1		100	3000.0	4153.3
	167	6000.0	8654.6		167	6000.0	8734.9
1620.0	55	2200.0	2200.0	1628.0	60	2357.0	2357.0
	72	2300.0	2597.3		75	2500.0	3004.7
	103	3200.0	4662.3		103	3000.0	4045.5
	131	4000.0	6098.2		167	6000.0	8913.6
	183	6000.0	9294.3				
1640.0	51	2200.0	2200.0	1646.0	60	2100.0	2100.0
	81	2350.0	2585.1		88	2208.0	2423.3
	102	2500.0	3009.3		131	2750.0	3614.1
	145	3200.0	4439.0		178	6000.0	10736.0
	176	6000.0	12509.6				
1654.0	56	2100.0	2100.0				
	85	2300.0	2643.7				
	131	3651.0	5309.0				
	178	6000.0	9959.3				

9 3 1 0 9 0 4 1 9 7 0

LINE 8-5-2 SOUTH

CMP	TIME	NMO VELOCITY	INTERVAL VELOCITY	CMP	TIME	NMO VELOCITY	INTERVAL VELOCITY
44.0	50	1954.0	1954.0	110.0	49	2071.0	2071.0
	95	2132.0	2313.8		65	2093.0	2159.0
	187	4500.0	6038.8		84	2380.0	3171.1
					190	3622.0	4361.9
192.0	55	1950.0	1950.0	234.0	59	2091.0	2091.0
	69	2015.0	2252.3		74	2315.0	3039.9
	116	2596.0	3266.8		135	3000.0	3662.9
	172	3802.0	5517.1		183	4500.0	7203.5
252.0	65	2070.0	2070.0	298.0	38	1933.0	1933.0
	81	2213.0	2717.6		58	2124.0	2446.2
	154	2742.0	3229.1		82	2459.0	3123.6
	193	5367.0	10623.4		173	4152.0	5227.3
398.0	56	2096.0	2096.0	404.0	42	2067.0	2067.0
	134	2490.0	2738.1		66	2063.0	2056.0
	145	2789.0	5196.8		108	2374.0	2793.6
	169	4200.0	8787.5		185	4018.0	5557.3
430.0	46	2350.0	2350.0	468.0	42	2263.0	2263.0
	87	2417.0	2490.0		58	2337.0	2520.9
	192	3900.0	4792.9		140	3123.0	3576.1
					189	4324.0	6652.1
492.0	35	2151.0	2151.0	618.0	59	2121.0	2121.0
	83	2257.0	2331.3		92	2528.0	3126.3
	145	2447.0	2680.4		115	3211.0	5098.0
	192	3643.0	5978.5		161	3756.0	4858.0
674.0	56	2322.0	2322.0	780.0	51	1895.0	1895.0
	104	2620.0	2929.6		62	2179.0	3180.0
	171	3059.0	3636.9		87	2245.0	2400.9
					147	3306.0	4412.4
					189	4324.0	6773.7

9 1 1 0 9 0 4 1 0 7 1

CMP	TIME	NMO VELOCITY	INTERVAL VELOCITY	CMP	TIME	NMO VELOCITY	INTERVAL VELOCITY
872.0	62	2053.0	2053.0				
	102	2342.0	2730.1				
	147	3050.0	4237.4				
	183	4603.0	8349.8				
LINE 4-5							
44.0	46	1850.0	1850.0	50.0	46	1850.0	1850.0
	75	2250.0	2768.4		77	2107.0	2438.9
	95	2500.0	3271.6		97	2300.0	2926.5
	117	2900.0	4211.6		120	3000.0	4964.5
	147	3500.0	5217.9		178	5368.0	8355.4
62.0	49	1925.0	1925.0	80.0	42	1975.0	1975.0
	69	2050.0	2328.1		59	2212.0	2710.1
	95	2300.0	2859.4		83	2415.0	2853.3
	112	2500.0	3408.0		115	3194.0	4640.6
	147	3500.0	5608.0		167	5800.0	9245.3
	165	6000.0	15164.4				
96.0	45	1800.0	1800.0	104.0	47	1861.0	1861.0
	74	2065.0	2419.4		70	1900.0	1977.3
	94	2400.0	3360.7		95	2300.0	3161.3
	125	3000.0	4338.7		125	2900.0	4276.7
	147	5500.0	12287.7		147	3500.0	5836.8
					173	6000.0	13049.1
136.0	49	1721.0	1721.0	148.0	52	1700.0	1700.0
	70	1800.0	1972.1		70	1800.0	2061.8
	97	2300.0	3256.5		97	2300.0	3256.5
	111	2600.0	4116.4		111	2600.0	4116.4
	147	3500.0	5401.6		147	3500.0	5401.6
162.0	53	1727.0	1727.0	166.0	58	1800.0	1800.0
	74	1960.0	2451.5		74	1960.0	2454.1
	84	2100.0	2935.3		87	2150.0	3011.2
	115	2686.0	3848.9		117	2554.0	3469.0
	160	3550.0	5135.3		147	3500.0	5881.0

9 3 1 4 9 0 4 7 2

CMP	TIME	NMO VELOCITY	INTERVAL VELOCITY	CMP	TIME	NMO VELOCITY	INTERVAL VELOCITY
182.0	58	1850.0	1850.0	204.0	57	1971.0	1971.0
	71	1922.0	2214.9		84	2100.0	2349.2
	87	2150.0	2956.7		115	2686.0	3848.9
	115	2600.0	3660.8		160	3550.0	5135.3
	147	3500.0	5655.1				
234.0	57	1971.0	1971.0	240.0	58	1850.0	1850.0
	84	2100.0	2349.2		91	2200.0	2707.6
	115	2686.0	3848.9		115	2759.0	4257.1
	160	3550.0	5135.3		147	3500.0	5377.5
288.0	62	1950.0	1950.0	344.0	69	1900.0	1900.0
	84	2050.0	2308.6		93	2000.0	2263.0
	115	2500.0	3434.8		117	2389.0	3510.4
	147	3500.0	5814.9		175	3800.0	5661.8
376.0	64	2000.0	2000.0	380.0	64	2000.0	2000.0
	99	2186.0	2490.4		99	2186.0	2490.4
	115	2500.0	3918.5		115	2500.0	3918.5
	158	3600.0	5559.3		158	3600.0	5559.3
				180	3924.0	5736.3	
410.0	61	2000.0	2000.0	426.0	61	2100.0	2100.0
	99	2186.0	2455.3		99	2186.0	2317.4
	115	2500.0	3918.5		115	2500.0	3918.5
	158	3600.0	5559.3		158	3600.0	5559.3
	180	3924.0	5736.3		180	3924.0	5736.3
430.0	61	2100.0	2100.0	442.0	61	2100.0	2100.0
	99	2200.0	2351.7		99	2200.0	2351.7
	115	2500.0	3869.7		110	2454.0	4081.8
	158	3600.0	5559.3		158	3600.0	5372.1
	180	3924.0	5736.3		180	3924.0	5736.3

9 3 1 3 9 0 4 0 7 3

CMP	TIME	NMO VELOCITY	INTERVAL VELOCITY	CMP	TIME	NMO VELOCITY	INTERVAL VELOCITY
452.0	59	2000.0	2000.0	464.0	59	2000.0	2000.0
	87	2130.0	2380.8		87	2130.0	2380.8
	112	2700.0	4107.4		112	2700.0	4107.4
	132	3000.0	4310.0		132	3000.0	4310.0
	176	3940.0	5924.1		176	3940.0	5924.1
476.0	64	2105.0	2105.0	482.0	47	1900.0	1900.0
	90	2200.0	2418.0		64	2105.0	2588.6
	105	2400.0	3358.6		90	2200.0	2418.0
	132	3000.0	4647.6		105	2400.0	3358.6
	175	3950.0	5989.2		132	3000.0	4647.6
					175	3950.0	5989.2
520.0	69	2075.0	2075.0	524.0	47	1900.0	1900.0
	84	2115.0	2290.0		66	2100.0	2527.6
	104	2500.0	3703.0		87	2200.0	2488.3
	122	3300.0	6139.9		104	2500.0	3669.6
	147	4500.0	8119.5		132	3500.0	5876.7
					158	4700.0	8488.0
534.0	55	2000.0	2000.0	536.0	55	2000.0	2000.0
	69	2050.0	2235.6		69	2050.0	2235.6
	87	2400.0	3425.0		87	2400.0	3425.0
	126	4009.0	6251.1		126	4009.0	6251.1
	149	4600.0	7002.4		145	4600.0	7409.5
556.0	41	1900.0	1900.0	564.0	55	2000.0	2000.0
	59	2150.0	2632.3		69	2050.0	2235.6
	83	2496.0	3190.9		87	2300.0	3075.5
	116	2700.0	3155.3		115	3800.0	6547.5
	130	3000.0	4813.4		126	4009.0	5756.3
	158	3500.0	5228.7		149	4600.0	7002.4

9 1 1 9 0 4 0 3 7 4

CMP	TIME	NMO VELOCITY	INTERVAL VELOCITY	CMP	TIME	NMO VELOCITY	INTERVAL VELOCITY
570.0	41	1900.0	1900.0				
	54	1997.0	2276.0				
	62	2102.0	2706.2				
	83	2496.0	3402.7				
	116	2700.0	3155.3				
	158	3500.0	5094.0				
LINE 8-1							
96.0	62	2100.0	2100.0	112.0	66	1650.0	1650.0
	112	2150.0	2210.4		78	1750.0	2220.9
	176	4000.0	5992.5		90	1850.0	2400.5
	220	6000.0	10770.3		112	2100.0	2906.8
					142	2550.0	3783.5
					176	4000.0	7461.0
			220	6000.0	10770.3		
128.0	58	1800.0	1800.0	140.0	67	1900.0	1900.0
	74	1884.0	2161.3		85	2200.0	3068.9
	94	2250.0	3265.1		135	2900.0	3805.1
	176	4000.0	5342.1		174	4000.0	6501.8
	220	6000.0	10770.3				
156.0	65	2000.0	2000.0	172.0	61	1886.0	1886.0
	80	2100.0	2487.3		96	2045.0	2295.9
	113	2250.0	2577.7		113	2250.0	3167.7
	139	2580.0	3685.6		139	2580.0	3685.6
	158	3586.0	7631.5		158	3600.0	7686.1
186.0	51	1600.0	1600.0	202.0	68	2075.0	2075.0
	81	1880.0	2278.4		84	2212.0	2718.3
	96	2045.0	2771.1		98	2425.0	3436.1
	113	2250.0	3167.7		179	3800.0	4979.5
	139	2580.0	3685.6				
	158	3200.0	6038.0				
	180	3900.0	7134.7				

9 1 1 3 9 0 4 1 9 7 5

CMP	TIME	NMO VELOCITY	INTERVAL VELOCITY	CMP	TIME	NMO VELOCITY	INTERVAL VELOCITY
268.0	63	1975.0	1975.0	286.0	63	1950.0	1950.0
	73	2037.0	2390.9		85	2100.0	2479.9
	85	2124.0	2591.1		103	2175.0	2498.9
	103	2175.0	2401.2		162	3000.0	4056.3
	160	3500.0	5083.1		183	5000.0	12183.1
294.0	67	1950.0	1950.0	340.0	56	2050.0	2050.0
	82	2100.0	2669.0		82	2325.0	2827.9
	125	3000.0	4213.4		127	3000.0	3943.3
	163	4000.0	6247.1		152	4000.0	7180.5
350.0	56	2050.0	2050.0	402.0	53	1900.0	1900.0
	82	2325.0	2827.9		73	2000.0	2243.5
	127	3000.0	3943.3		143	2950.0	3688.7
	152	4000.0	7180.5		166	4000.0	7834.0
414.0	43	1850.0	1850.0	438.0	43	1850.0	1850.0
	77	2300.0	2766.2		62	2150.0	2708.9
	179	4500.0	5616.3		110	2650.0	3181.6
			179		5000.0	7325.3	
456.0	43	1850.0	1850.0	482.0	40	1775.0	1775.0
	62	2150.0	2708.9		67	2332.0	2971.1
	110	2662.0	3204.5		93	2700.0	3473.0
	179	5000.0	7318.3		107	2925.0	4118.6
			179		5000.0	7031.2	
510.0	40	1750.0	1750.0	522.0	38	1900.0	1900.0
	64	2300.0	3000.4		66	2350.0	2849.2
	85	2400.0	2681.9		85	2400.0	2566.1
	114	2700.0	3431.4		114	2700.0	3431.4
	184	5000.0	7337.7		184	5000.0	7337.7

9 4 1 1 9 0 4 1 8 7 6

CMP	TIME	NMO VELOCITY	INTERVAL VELOCITY	CMP	TIME	NMO VELOCITY	INTERVAL VELOCITY
532.0	39	1800.0	1800.0	568.0	49	2000.0	2000.0
	62	2200.0	2748.3		69	2463.0	3336.0
	80	2350.0	2805.9		87	3050.0	4659.1
	115	2700.0	3366.0		106	3400.0	4679.4
	172	4000.0	5794.2		153	5000.0	7437.2
578.0	40	1900.0	1900.0	594.0	42	1900.0	1900.0
	62	2100.0	2421.7		65	2266.0	2814.1
	87	2750.0	3921.8		83	2700.0	3882.4
	101	3126.0	4847.8		108	3400.0	5073.1
	155	5000.0	7313.2		155	5000.0	7475.5
612.0	37	1900.0	1900.0	636.0	45	1950.0	1950.0
	66	2400.0	2916.0		72	2600.0	3418.9
	82	2500.0	2876.0		85	2700.0	3197.7
	105	3300.0	5237.6		108	3700.0	6110.8
	175	4711.0	6256.9		179	5000.0	6496.5
642.0	45	1950.0	1950.0	666.0	55	2200.0	2200.0
	64	2500.0	3470.8		70	2500.0	3379.3
	87	2700.0	3191.2		84	2700.0	3534.1
	108	3700.0	6340.7		108	3700.0	6007.5
	179	5000.0	6496.5		179	5000.0	6496.5
702.0	38	2100.0	2100.0	720.0	37	2185.0	2185.0
	55	2200.0	2408.6		65	2612.0	3086.9
	66	2500.0	3646.9		94	2884.0	3415.9
	78	2600.0	3092.7		153	4075.0	5459.9
	108	3700.0	5631.0				
	179	5000.0	6496.5				
722.0	41	2416.0	2416.0	740.0	37	1925.0	1925.0
	67	2500.0	2627.0		63	2200.0	2540.5
	83	2600.0	2982.6		109	3026.0	3881.8
	116	3800.0	5810.0		165	4100.0	5630.9
	159	5000.0	7313.5				

9 1 1 9 9 0 4 0 9 7 7

CMP	TIME	NMO VELOCITY	INTERVAL VELOCITY	CMP	TIME	NMO VELOCITY	INTERVAL VELOCITY
750.0	39	1900.0	1900.0	764.0	59	2086.0	2086.0
	65	2250.0	2691.0		65	2178.0	2932.8
	88	2700.0	3685.8		77	2288.0	2810.0
	116	3800.0	6075.5		89	2626.0	4189.7
	159	5000.0	7313.5		147	4000.0	5474.5
				192	6000.0	10066.4	
796.0	59	1900.0	1900.0	806.0	58	1994.0	1994.0
	69	1938.0	2148.6		72	2158.0	2734.6
	87	1974.0	2106.3		108	3027.0	4263.1
	106	2219.0	3102.9		161	4000.0	5471.1
	150	3000.0	4338.1				
	186	4200.0	7323.9				
810.0	44	1900.0	1900.0	846.0	52	2130.0	2130.0
	57	2050.0	2491.6		87	2175.0	2240.2
	87	2175.0	2394.6		106	2374.0	3127.5
	106	2374.0	3127.5		150	3000.0	4135.8
	150	3000.0	4135.8		186	4200.0	7323.9
	186	4200.0	7323.9				
850.0	44	2150.0	2150.0	852.0	51	2250.0	2250.0
	87	2175.0	2200.3		96	2350.0	2458.4
	106	2374.0	3127.5		134	3500.0	5407.9
	150	3000.0	4135.8		152	4650.0	9560.1
	186	4203.0	7332.8				
854.0	51	2250.0	2250.0	860.0	47	2100.0	2100.0
	96	2346.0	2450.3		66	2200.0	2429.7
	134	3500.0	5412.3		102	3100.0	4284.3
	152	4650.0	9560.1		141	4500.0	6933.8

9 2 1 0 9 0 4 1 9 7 8

CMP	TIME	NMO VELOCITY	INTERVAL VELOCITY	CMP	TIME	NMO VELOCITY	INTERVAL VELOCITY
874.0	52	2313.0	2313.0				
	69	2400.0	2648.4				
	102	3100.0	4202.4				
	115	3300.0	4575.3				
	158	3500.0	3985.9				

9 0 1 0 9 0 4 1 2 7 9

APPENDIX D

INTERPRETED SEISMIC SECTIONS

9 3 1 3 9 0 4 7 8 9 0

This page intentionally left blank.

9 7 1 3 9 0 4 7 8 8 1

APPENDIX D

INTERPRETED SEISMIC SECTIONS

Three seismic reflection lines are included in this appendix, lines 3-5, 2-3, and 4-2. The interpreted Hanford/Ringold contact and the lower mud unit are plotted on the sections. The measured drill depths to the sedimentary units is displayed below the well locations. A detailed discussion of these seismic sections is presented in Chapter 4.0 of the main body of the text.

9 7 1 2 9 0 4 0 3 9 2

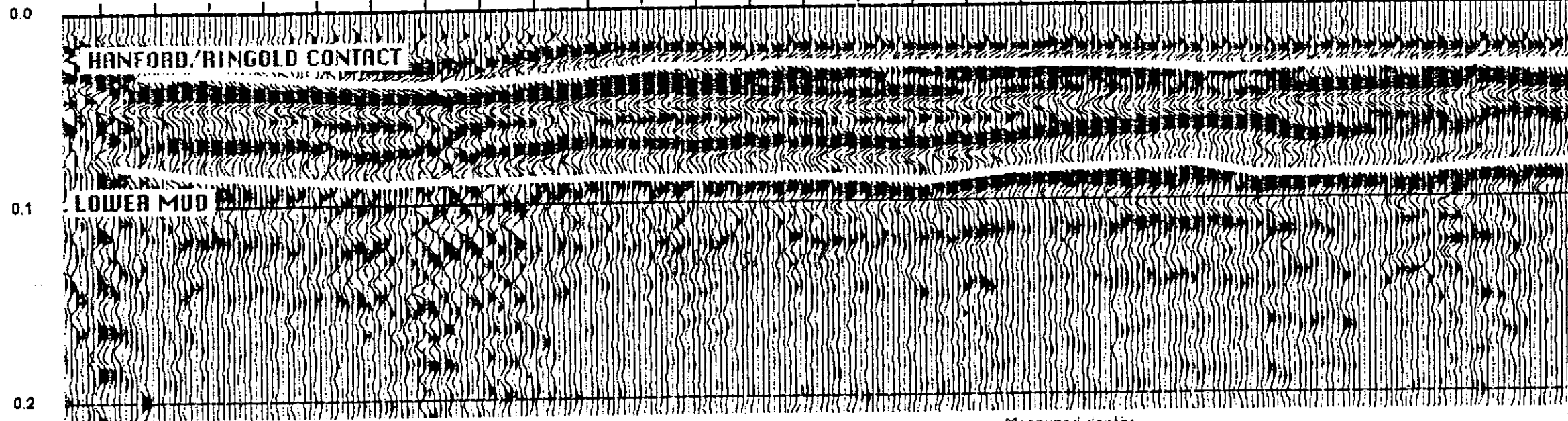
This page intentionally left blank.

9 3 1 0 9 2 4 1 8 0 3

WELL 399-1-13



39.0 373.5 378.5 383.5 386.5 393.5 398.5 403.5 408.5 413.5 418.5 423.5 428.5 433.5 438.5 443.5 448.5 453.5 458.5 463.5 468.5 473.5 478.5 483.5 488.5 493.5 498.5 503.5 50



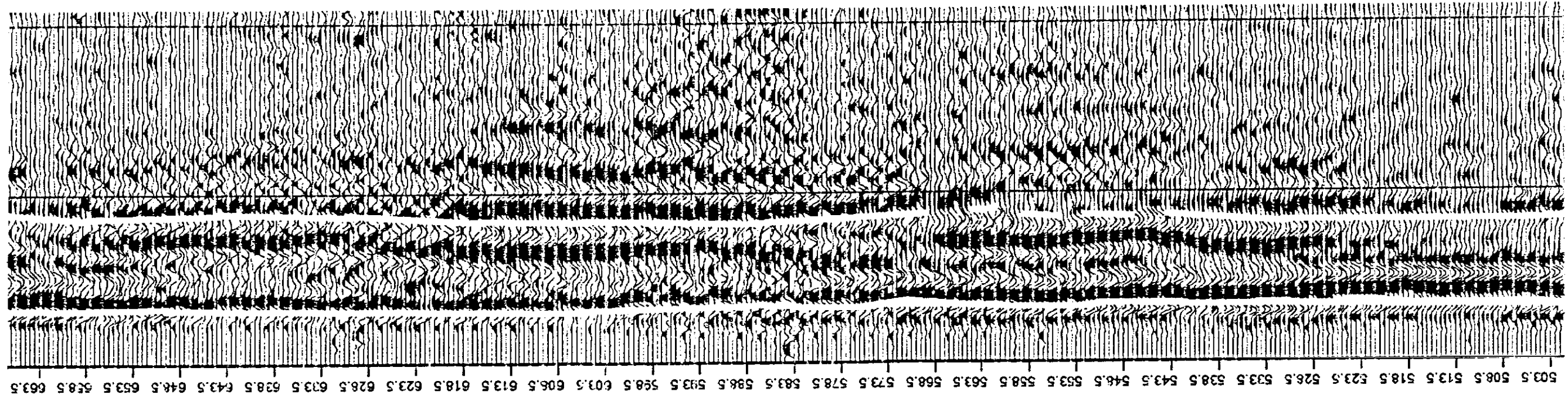
Measured depths
water table - 42 ft
Ringold - 48 ft
Lower Mud - 113 ft
Basalt - 144 ft

9 8 1 2 9 0 4 0 8 8 4

start

**THIS PAGE INTENTIONALLY
LEFT BLANK**

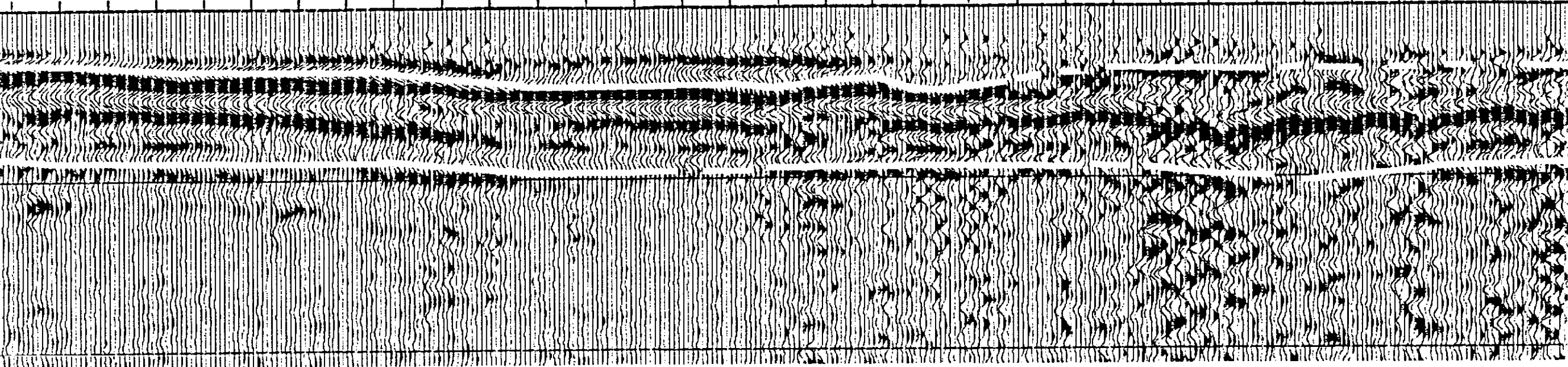
Middle 1



**THIS PAGE INTENTIONALLY
LEFT BLANK**

Jct

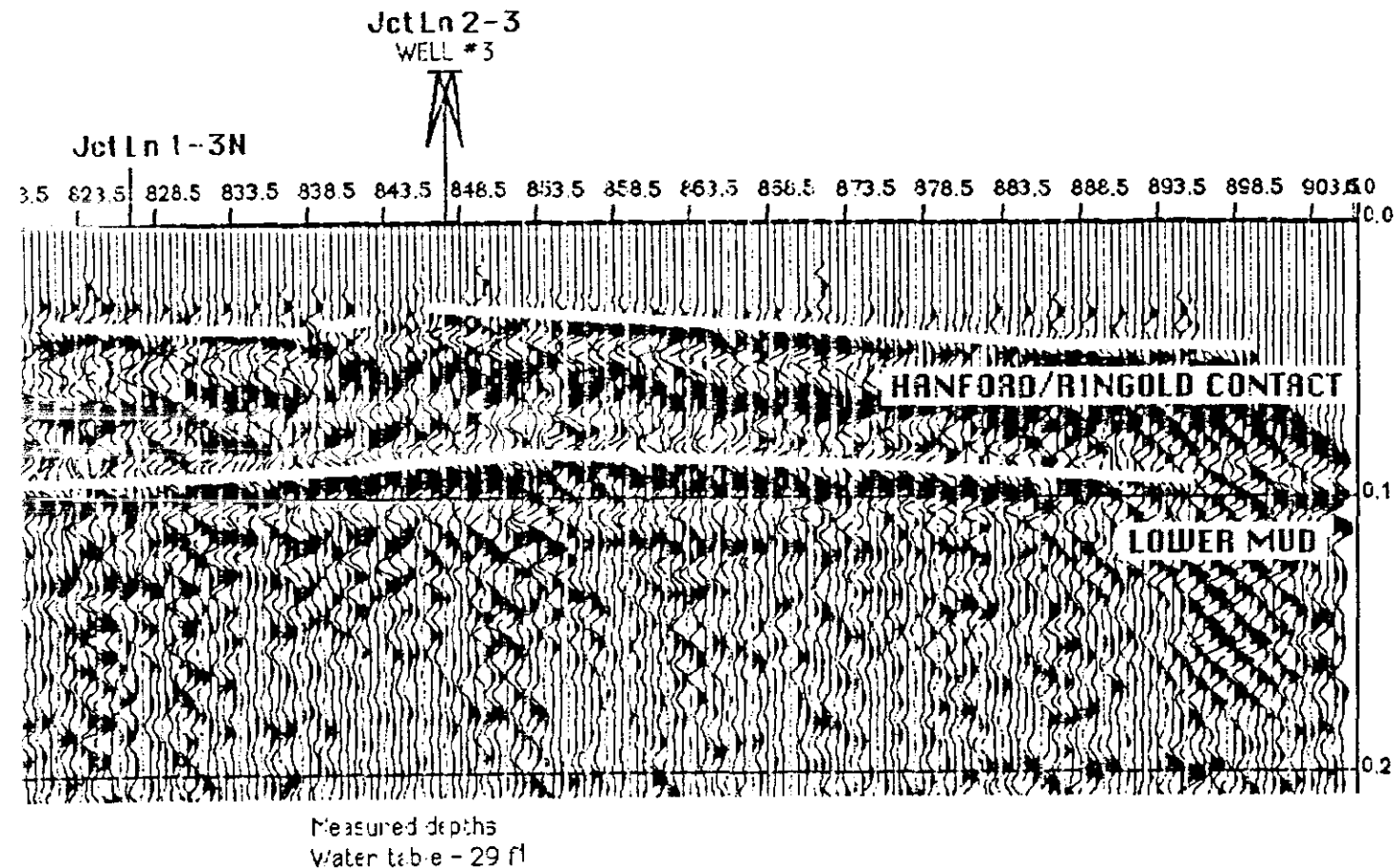
663.5 668.5 673.5 678.5 683.5 688.5 693.5 698.5 703.5 708.5 713.5 718.5 723.5 728.5 733.5 738.5 743.5 748.5 753.5 758.5 763.5 768.5 773.5 778.5 783.5 788.5 793.5 798.5 803.5 808.5 813.5 818.5 823.5



Middle 2

1950

1950
1950



Project **300 - FF - 5**

Line **Line 3-5**

LN 3-5 STACK

Field Parameters

Source - Dinoseis
 Shot Interval - 3.0 m (10ft)
 Receiver Interval - 1.5m (5ft)
 Near Offset - 3.0 m (10ft)
 Far Offset - 38m (125ft)

Recording Unit - EG&G ES2401
 Sample Rate - 0.2 millsec
 Record Length - 0.409 sec
 No. Channels - 24
 Filters Low - 35 hz
 Notch - IN
 High - 250 hz

Processing Parameters

Create Trace Headers
 Automatic Gain Control - 100 msec window
 Dip Filter - Reject 400 - 1700 ft/sec
 Apply Filter - pass 60hz @18db/oct - 180 hz @ 18db/oct 30msec operator
 Apply Static Shifts - Record statics for Dinoseis delays
 CMP Sort
 NMO Correction - stretch mute - 97% with 20msec taper
 Apply Static Shifts - Datum Elev = 375 ft
 CMP Stack

Display Parameters

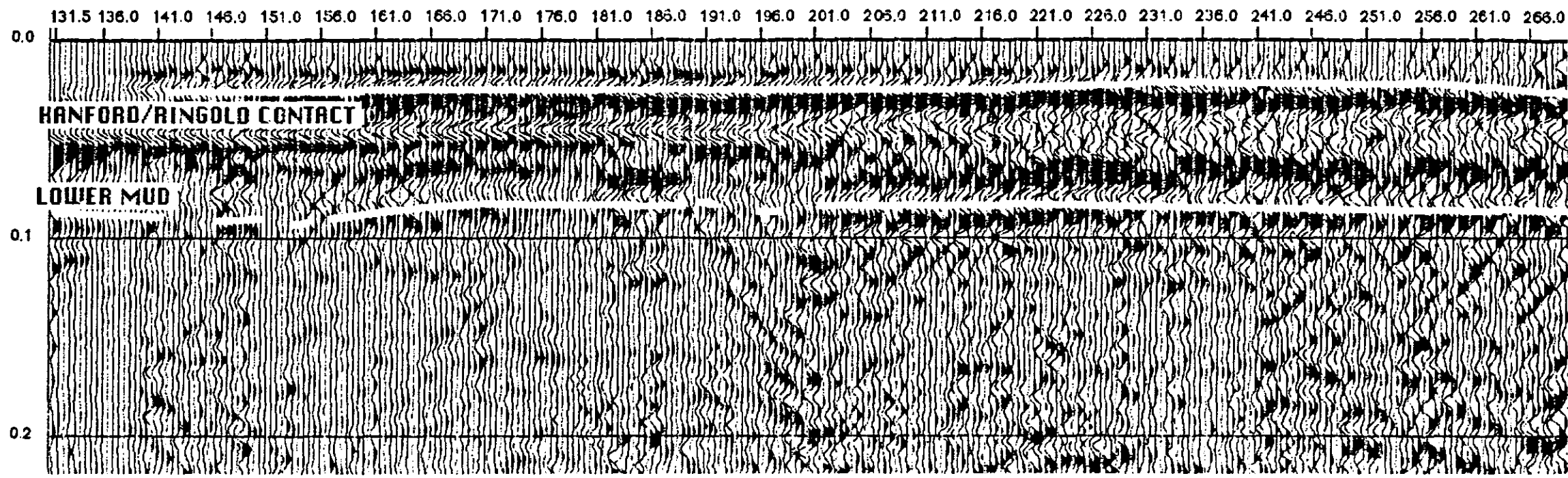
Inches/Second 15.0
 Traces/inch 24
 Plot Polarity Normal

Processed using SPW™ from Parallel Geoscience Corporation

Figure D-1. Seismic Line 3-5.

**THIS PAGE INTENTIONALLY
LEFT BLANK**

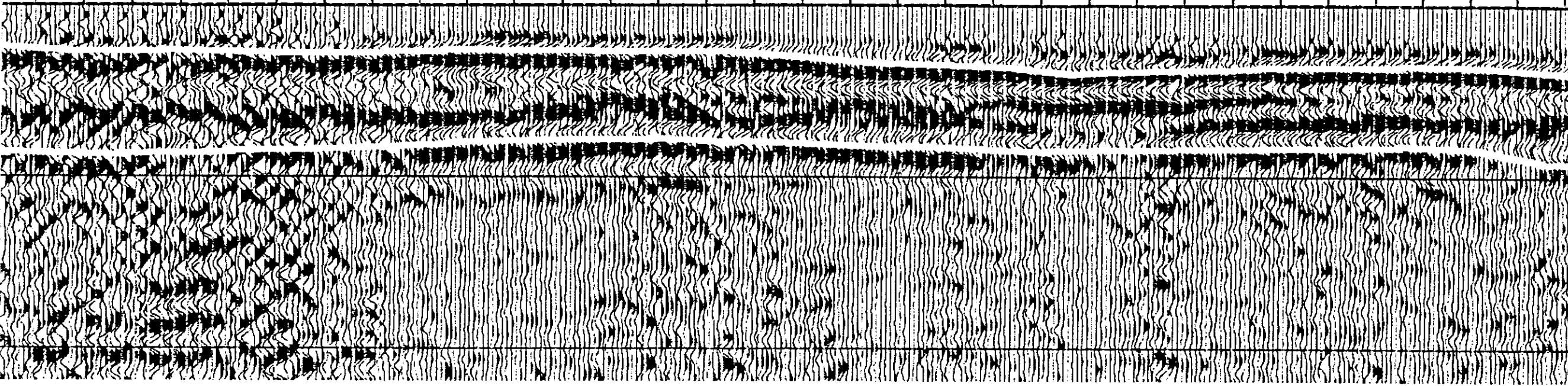
93129047005



start

**THIS PAGE INTENTIONALLY
LEFT BLANK**

0 266.0 271.0 276.0 281.0 286.0 291.0 296.0 301.0 306.0 311.0 316.0 321.0 326.0 331.0 336.0 341.0 346.0 351.0 356.0 361.0 366.0 371.0 376.0 381.0 386.0 391.0 396.0 401.0 406.0 411.0 416.0 421.0 42



Middle 1

**THIS PAGE INTENTIONALLY
LEFT BLANK**

1/1/1992

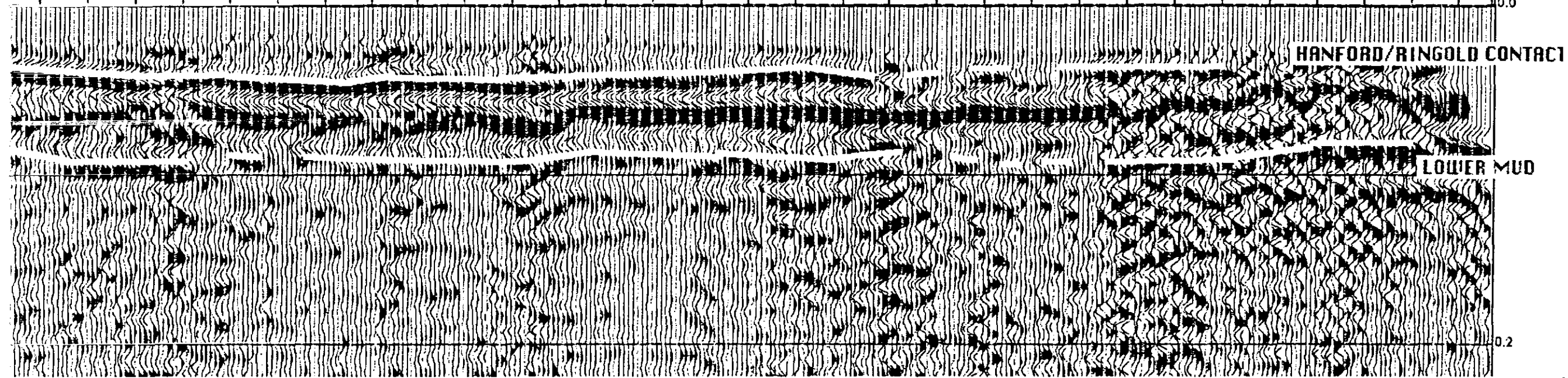
WELL #3



JCT Line 1-3N

JCT Line 3-5

0 421.0 426.0 431.0 436.0 441.0 446.0 451.0 456.0 461.0 466.0 471.0 476.0 481.0 486.0 491.0 496.0 501.0 506.0 511.0 516.0 521.0 526.0 531.0 536.0 541.0 546.0 551.0 556.0 561.0 566.0 571.0 574.5



Middle 2

**THIS PAGE INTENTIONALLY
LEFT BLANK**

7-11-63

WELL #3



JCT Line 3-5

9 551.0 556.0 561.0 566.0 571.0 574.5

0.0

HANFORD/RINGOLD CONTACT

LOWER MUD

0.2

Project **300 - FF - 5**

Line **Line 2-3**

LN 2-3 STACK

Field Parameters

Source - Dinoseis	Recording Unit - EG&G ES2401
Shot Interval - 3.0 m (10ft)	Sample Rate - 0.2 millsec
Receiver Interval - 1.5m (5ft)	Record Length - 0.409 sec
Near Offset - 3.0 m (10ft)	No. Channels - 24
Far Offset - 38m (125ft)	Filters Low - 35 hz
	Notch - IN
	High - 250 hz

Processing Parameters

Create Trace Headers
 Automatic Gain Control - 100 msec window
 Apply Static Shifts - Record statics for Dinoseis delays
 Dip Filter - Reject 400 - 1700 ft/sec
 Apply Filter - pass 60hz @18db/oct - 120 hz @ 18db/oct 30msec operator
 NMO Correction - stretch mute - 90% with 20msec taper
 Apply Static Shifts - Datum Elev = 375 ft
 CMP Stack

Display Parameters

Inches/Second	15.0
Traces/Inch	24
Plot Polarity	Normal

Processed using SPW™ from Parallel Geoscience Corporation

Figure D-2. Seismic Line 2-3.

end

**THIS PAGE INTENTIONALLY
LEFT BLANK**

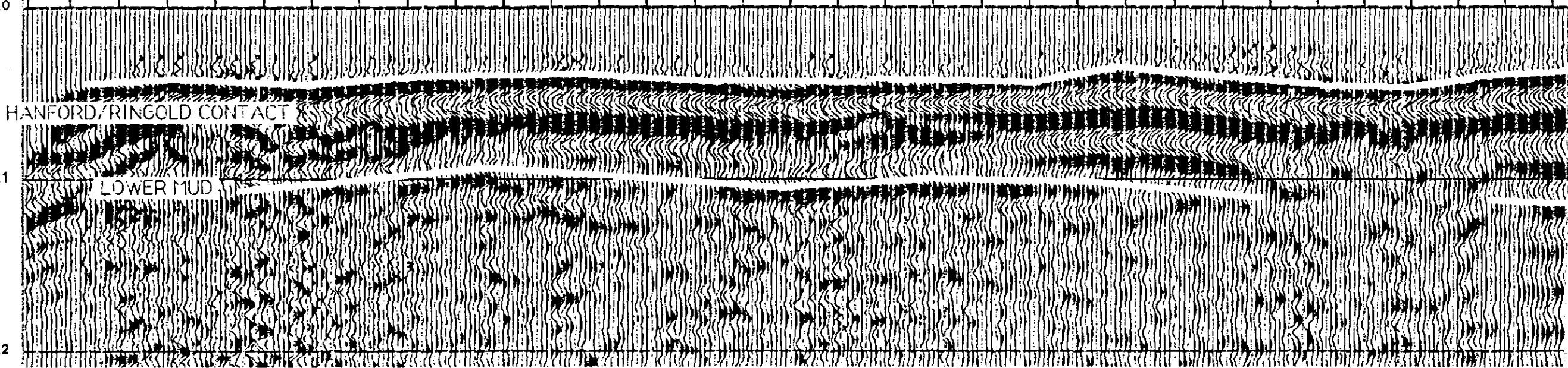
WELL #4



JCT Line 7-4

JCT Line 4-5

33.5 38.0 43.0 48.0 53.0 58.0 63.0 68.0 73.0 78.0 83.0 88.0 93.0 98.0 103.0 108.0 113.0 118.0 123.0 128.0 133.0 138.0 143.0 148.0 153.0 158.0 163.0 168.0 173.0 178.0 183.0 188.0 193.0



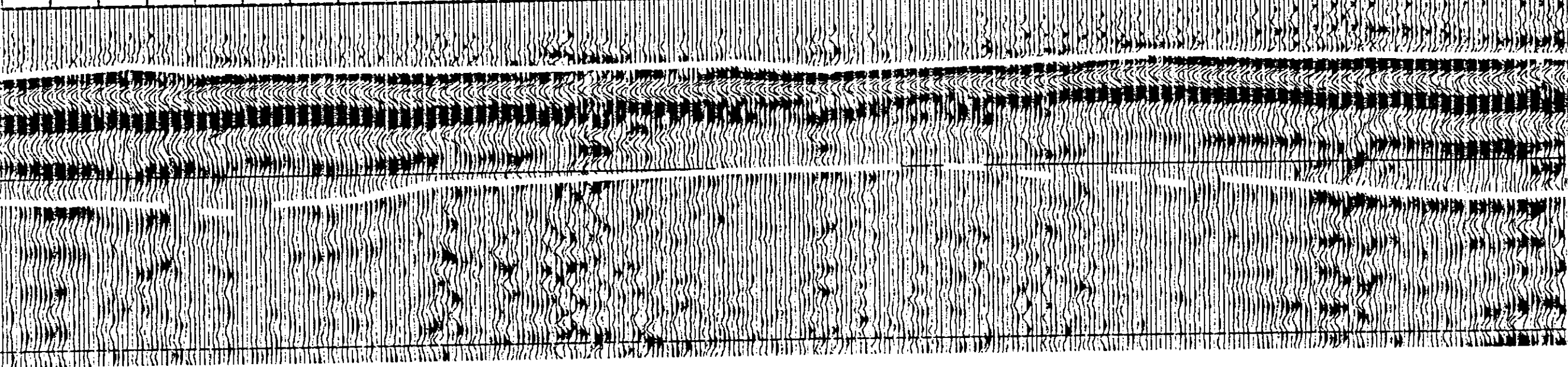
start

L

**THIS PAGE INTENTIONALLY
LEFT BLANK**

Handwritten mark

188.0 193.0 198.0 203.0 208.0 213.0 218.0 223.0 228.0 233.0 238.0 243.0 248.0 253.0 258.0 263.0 268.0 273.0 278.0 283.0 288.0 293.0 298.0 303.0 308.0 313.0 318.0 323.0 328.0 333.0 338.0 343.0 348.0

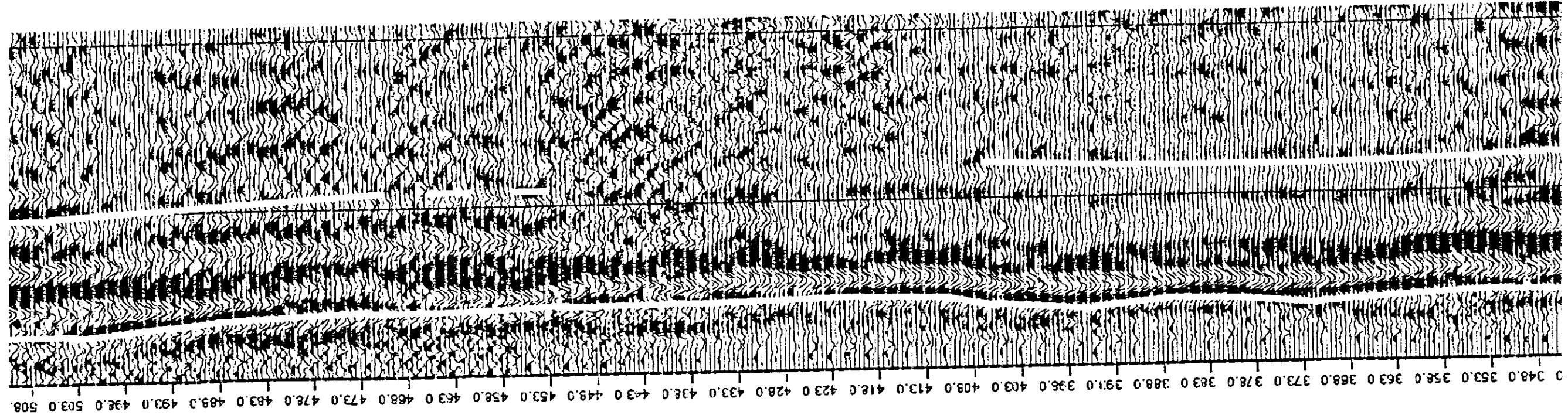


Middle 1

**THIS PAGE INTENTIONALLY
LEFT BLANK**

1 000000

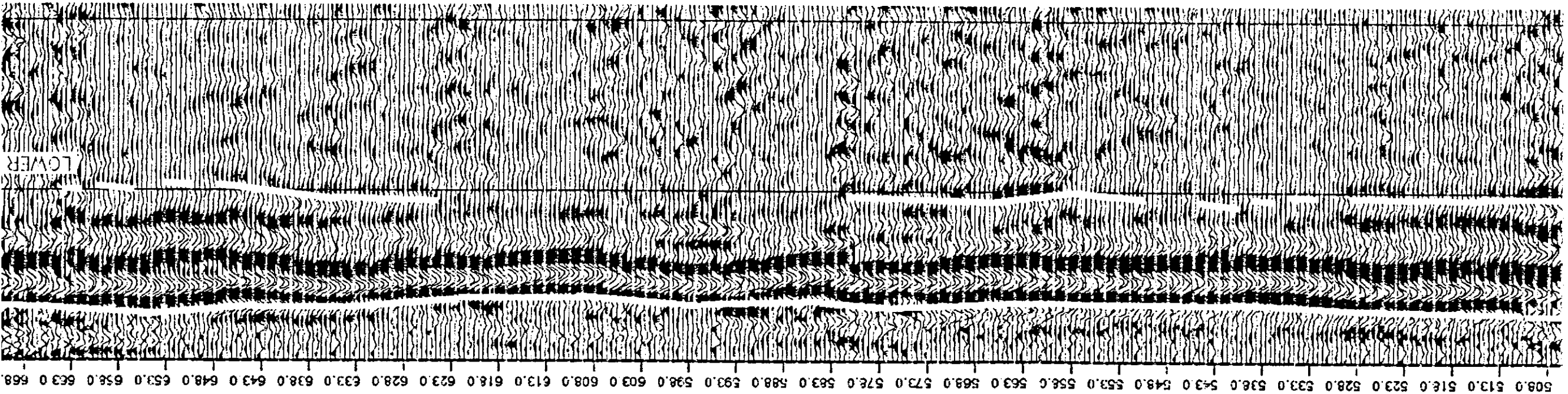
Middle 2

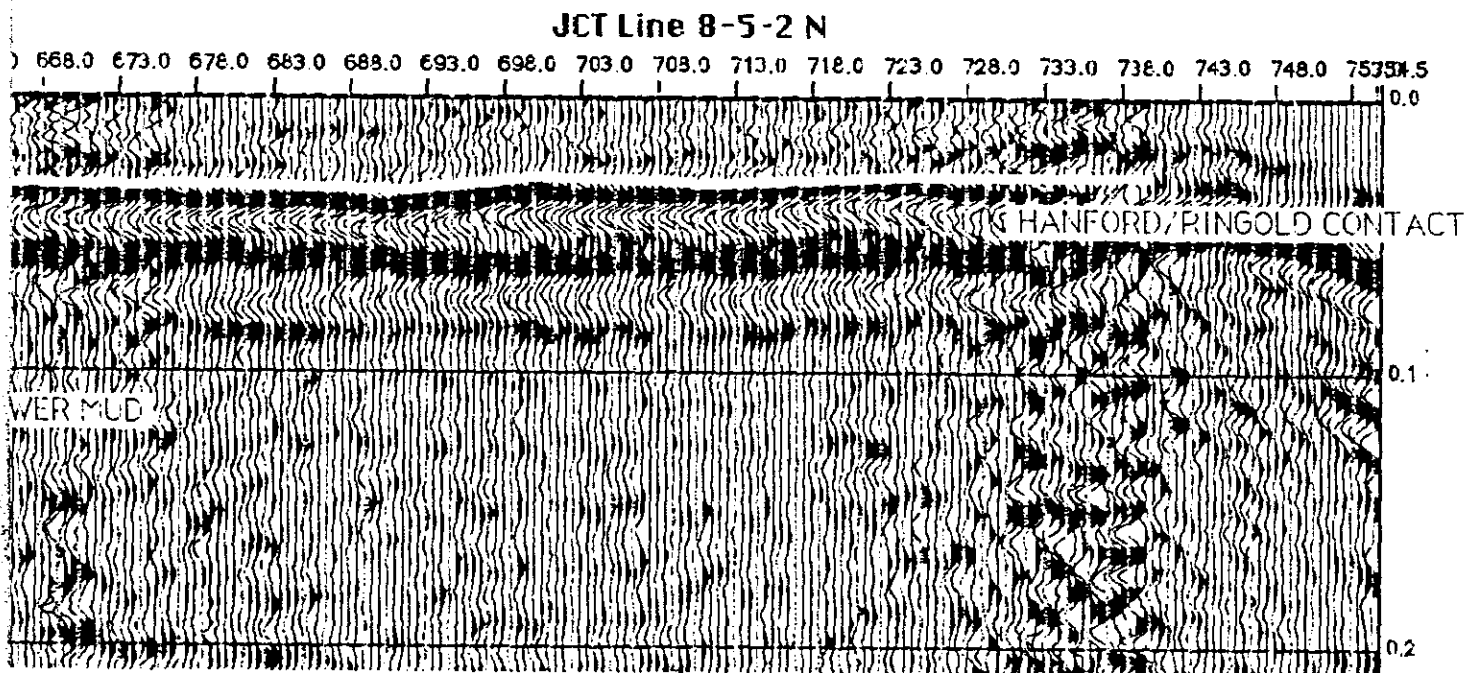


**THIS PAGE INTENTIONALLY
LEFT BLANK**

2 10/10

Middler 3





Project **300 - FF - 5**

Line **Line 4-2**

LN 4-2 STACK

Field Parameters

Source - Dinosaurs
 Shot Interval - 3.0 m (10ft)
 Receiver Interval - 1.5m (5ft)
 Near Offset - 3.0 m (10ft)
 Far Offset - 38m (125ft)

Recording Unit - EG&G ES2401
 Sample Rate - 0.2 millsec
 Record Length - 0.409 sec
 No. Channels - 24
 Filters Low - 35 hz
 Notch - IN
 High - 250 hz

Processing Parameters

Create Trace Headers
 Automatic Gain Control - 100 msec window
 Dip Filter - Reject 400 - 1750 ft/sec
 Apply Filter - pass 60hz @36db/oct - 250 hz @ 18db/oct 25msec operator
 Apply Static Shifts - Record statics for Dinosaurs delays
 CMP Sort
 NMO Correction - stretch mute - 95% with 20msec taper
 Apply Static Shifts - Datum Elev = 375 ft
 CMP Stack

Display Parameters

Inches/Second 15.0
 Traces/Inch 24
 Plot Polarity Normal

Processed using SPW™ from Parallel Geoscience Corporation

Figure D-3. Seismic Line 4-2.

**THIS PAGE INTENTIONALLY
LEFT BLANK**

DISTRIBUTION SHEET

To: Those listed

From: J.R. Kunk

Date: 1/13/93

Project Title/Work Order:

Phase I Summary of Surface Geophysical Studies in the 300-FF-5 Operable Unit

EDT No.: 159213

ECN No.:

Name	MSIN	With Attachment	EDT/ECN & Comment	EDT/ECN Only
Hulstrom L.C. (15)	H4-55			
Kelty G.G (10)	H5-29			
Kunk J.R. (10)	G6-50			
EDMC (2)	L8-15			
Central Files	L8-04			

93139041087

**THIS PAGE INTENTIONALLY
LEFT BLANK**

Complete for all Types of Release

Purpose <input type="checkbox"/> Speech or Presentation <input type="checkbox"/> Full Paper (Check only one suffix) <input type="checkbox"/> Summary <input type="checkbox"/> Abstract <input type="checkbox"/> Visual Aid <input type="checkbox"/> Speakers Bureau <input type="checkbox"/> Poster Session <input type="checkbox"/> Videotape		<input type="checkbox"/> Reference <input checked="" type="checkbox"/> Technical Report <input type="checkbox"/> Thesis or Dissertation <input type="checkbox"/> Manual <input type="checkbox"/> Brochure/Flier <input type="checkbox"/> Software/Database <input type="checkbox"/> Controlled Document <input type="checkbox"/> Other	ID Number (include revision, volume, etc.) <u>WHC-SD-EN-TI-069 Rev 0</u> List attachments. Date Release Required <p align="center">1-8-1993</p>
---	--	---	--

Title Phase I Summary of Surface Geophysical Studies in the 300-FF-5 Operable Unit Unclassified Category UC-N/A Impact Level

New or novel (patentable) subject matter? No Yes
 If "Yes", has disclosure been submitted by WHC or other company?
 No Yes Disclosure No(s).

Copyrights? No Yes
 If "Yes", has written permission been granted?
 No Yes (Attach Permission)

Complete for Speech or Presentation

Title of Conference or Meeting NA Group or Society Sponsoring NA
 Date(s) of Conference or Meeting NA City/State NA
 Will proceedings be published? Yes No
 Will material be handed out? Yes No

Title of Journal NA

CHECKLIST FOR SIGNATORIES

Review Required per WHC-CM-3-4	Yes	No	Reviewer - Signature	Indicates Approval	Date
			Name (printed)	Signature	
Classification/Unclassified Controlled					
Nuclear Information	<input type="checkbox"/>	<input checked="" type="checkbox"/>			
Patent - General Counsel	<input checked="" type="checkbox"/>	<input type="checkbox"/>	<u>S. BERGLIN</u>	<u>[Signature]</u>	<u>1/12/93</u>
Legal - General Counsel	<input checked="" type="checkbox"/>	<input type="checkbox"/>			
Applied Technology/Export Controlled Information or International Program	<input type="checkbox"/>	<input checked="" type="checkbox"/>			
WHC Program/Project	<input type="checkbox"/>	<input checked="" type="checkbox"/>			
Communications	<input type="checkbox"/>	<input checked="" type="checkbox"/>			
AL Program/Project	<input type="checkbox"/>	<input checked="" type="checkbox"/>			
Publication Services	<input checked="" type="checkbox"/>	<input type="checkbox"/>	<u>M.S. Andrews</u>	<u>M.A. Andrews</u>	<u>1/18/93</u>
Other Program/Project	<input type="checkbox"/>	<input checked="" type="checkbox"/>			


Information conforms to all applicable requirements. The above information is certified to be correct.

References Available to Intended Audience Yes No
 Transmit to DOE-HQ/Office of Scientific and Technical Information Yes No
 Author/Requestor (Printed/Signature) Faye Stone for J.R. KUNK Date 1/12/92

Intended Audience
 Internal Sponsor External
 Responsible Manager (Printed/Signature) Faye Stone for A.J. KNEPP Date 1/12/92

INFORMATION RELEASE ADMINISTRATION APPROVAL STAMP

Stamp is required before release. Release is contingent upon resolution of mandatory comments.



Date Cancelled Date Disapproved

**THIS PAGE INTENTIONALLY
LEFT BLANK**

ID Number

Lead Author J.R. Kunk	Phone 6-4024	MSIN G6-50	Other Author(s) or Requestor See Below		
Project or Program 300-FF-5 Operable Unit	Lead Org Code 81234		Sponsor Agency (DOE, DOT, NRC, USGS, etc.) DOE		
Editor M.S. Andrews	Phone 6-4386	MSIN H4-17	DOE/HQ Program (DP, EH, EM, NE, etc.)		
Mandatory Comments (Only mandatory comments are to be documented. All other comments should be made on a copy of the information submitted for review and returned to the author.)	Reviewer Name & Signature	Date	Resolution	Reviewer Name & Signature	Date

Legends/Notices/Markings (required per WHC-CM-3-4 or guidance organization.) (Reviewer initials)

	Affix			Affix	
	Yes	No		Yes	No
Applied Technology	[]	[]	Predecisional Information	[]	[]
Business-Sensitive Information	[]	[]	Programmatic Notice		
Computer Software Notice	[]	[]	Proprietary Information	[]	[]
Copyright License Notice	[]	[]	Purpose and Use	[]	[X]
Export Controlled Information	[]	[]	Thesis/Dissertation	[]	[]
Legal Disclaimer	[X]	[]	Trademark Disclaimer	[]	[]
Limited Disclosure	[]	[X]	Unclassified Controlled Nuclear Information/Official Use Only	[]	[]
Patent Status	[]	[X]			

Responsible Manager (Printed/Signature)
NA

Additional Information Other authors include S.M. Narbutovskih, K.A. Bergstrom and T.H. Mitchell

**THIS PAGE INTENTIONALLY
LEFT BLANK**